Measurement of $e^+e^- \rightarrow \Lambda\bar{\Lambda}\phi$ using data samples at $\sqrt{s} = 4.190, 4.200, 4.210, 4220, 4.237, 4.246, 4.260, 4.270$ *and* 4.280 GeV

Aamir Khalid, Talab Hussain

Centre for High Energy Physics,
University of the Punjab

BESIII Charmonium Group Meeting
Tuesday, May 7, 2019

Highlights

- *Our decay process*
- *Comments in Previous Presentation presented on 10 April 2019*
- *Data sample and MC simulation*
- *Initial event selection criteria*
- *Kinematic fitting*
- $e^+e^- \rightarrow \Lambda\bar{\Lambda}\phi$ *plots*
- *Time distribution plots*
- *Final event selection*
- *Plots after final event selection*
- *Scatter Plot*
- *Background analysis*
- *Detection efficiency*
- *Cross section calculation of* $XYZ \rightarrow \Lambda\bar{\Lambda}\phi$
- *Systematic uncertainty estimation*
- Statistical significance of ϕ signal
- *Summary and analysis results*

Comments in previous presentation presented on 10 April 2019

- Deduce results for 4C and 1C Separately
- Plot proper time distribution for

  $\boldsymbol{p\pi^-}, \boldsymbol{\bar{p}\pi^+} and\ \boldsymbol{K^+K^-}$

- Draw Scatter Plot for $\boldsymbol{p\pi^-}$, $\boldsymbol{\bar{p}\pi^+} and\ \boldsymbol{K^+K^-}$

Our Decay Process

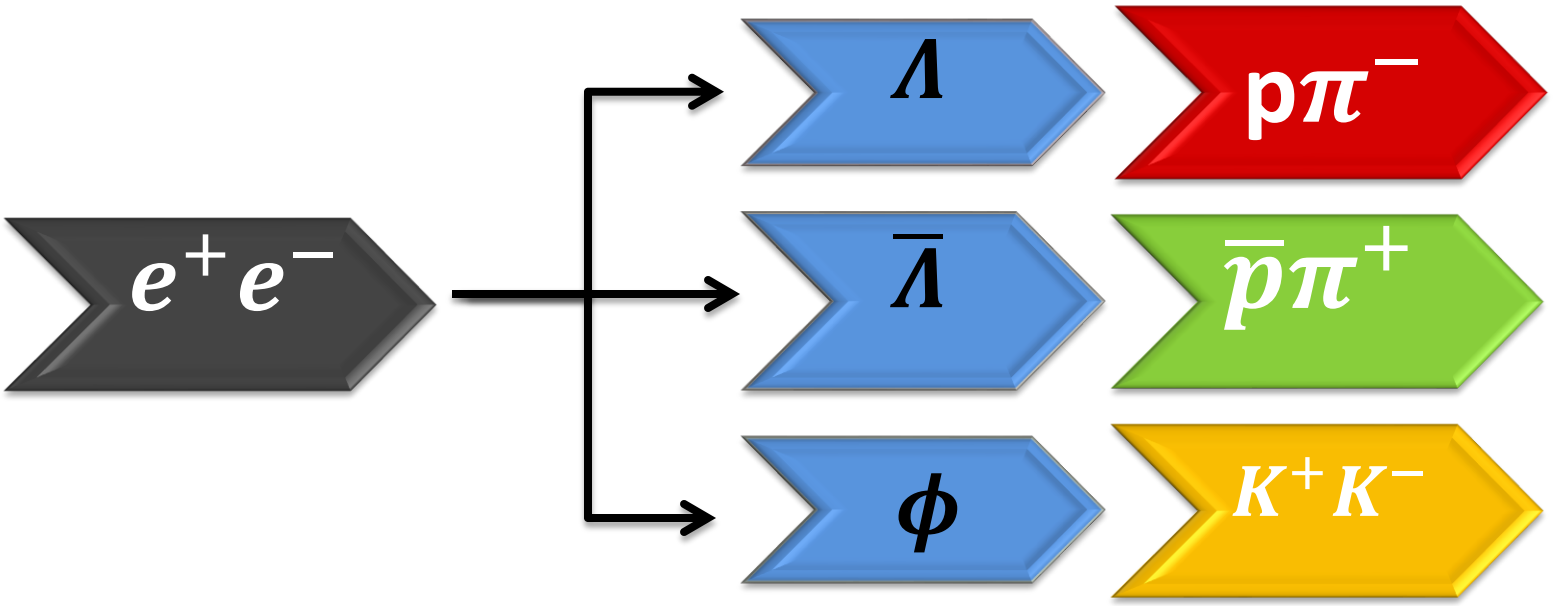

MC and Data Samples

- The analysis is performed under BOSS framework of 7.0.3 version.
- Phase Space (PHSP) model is used to study 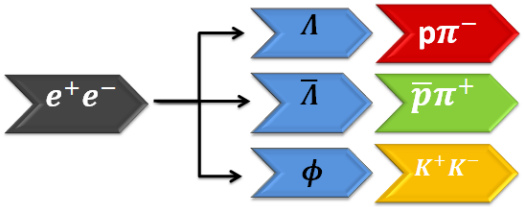

.
- Three kind of files used for analysis including (signal and exclusive MC root file) , inclusive MC data root file and real data root files. 500 pb^{-1} Inclusive data sample of Y(4260) is used for background analysis. Details of real data is given in table.
- Signal and exclusive MC root files are generated for 100,000 number of events while inclusive and real data root files are generated for 1 x 10^9 number of events.

Data Sample	Center of mass energy $\sqrt{s}$ (GeV)	$\mathcal{L}(pb^{-1})$	Run No.
Real	4.190	522.5 ± 0.1 ± 3.4	47543-48170
	4.200	424.6 ± 0.1 ± 2.5	48172-48713
	4.210	518.1 ± 0.1 ± 1.8	48714-49239
	4.220	514.3 ± 0.1 ± 1.9	49270-49787
	4.237	530.6 ± 0.1 ± 2.4	49788-50254
	4.246	537.4 ± 0.1 ± 2.6	50255-50793
	4.260	828.4 ± 0.1 ± 5.5	29677-30367, 31561-31981
	4.270	529.7 ± 0.1 ± 2.8	50796-51302
	4.280	175.5 ± 0.1 ± 0.9	51303-51498

Initial Event Selection Criteria

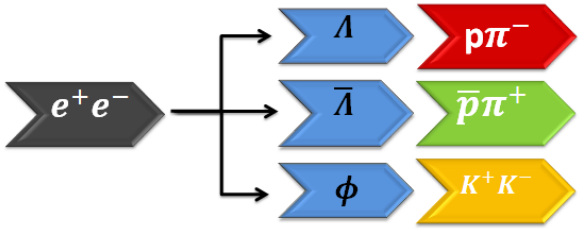

- One missing charged track technique is used. For 6 charged tracks, total electric charge should be equal to 0 and for 5 charged tracks (for missing charged track) the resulting net electric charge is +1 or -1.
- All the charged tracks are selected that lie with in the polar region of $|\cos(\theta)| < 0.93$.
- Each charged track is required to be within the interaction point in xy plane $V_{xy} = \sqrt{v_x^2 + v_y^2} < 10.0$ cm and in z direction $|v_z| < 15.0$ cm.
- Each track having transverse momentum $P_{xy} > 0.05$ GeV are selected and sent for further filtration.

Kinematic Fitting

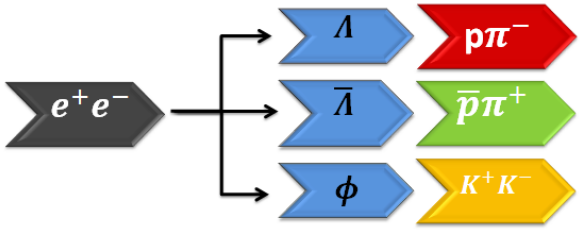

One missing charged track technique is used for kinematic fitting.

- For 6 (all) charged tracks only those events are selected that contain $N_p = 1,\ N_{\bar{p}} = 1,\ N_{\pi^+} = 1,\ N_{\pi^-} = 1,\ N_{K^+} = 1$ and $N_{K^-} = 1.$
- 4C fit is applied to the hypothesis $e^+e^- \to p\,\bar{p}\,\pi^+\pi^-K^+K^-$ by applying conservation of total energy and momentum.
- On the other hand for events having 5 (one missing) identified charged tracks from $p, \bar{p}, \pi^+, \pi^-, K^+ and K^-$ leads to the condition

$$N_p \le 1,\ N_{\bar{p}} \le 1,\ N_{\pi^+} \le 1,\ N_{\pi^-} \le 1,\ N_{K^+} \le 1 \text{ and } N_{K^-} \le 1.$$

- 1C fit is applied for one of the following hypothesis:

$$e^+e^- \to p\,\bar{p}\,\pi^+\pi^-K^+ (K^- \text{ missing})$$

$$e^+e^- \to p\,\bar{p}\,\pi^+\pi^-K^- (K^+ \text{ missing})$$

$$e^+e^- \to p\,\bar{p}\,\pi^+K^+K^- (\pi^- \text{ missing})$$

$$e^+e^- \to p\,\bar{p}\,\pi^-K^+K^- (\pi^+ \text{ missing})$$

$$e^+e^- \to p\,\pi^+\pi^-K^+K^- (\bar{p} \text{ missing})$$

and

$$e^+e^- \to \bar{p}\,\pi^+\pi^-K^+K^- (p \text{ missing})$$

$\chi^2_{4c\ and\ 1C}$ Distribution

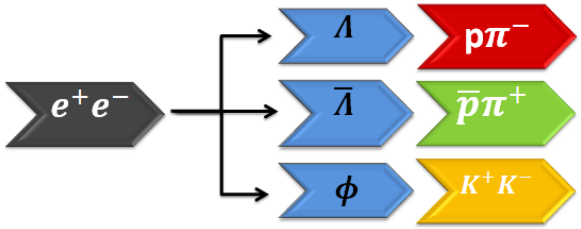

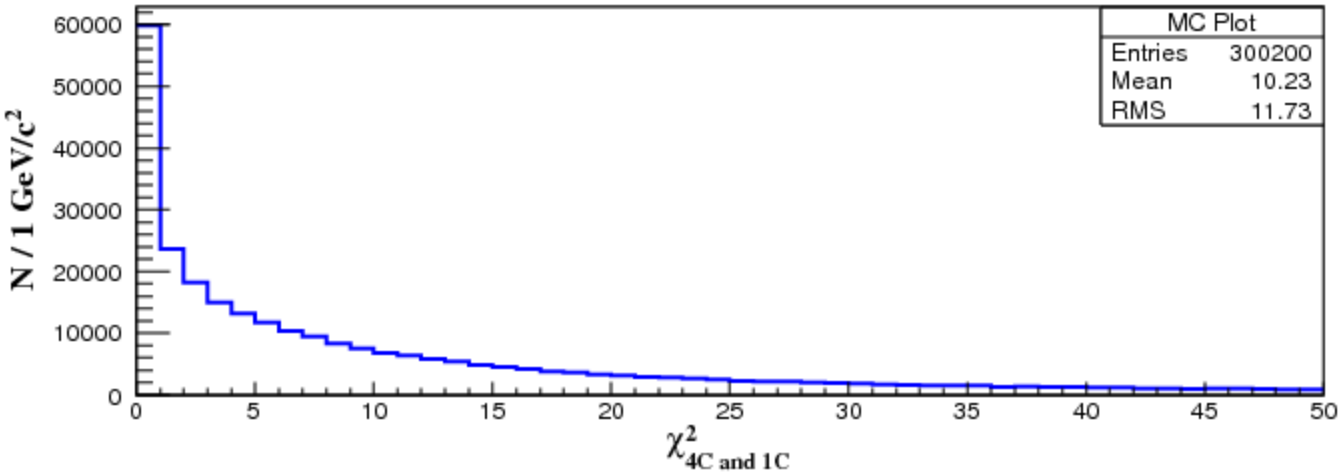

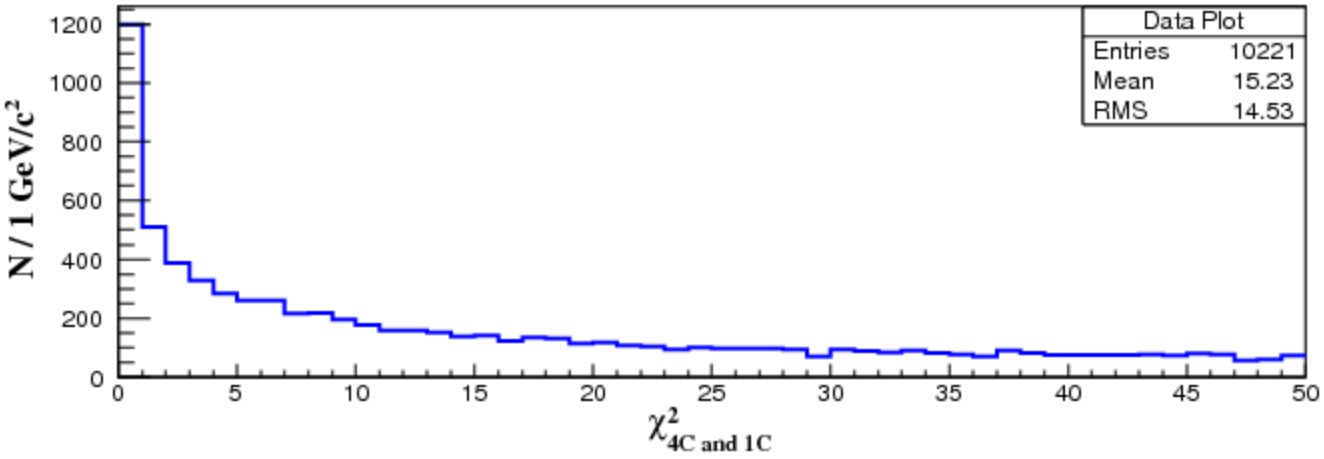

χ^2_{4c} Distribution

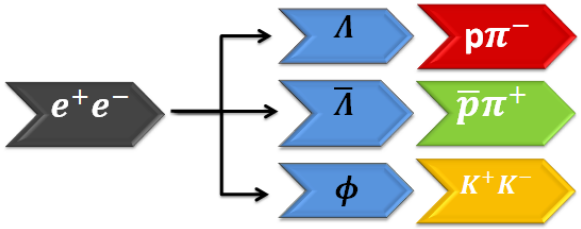

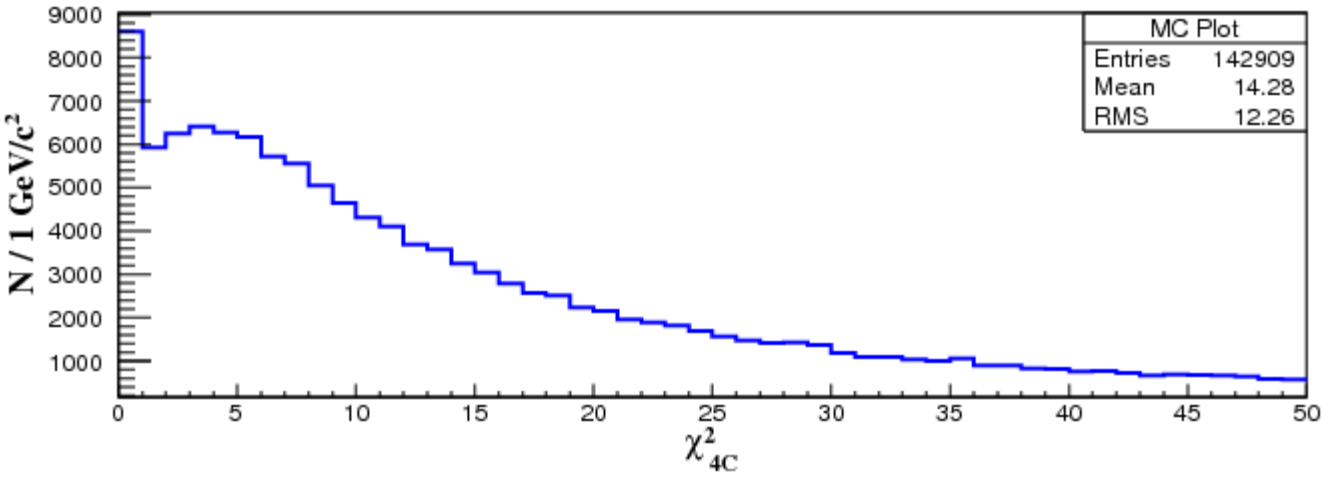

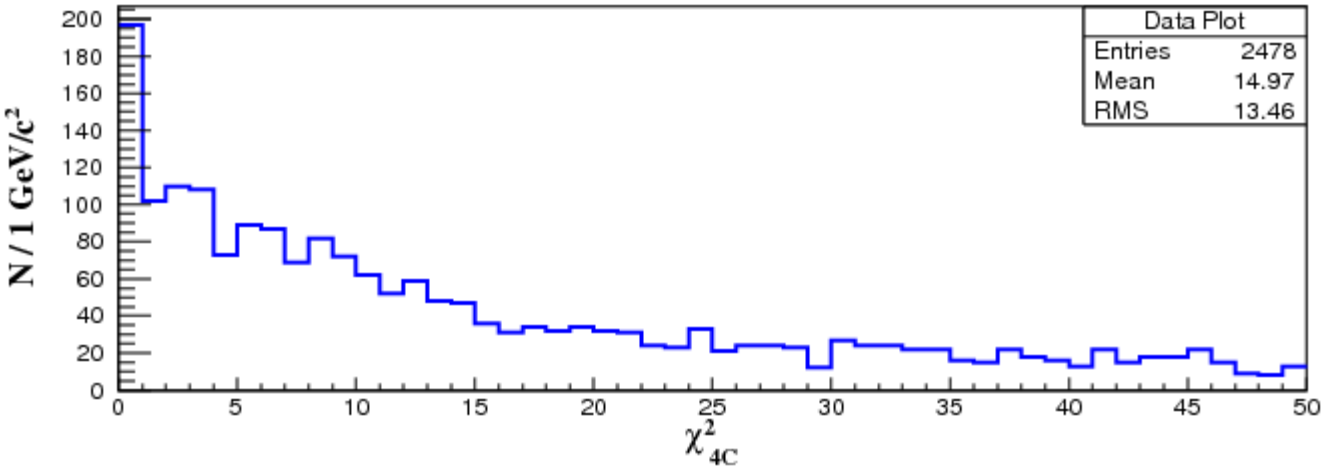

χ^2_{1c} Distribution

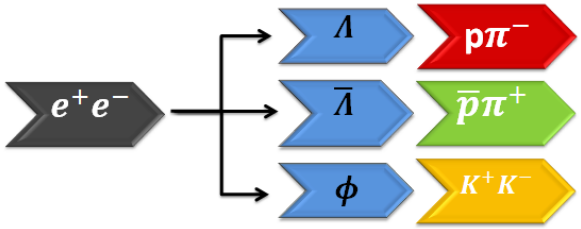

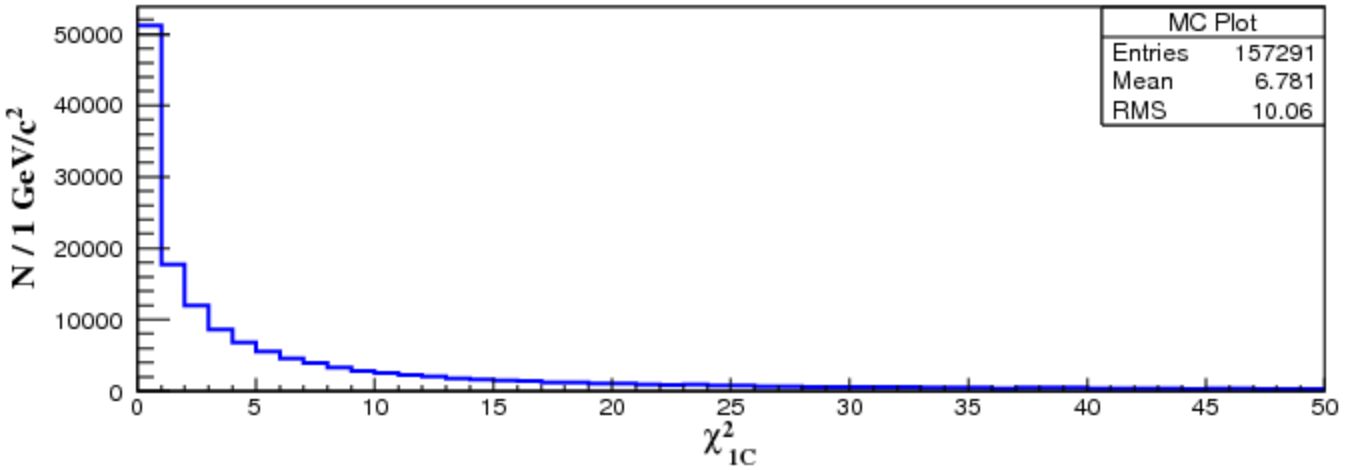

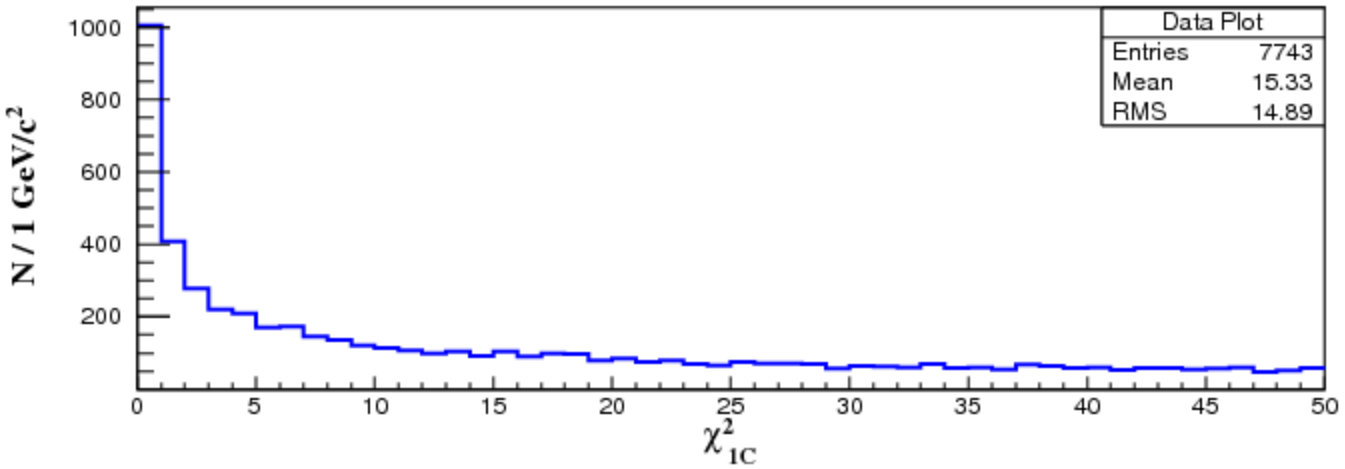

Momentum Distribution after 4C and 1C Kinematic Fit

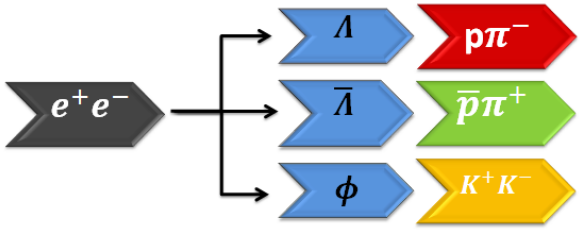

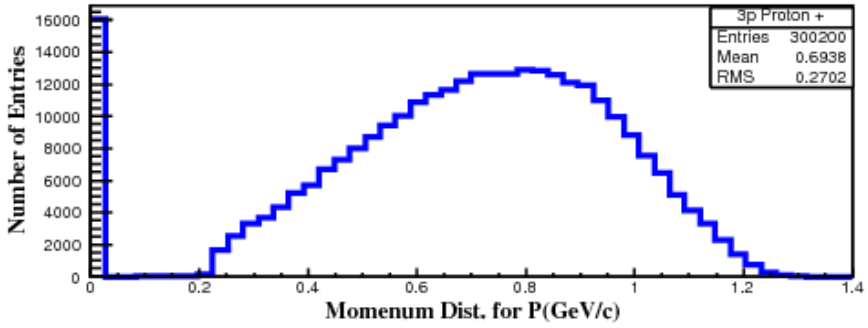

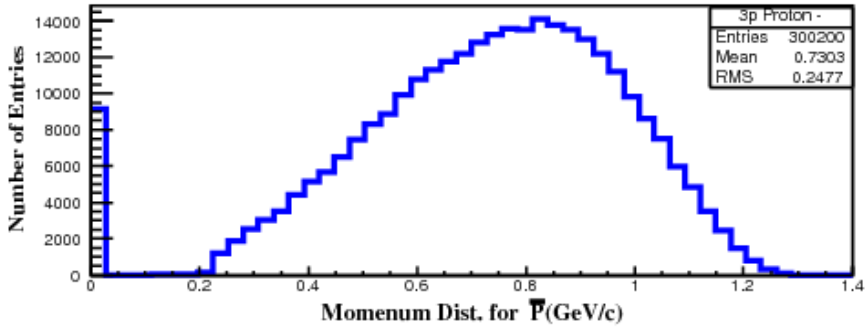

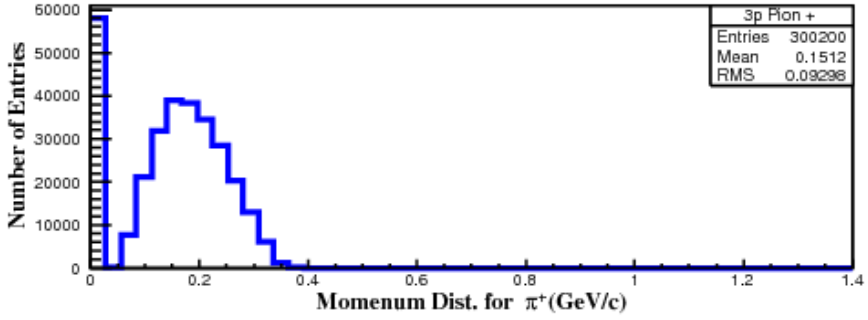

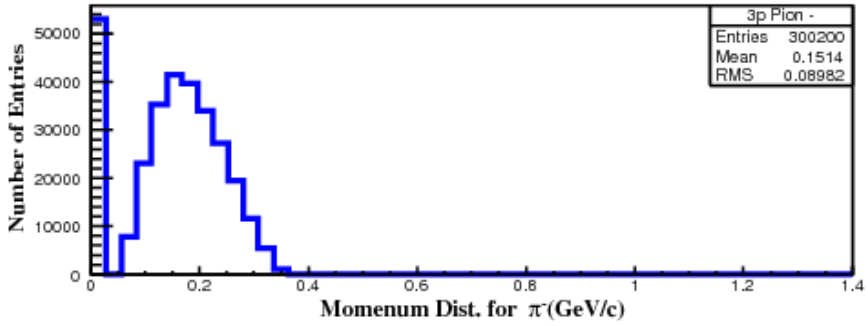

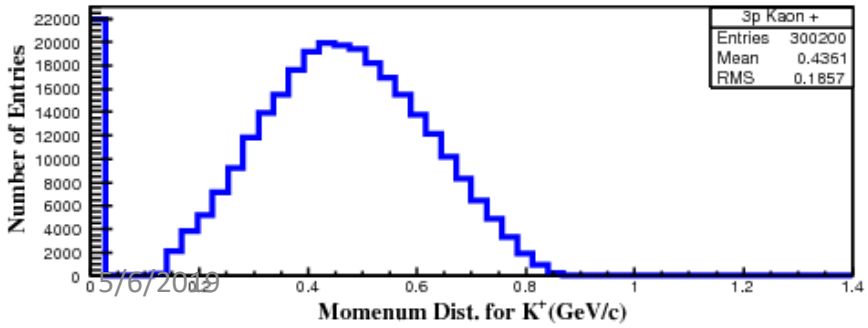

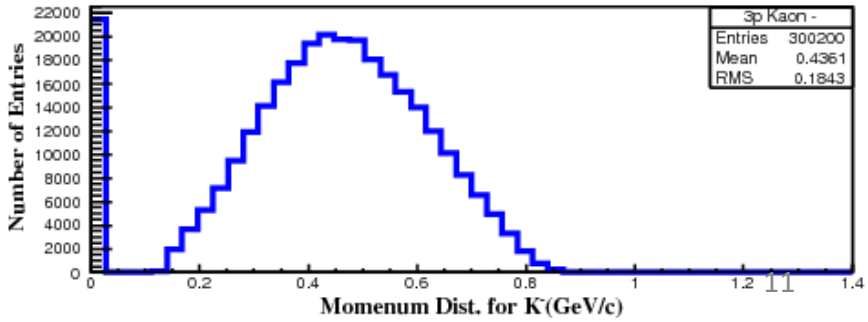

Momentum Distribution after 4C Kinematic Fit

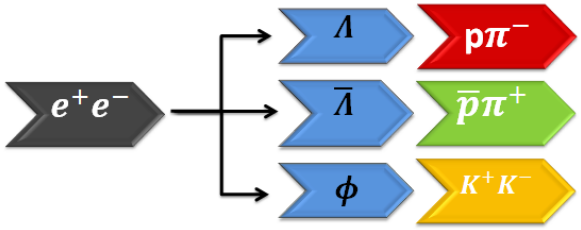

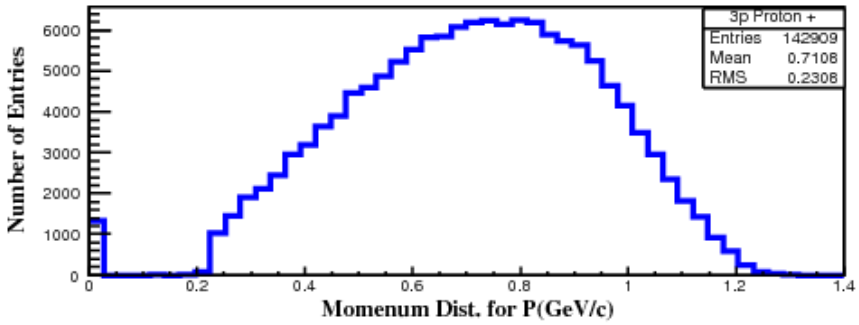

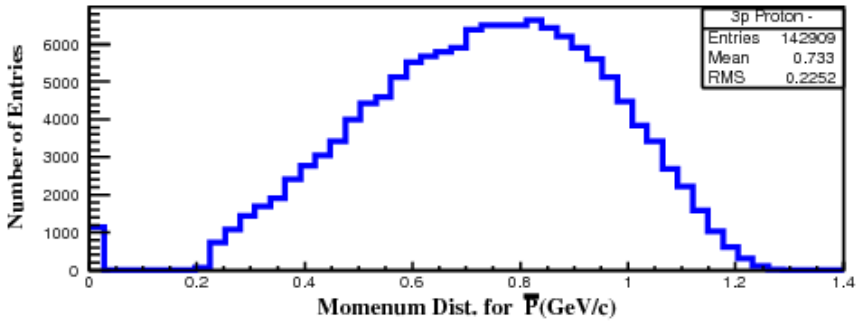

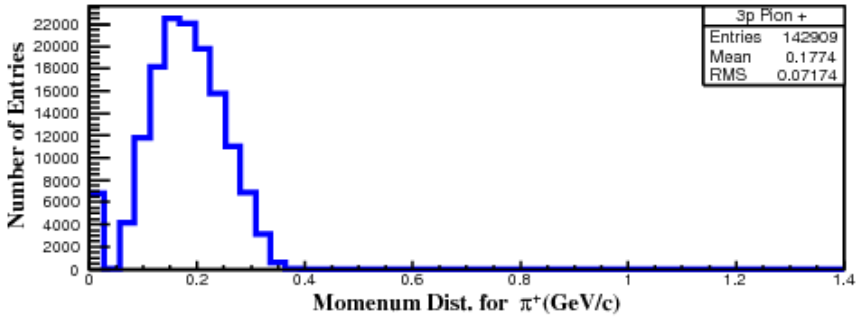

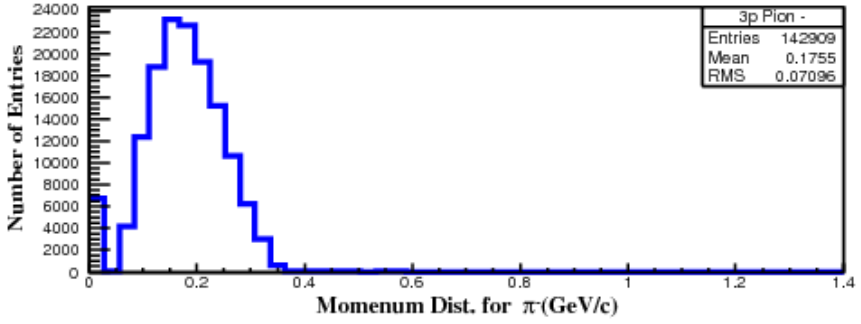

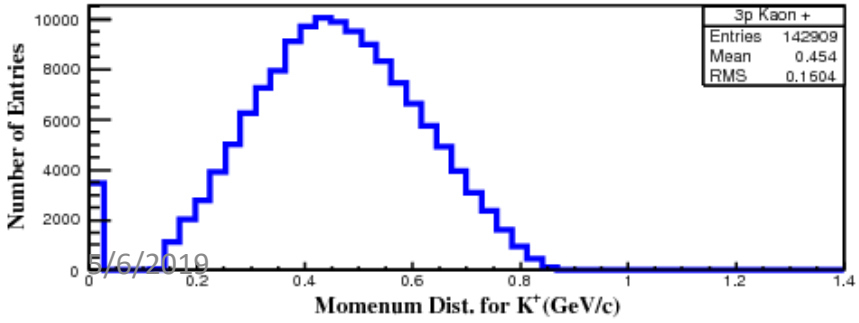

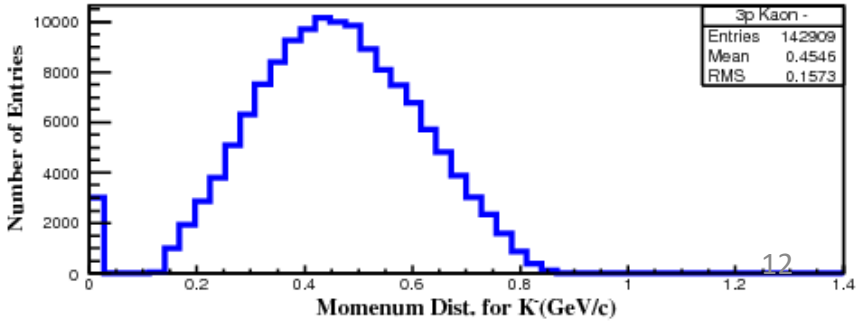

Momentum Distribution after 1C Kinematic Fit

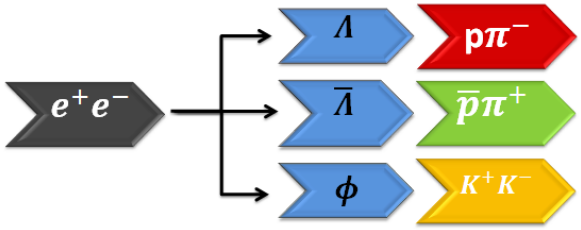

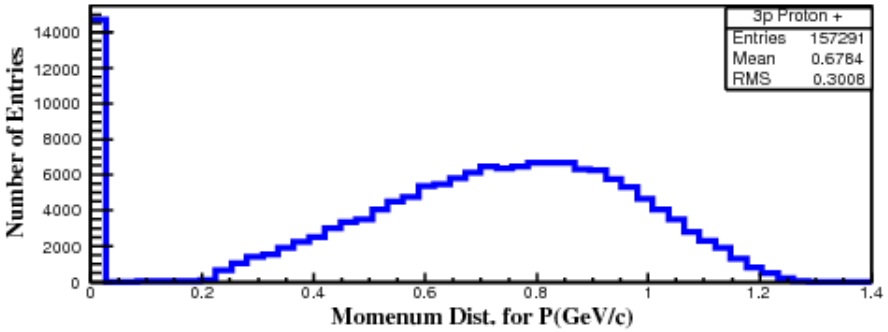

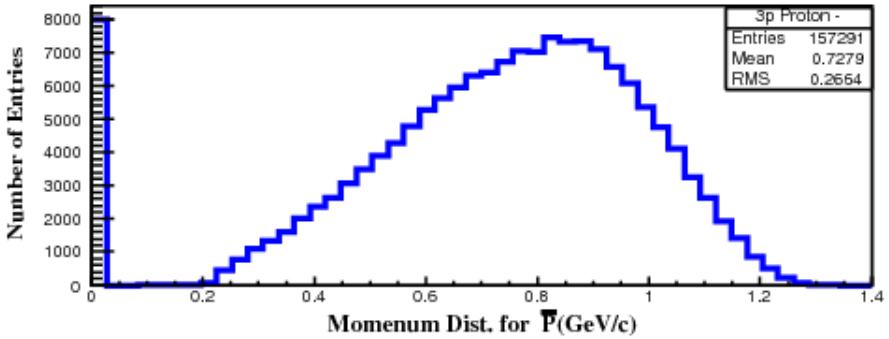

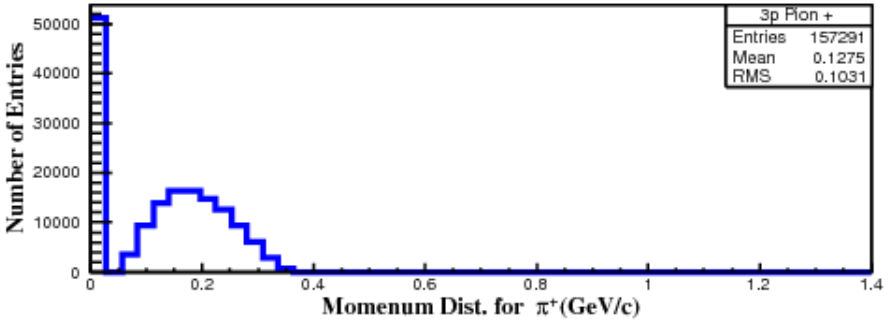

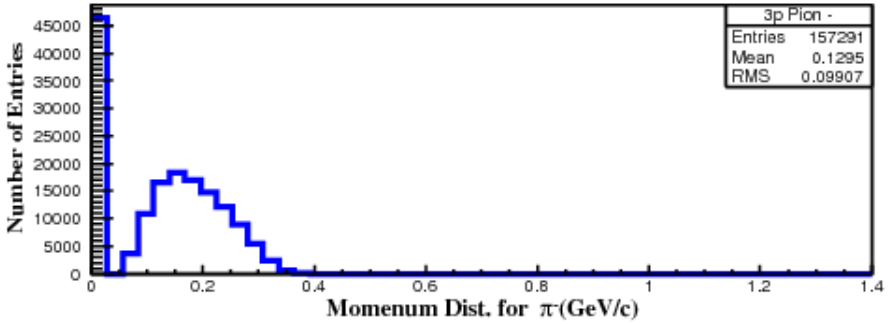

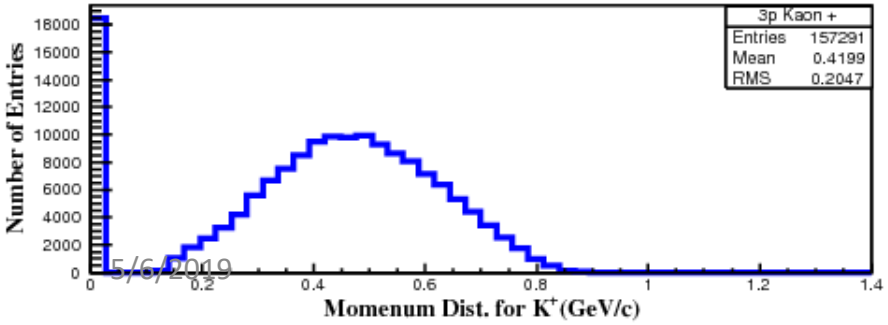

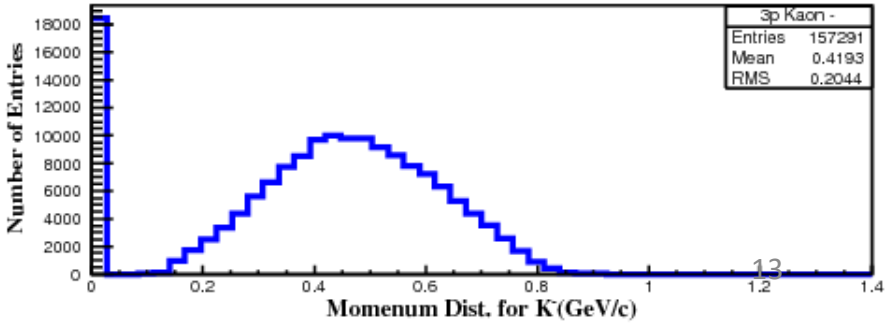

Invariant mass distribution of $p\pi^-$, $\bar{p}\pi^+$ and K^+K^- for (MC and DATA) of 4190 MEV energy after 4C and 1C kinematic fit and without mass, χ^2_{4c} and χ^2_{1c} cuts

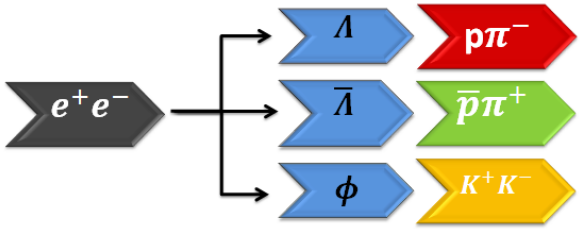

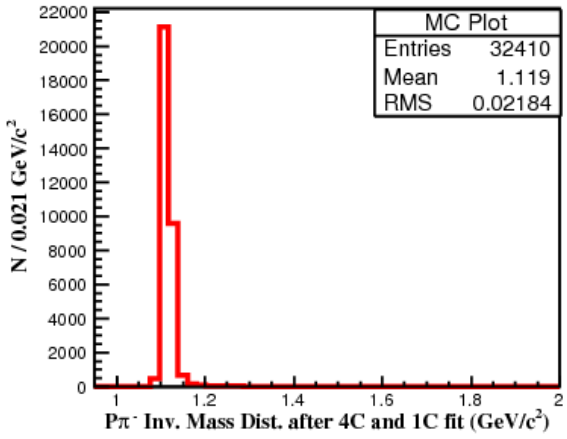

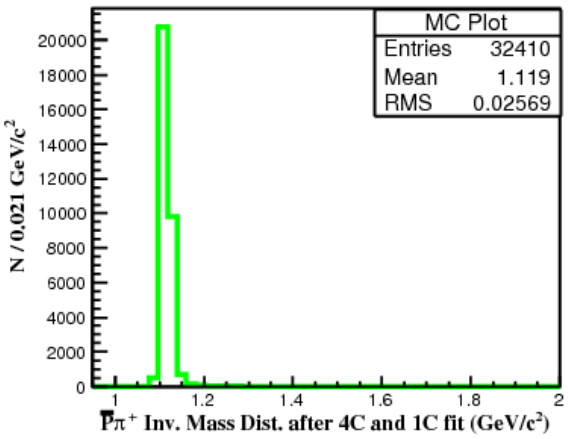

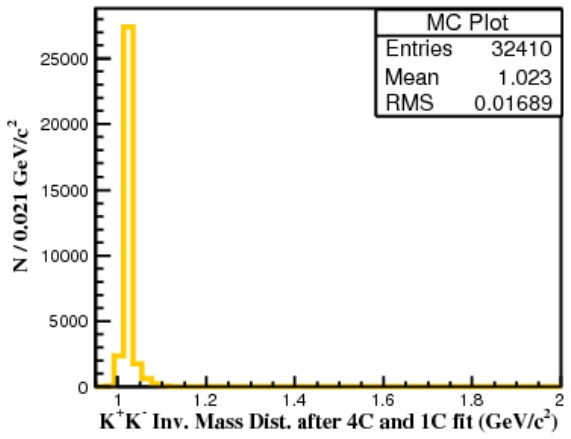

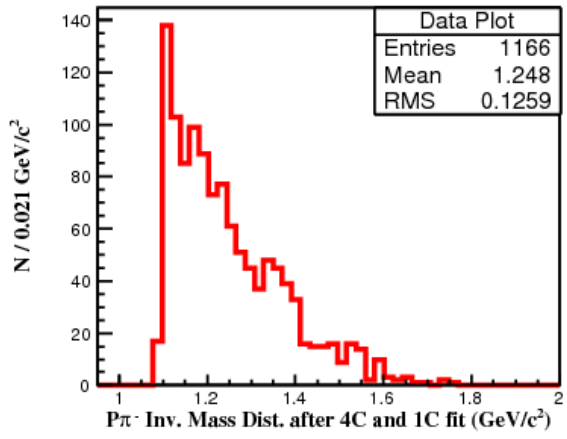

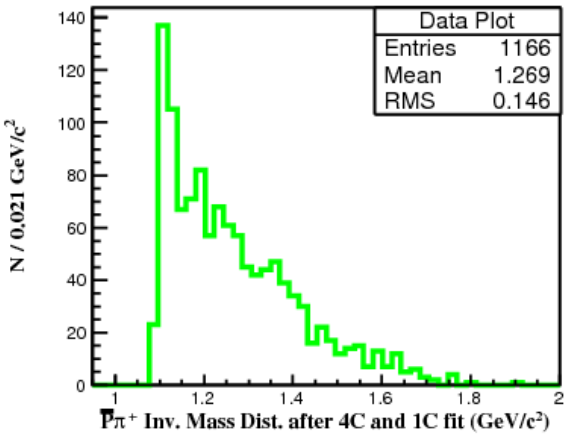

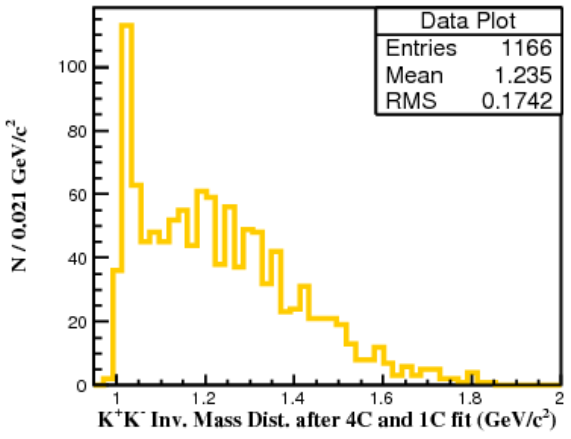

Invariant mass distribution of $p\pi^-$, $\bar{p}\pi^+$ and K^+K^- for (MC and DATA) of 4190 MEV energy after 4C kinematic fit and without mass, χ^2_{4c} and χ^2_{1c} cuts

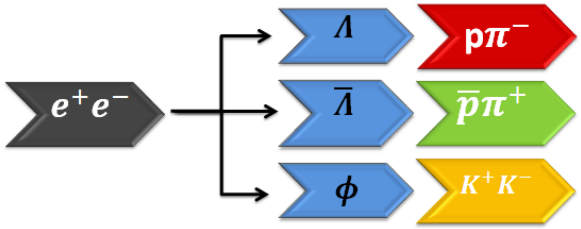

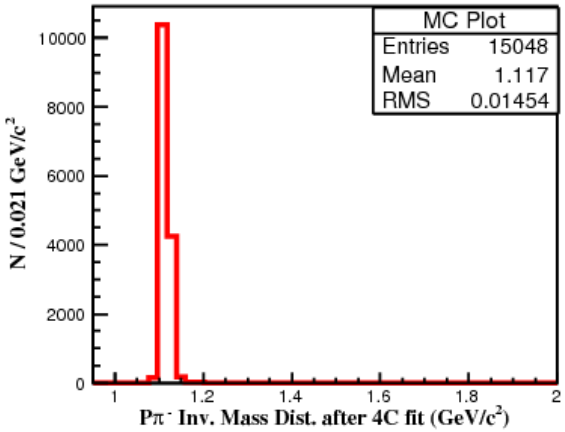

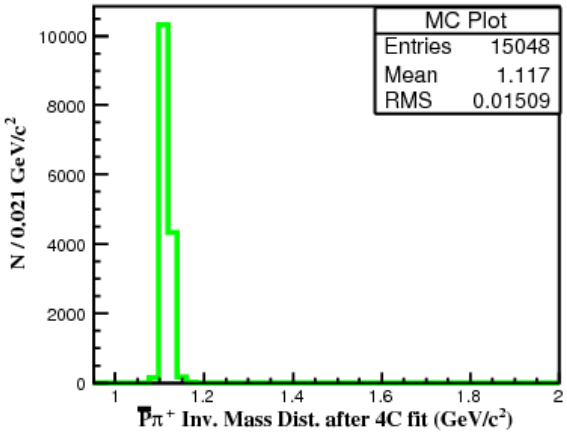

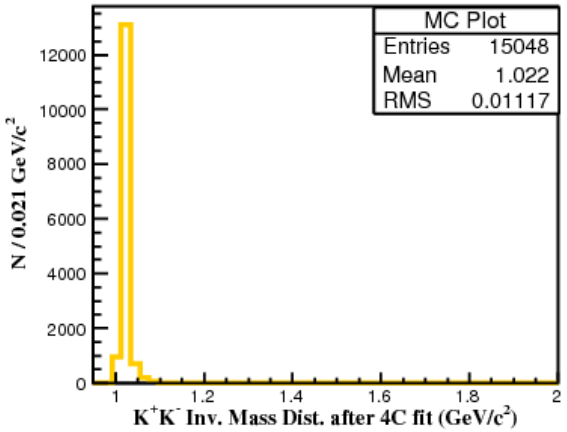

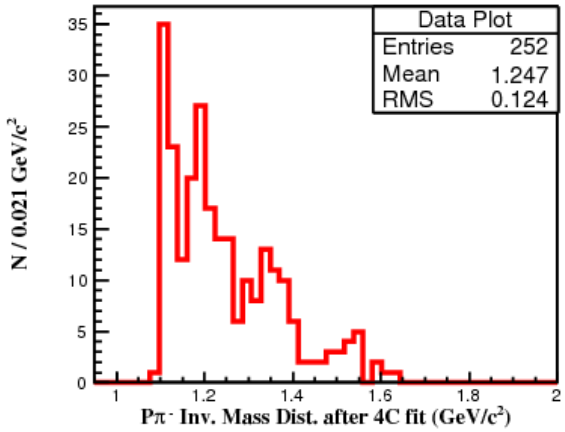

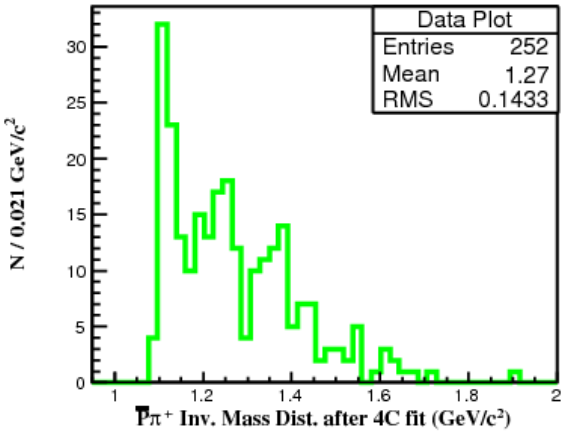

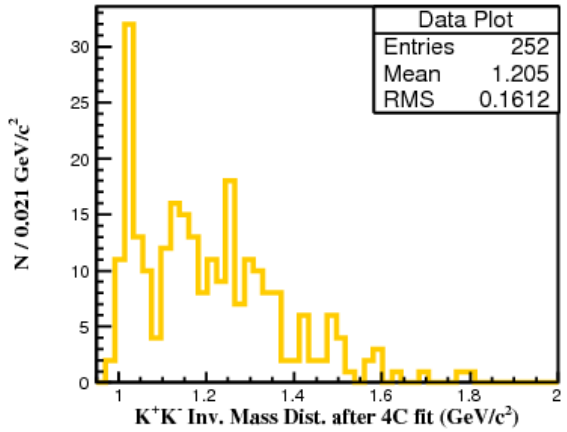

Invariant mass distribution of $p\pi^-$, $\bar{p}\pi^+$ and K^+K^- for (MC and DATA) of 4190 MEV energy after 1C kinematic fit and without mass, χ^2_{4c} and χ^2_{1c} cuts

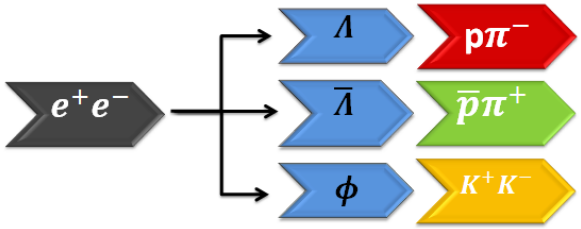

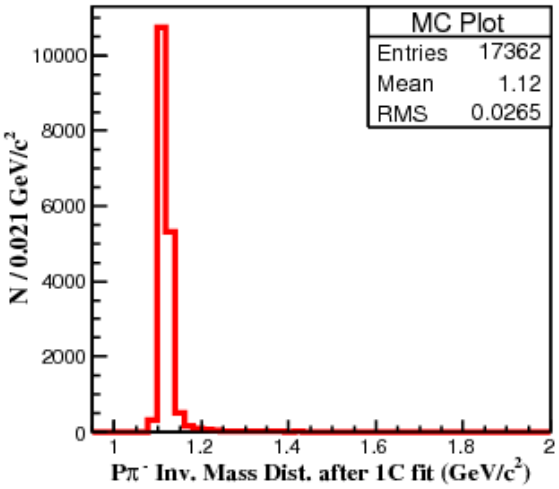

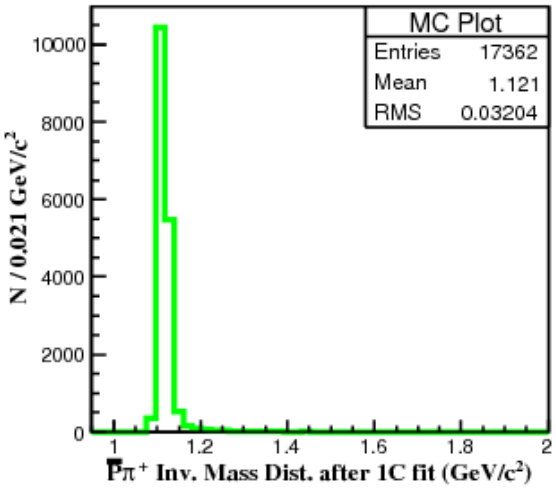

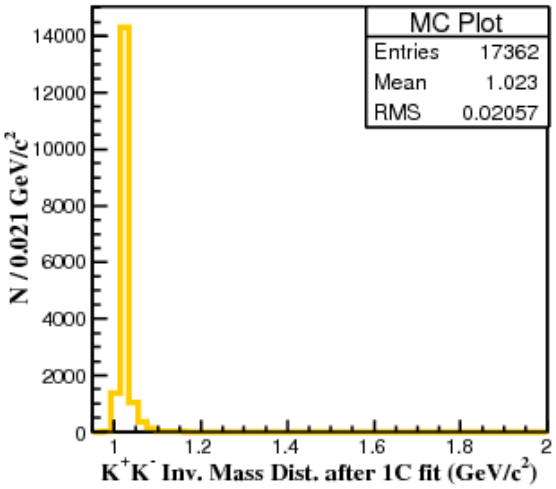

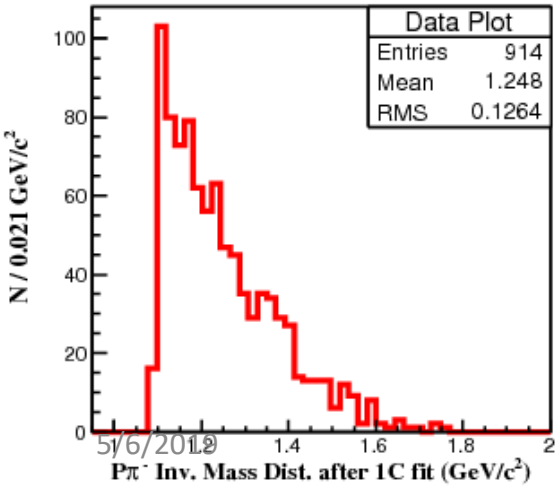

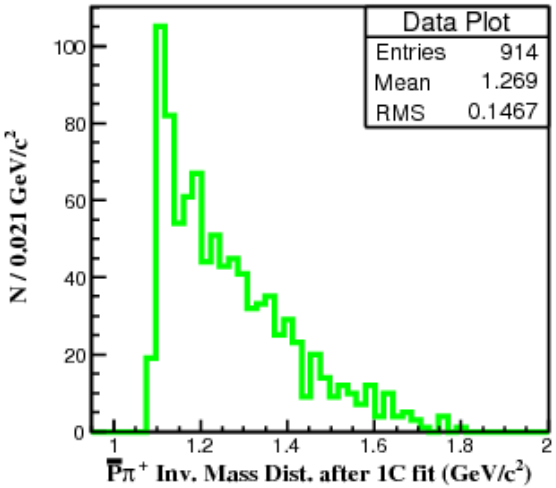

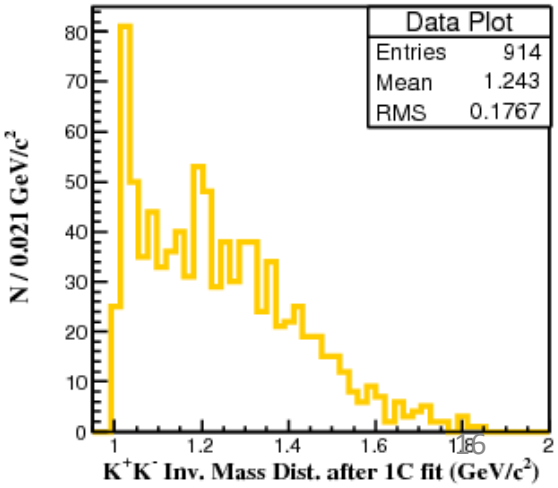

Invariant mass distribution of $p\pi^-$, $\bar{p}\pi^+$ and K^+K^- for (MC and DATA) of 4200 MEV energy after 4C and 1C kinematic fit and without mass, χ^2_{4c} and χ^2_{1c} cuts

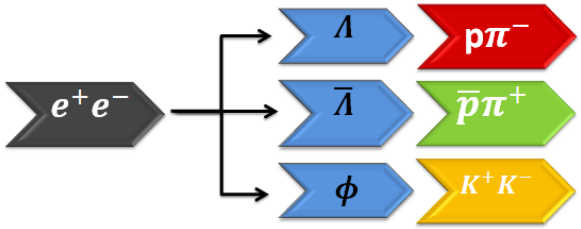

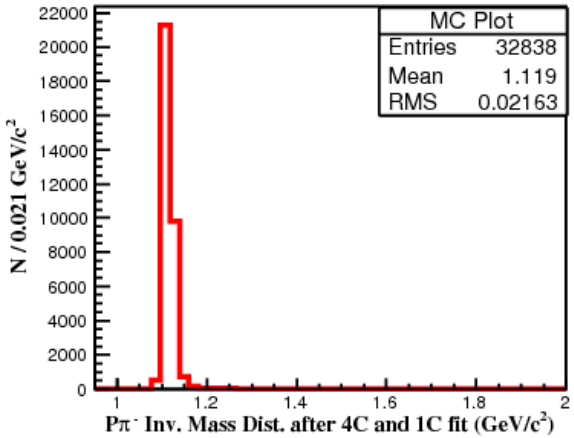

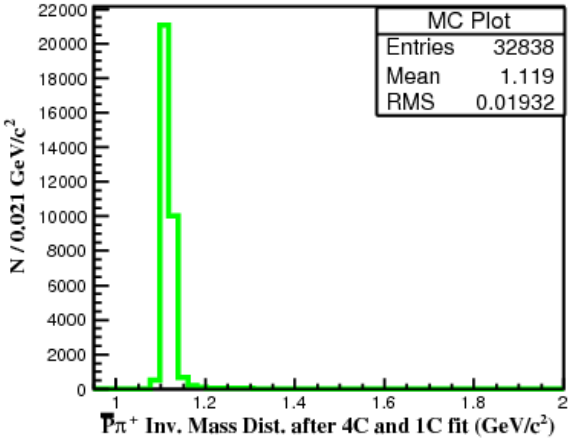

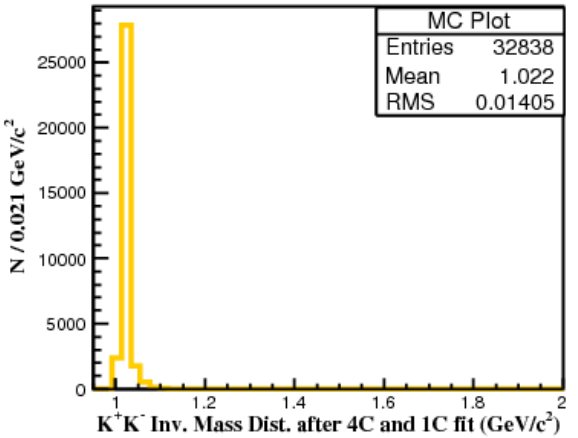

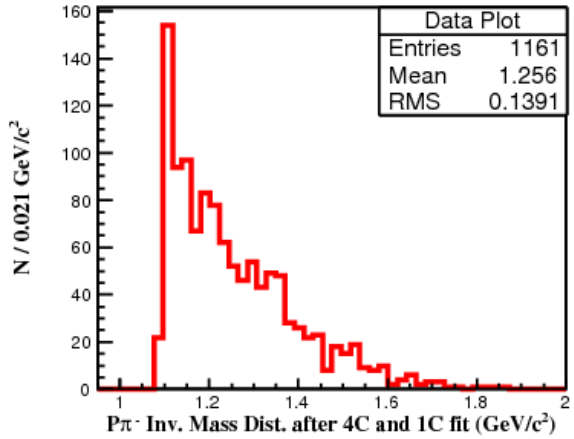

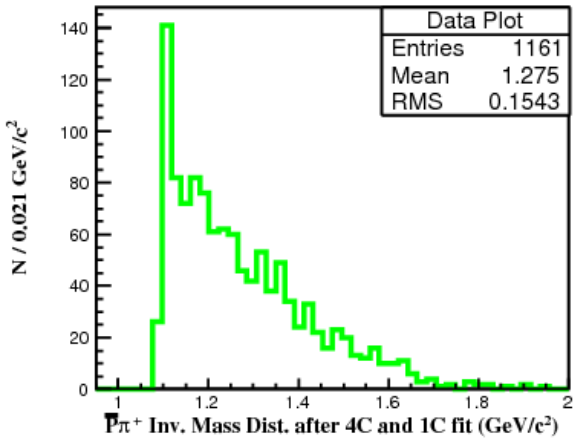

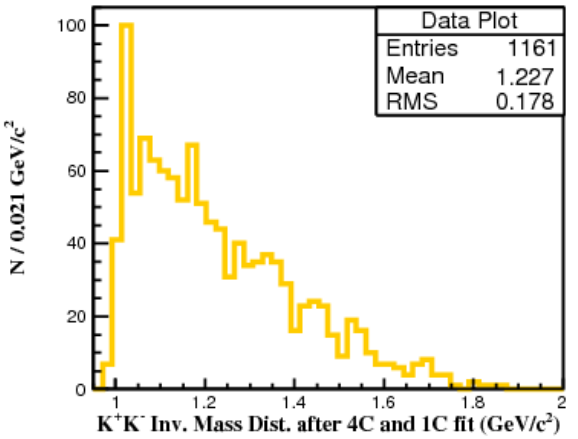

Invariant mass distribution of $p\pi^-$, $\bar{p}\pi^+$ and K^+K^- for (MC and DATA) of 4200 MEV energy after 4C kinematic fit and without mass, χ^2_{4c} and χ^2_{1c} cuts

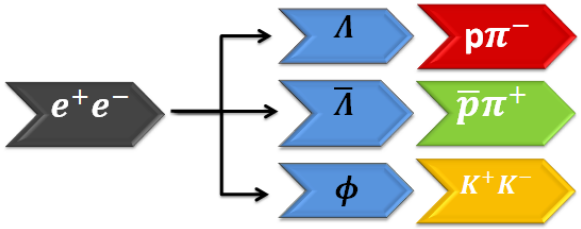

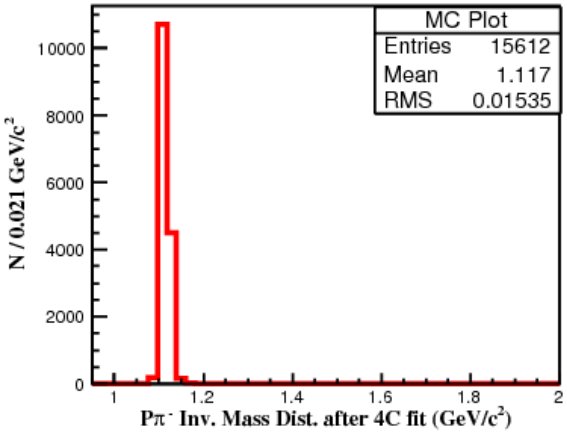

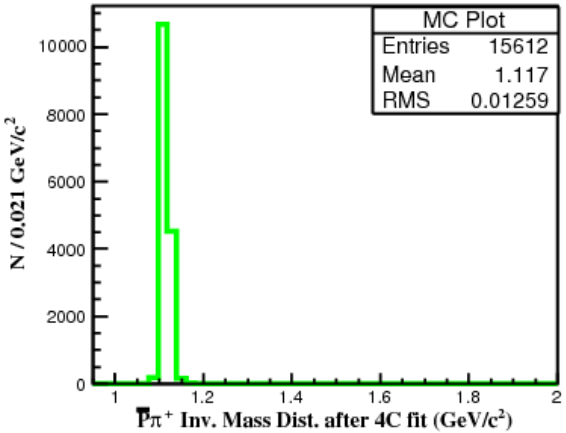

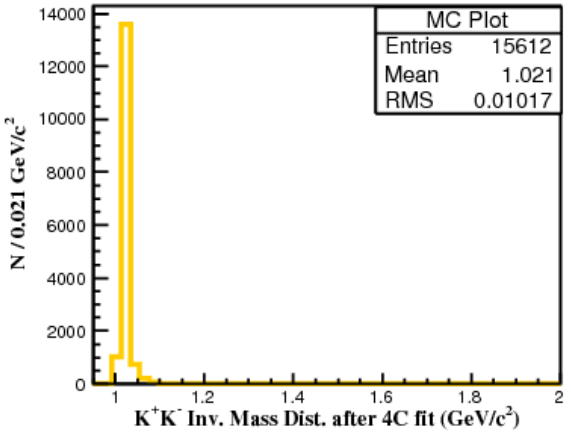

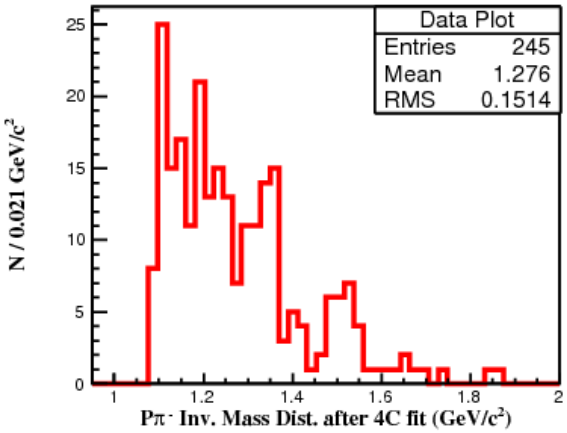

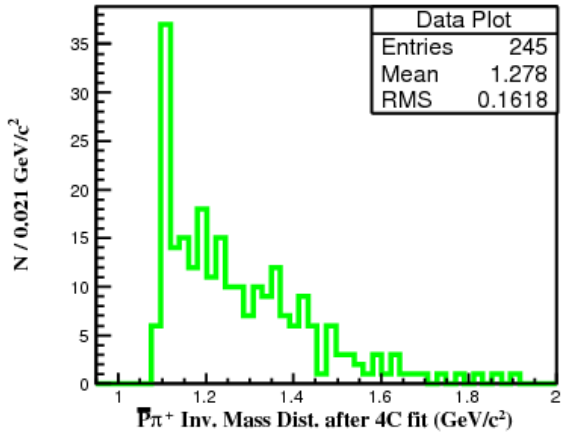

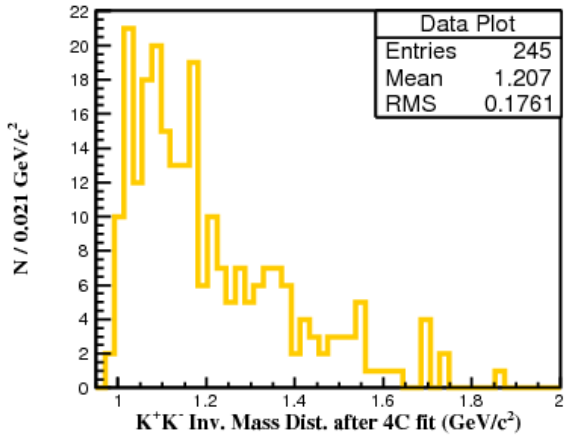

Invariant mass distribution of $p\pi^-$, $\bar{p}\pi^+$ and K^+K^- for (MC and DATA) of 4200 MEV energy after 1C kinematic fit and without mass, χ^2_{4c} and χ^2_{1c} cuts

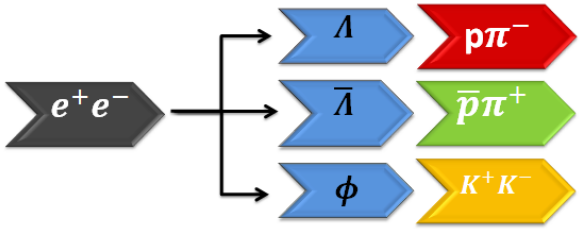

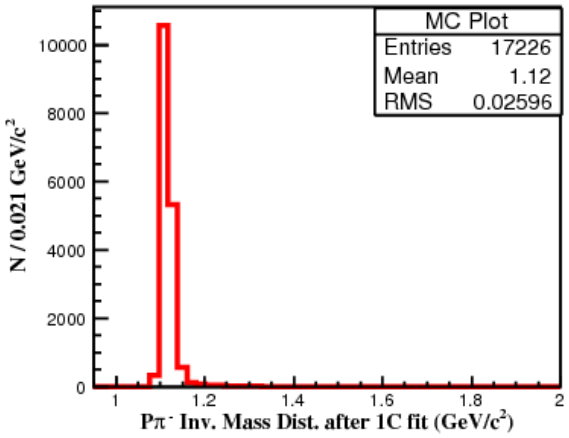

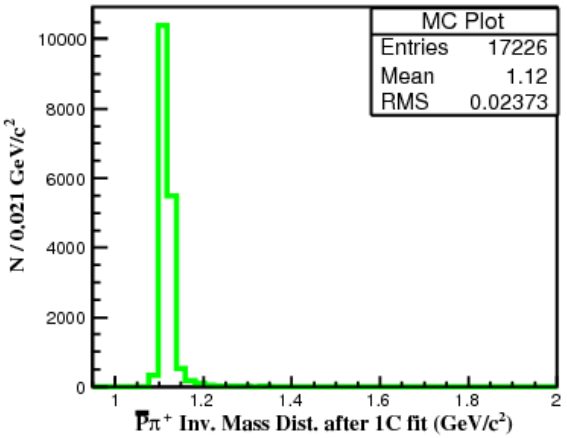

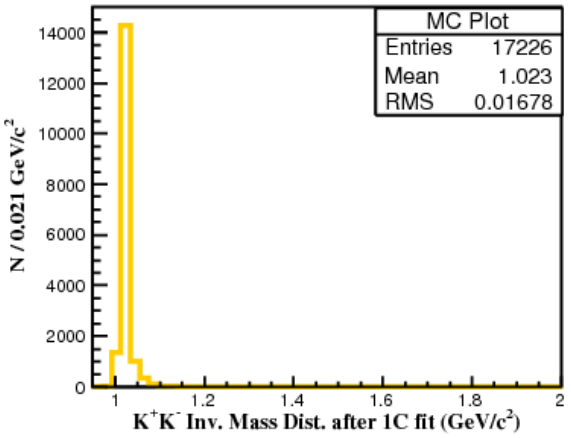

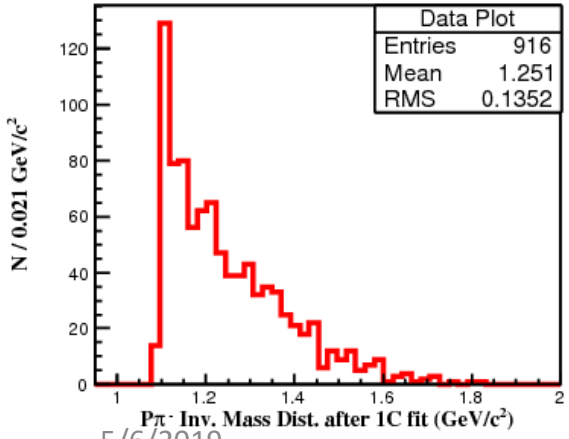

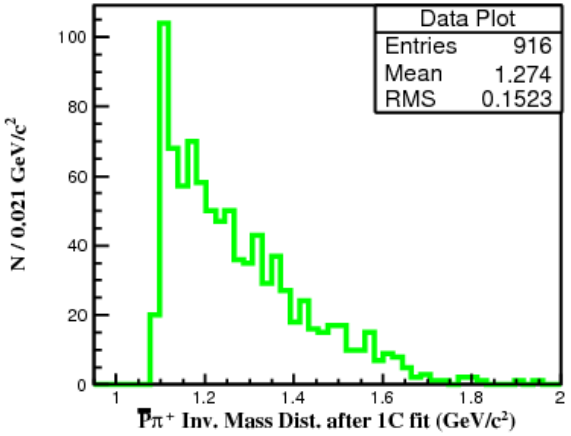

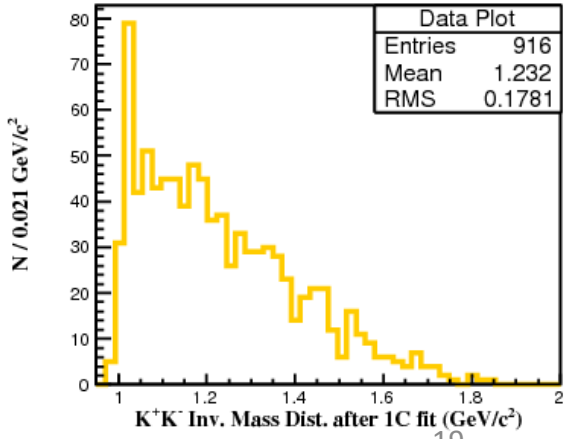

Invariant mass distribution of $p\pi^-$, $\bar{p}\pi^+$ and K^+K^- for (MC and DATA) of 4210 MEV energy after 4C and 1C kinematic fit and without mass, χ^2_{4c} and χ^2_{1c} cuts

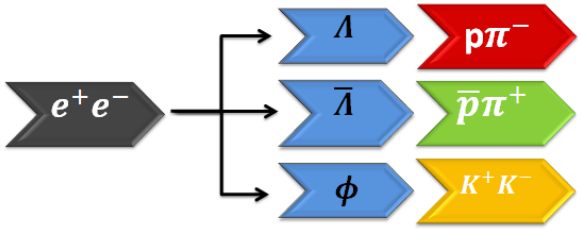

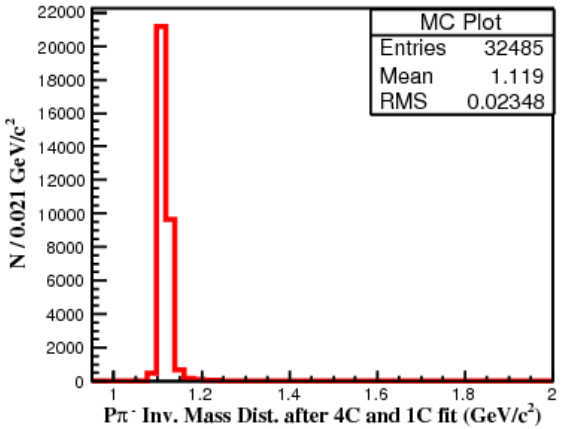

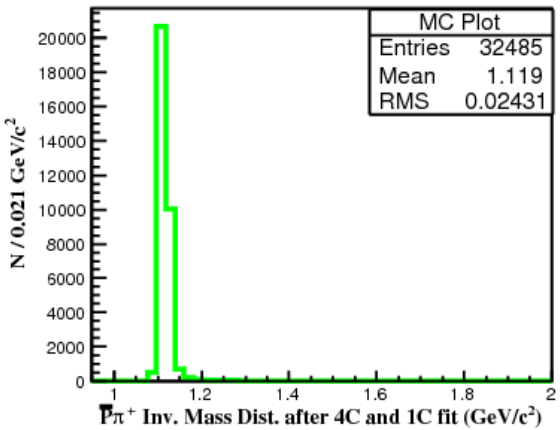

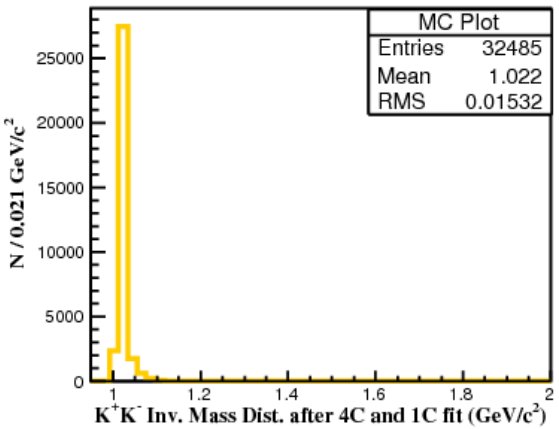

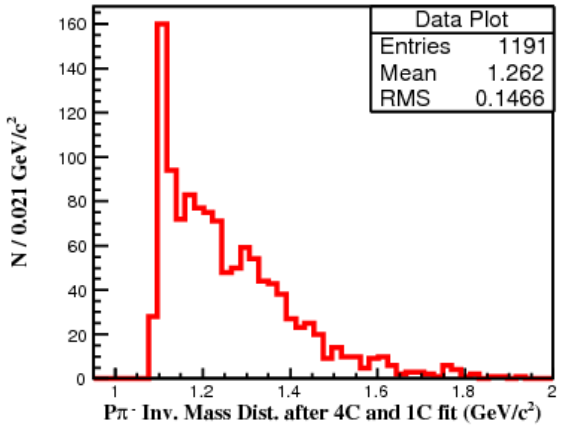

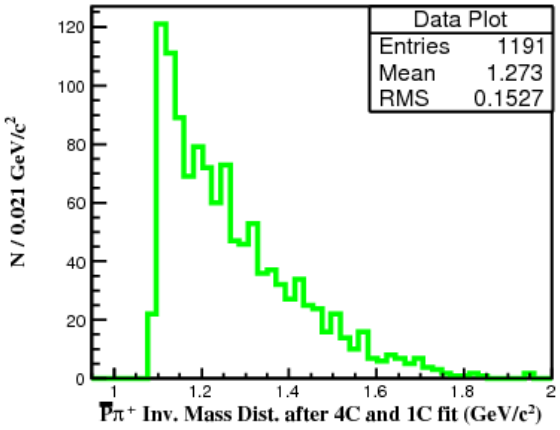

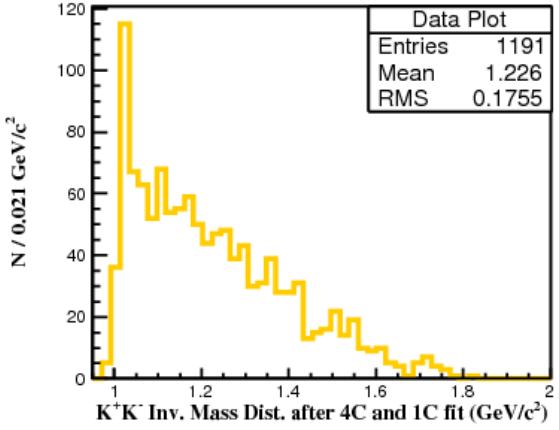

Invariant mass distribution of $p\pi^-$, $\bar{p}\pi^+$ and K^+K^- for (MC and DATA) of 4210 MEV energy after 4C kinematic fit and without mass, χ^2_{4c} and χ^2_{1c} cuts

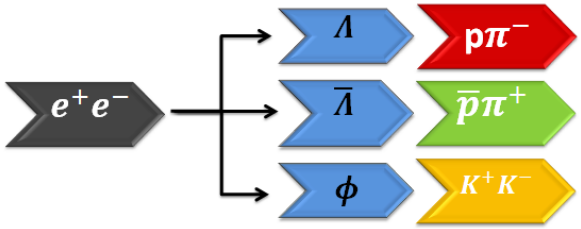

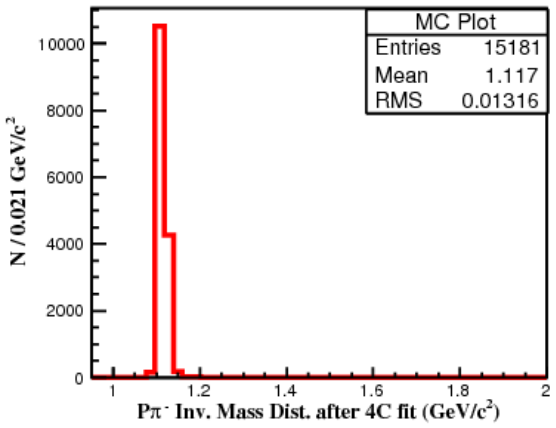

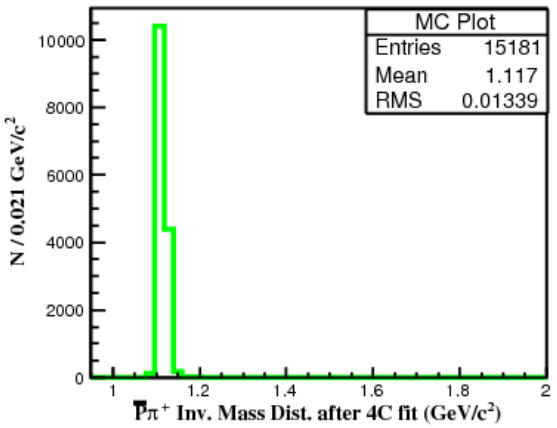

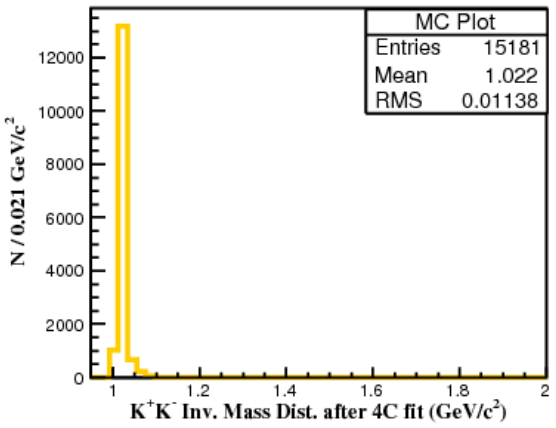

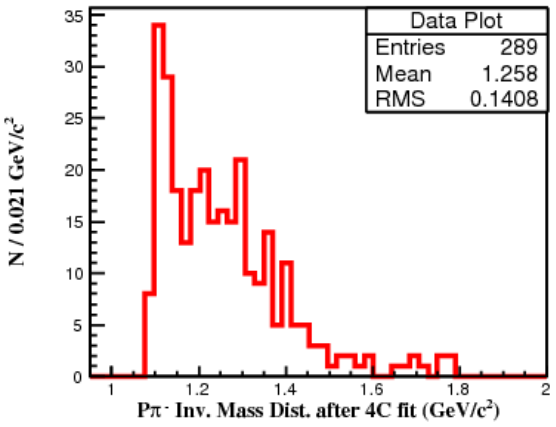

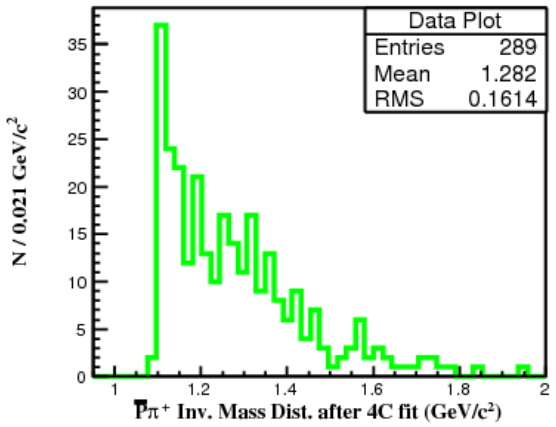

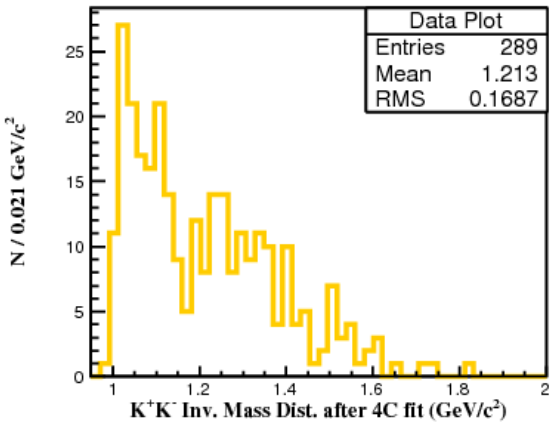

Invariant mass distribution of $p\pi^-$, $\bar{p}\pi^+$ and K^+K^- for (MC and DATA) of 4210 MEV energy after 1C kinematic fit and without mass, χ^2_{4c} and χ^2_{1c} cuts

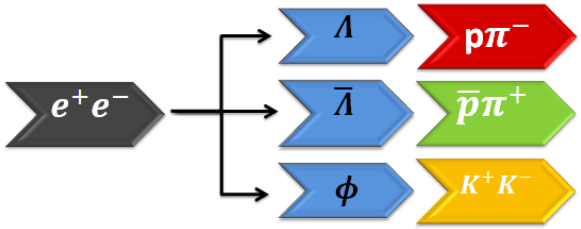

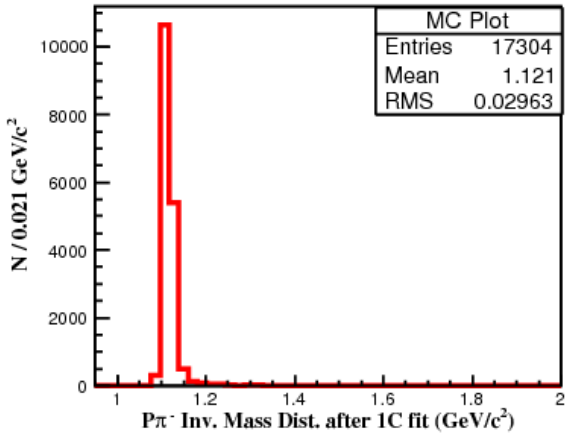

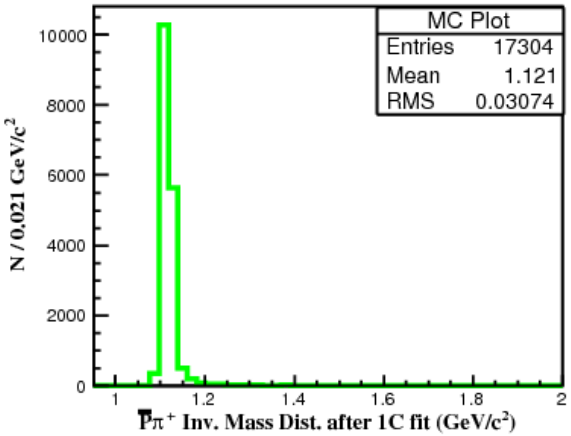

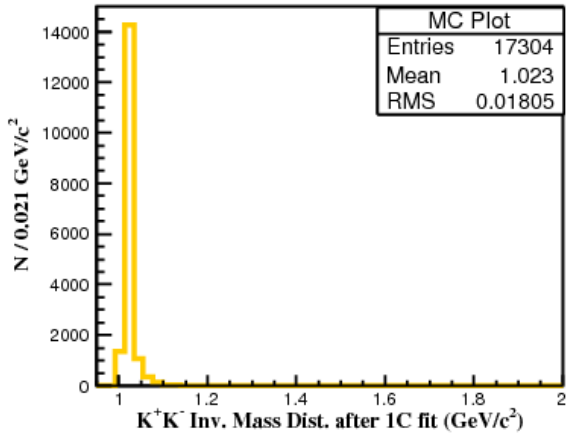

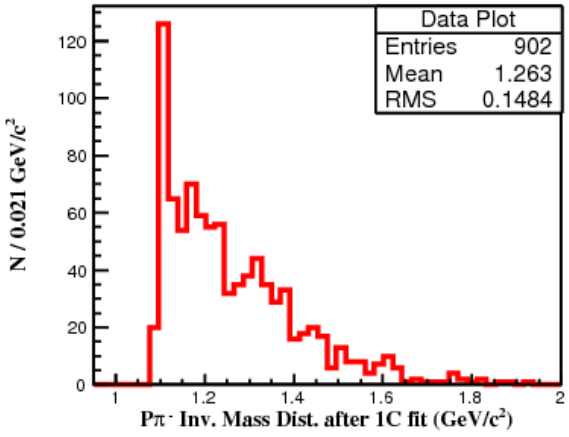

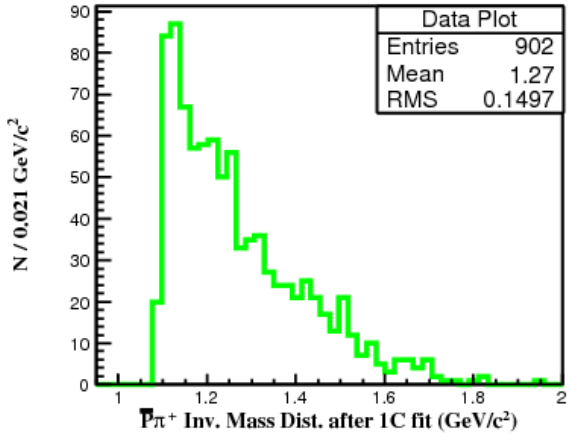

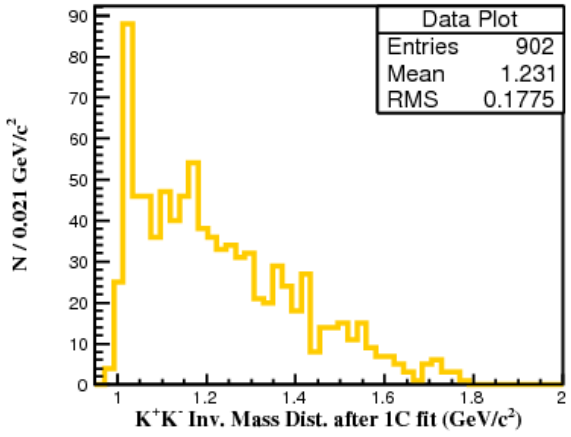

Invariant mass distribution of $p\pi^-$, $\bar{p}\pi^+$ and K^+K^- for (MC and DATA) of 4220 MEV energy after 4C and 1C kinematic fit and without mass, χ^2_{4c} and χ^2_{1c} cuts

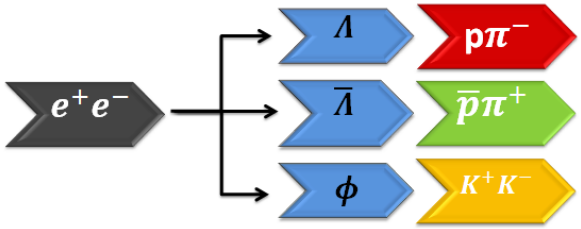

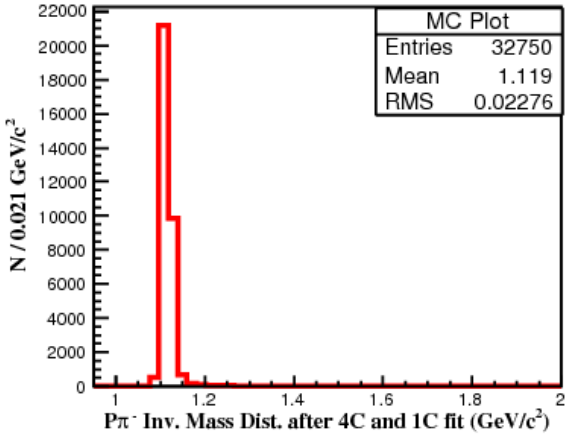

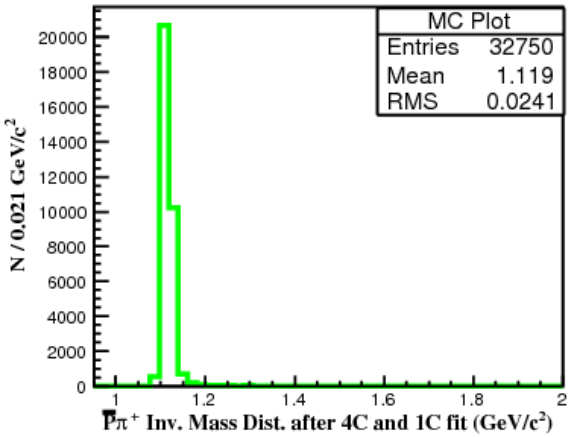

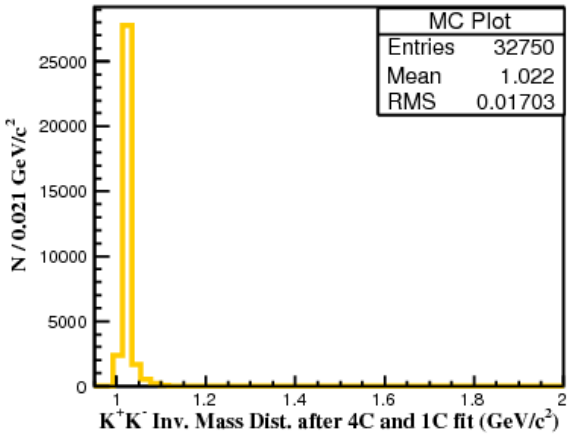

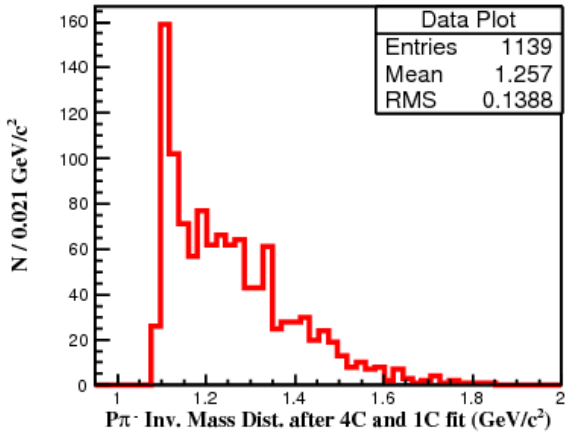

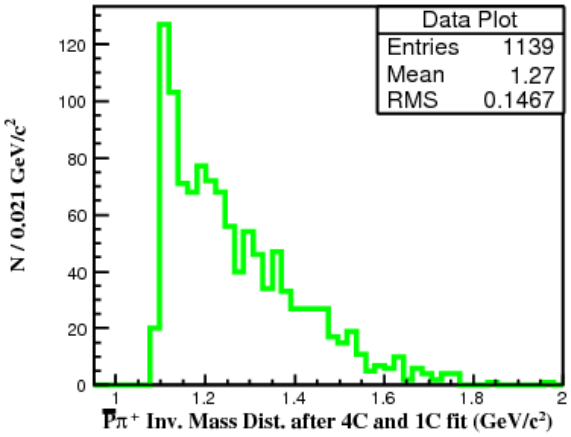

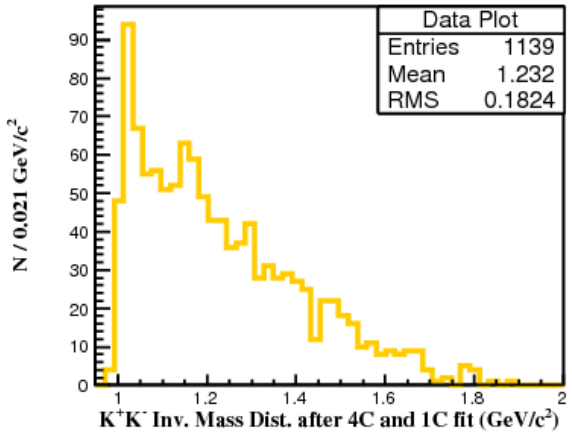

Invariant mass distribution of $p\pi^-$, $\bar{p}\pi^+$ and K^+K^- for (MC and DATA) of 4220 MEV energy after 4C kinematic fit and without mass, χ^2_{4c} and χ^2_{1c} cuts

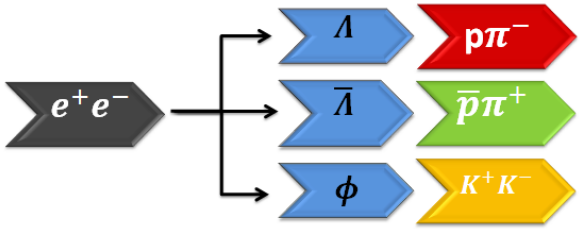

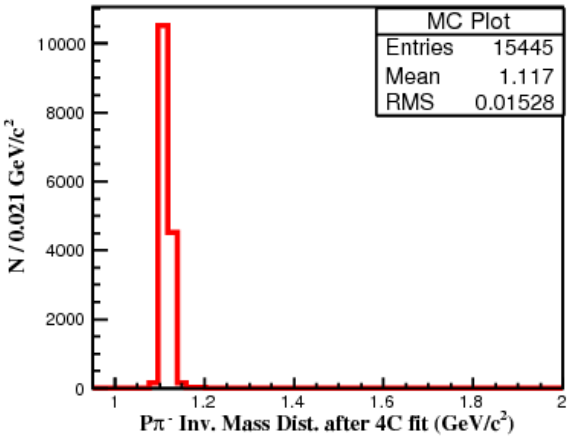

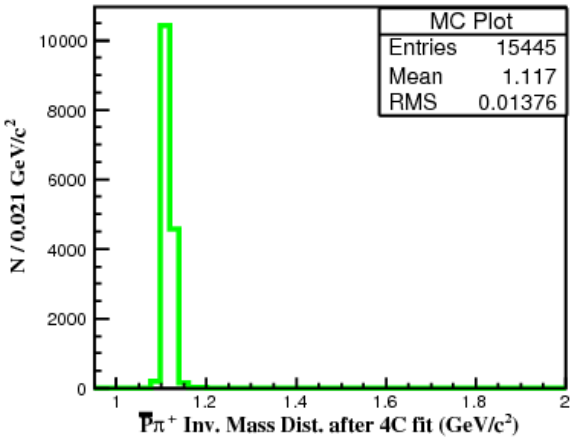

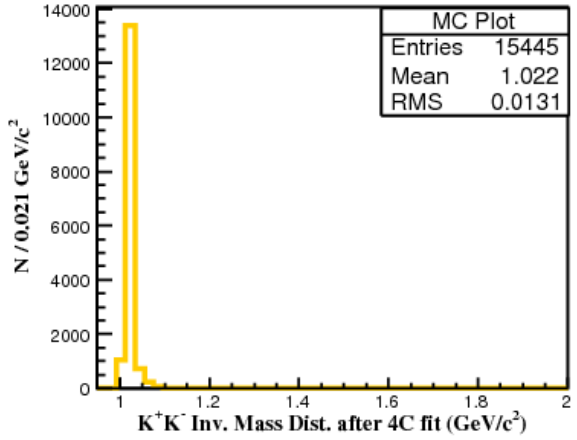

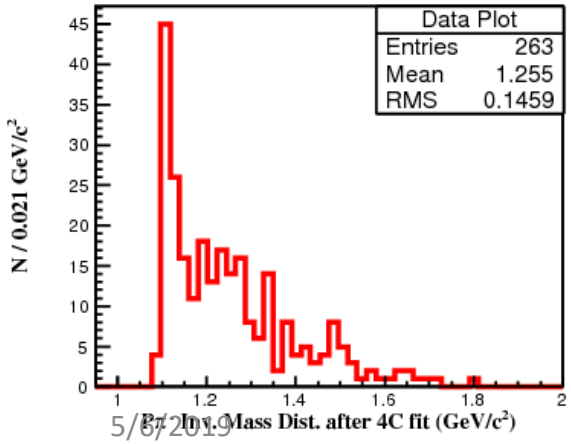

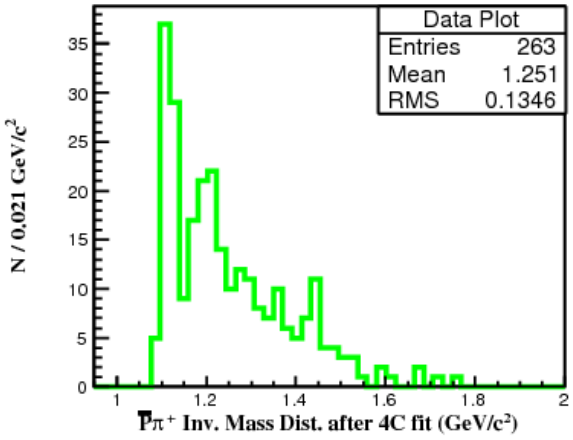

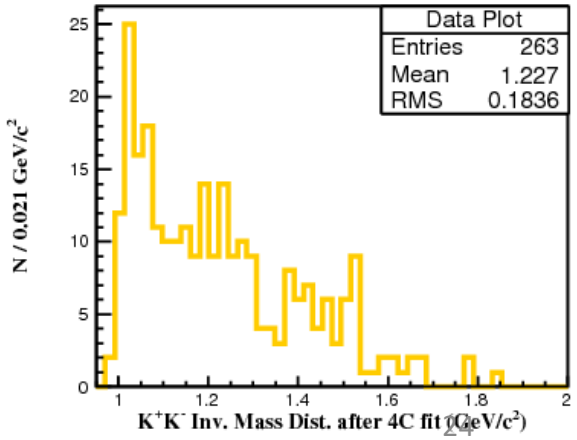

Invariant mass distribution of $p\pi^-$, $\bar{p}\pi^+$ and K^+K^- for (MC and DATA) of 4220 MEV energy after 1C kinematic fit and without mass, χ^2_{4c} and χ^2_{1c} cuts

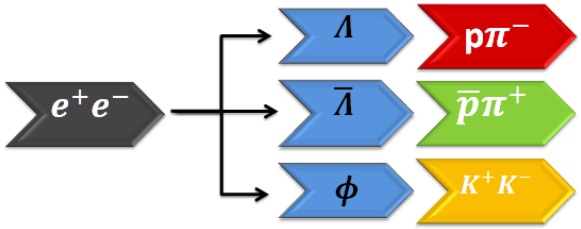

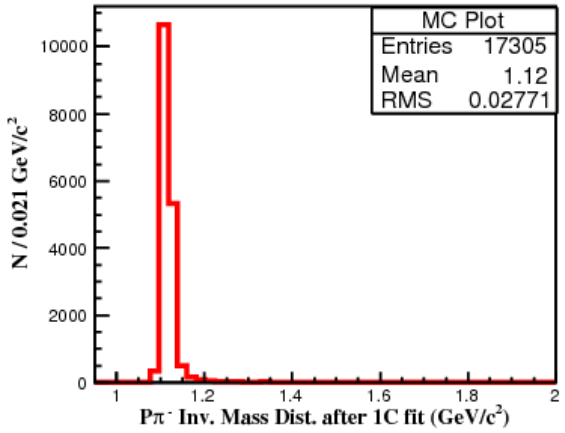

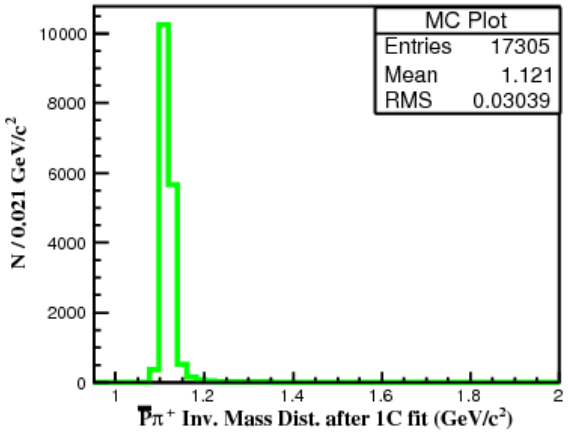

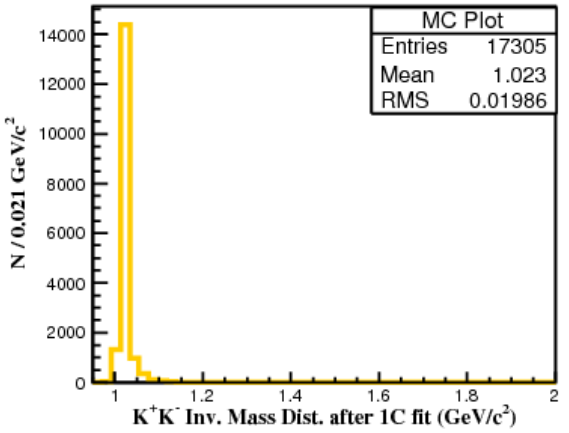

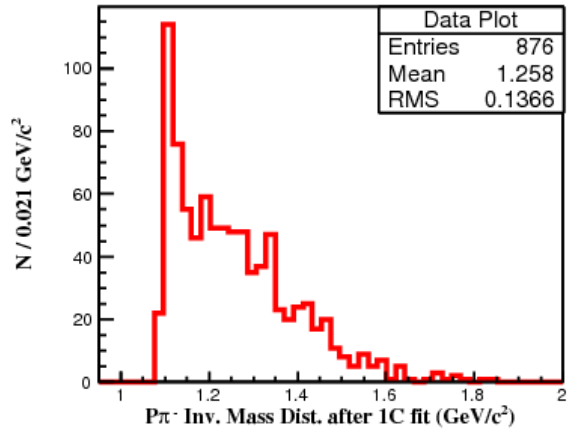

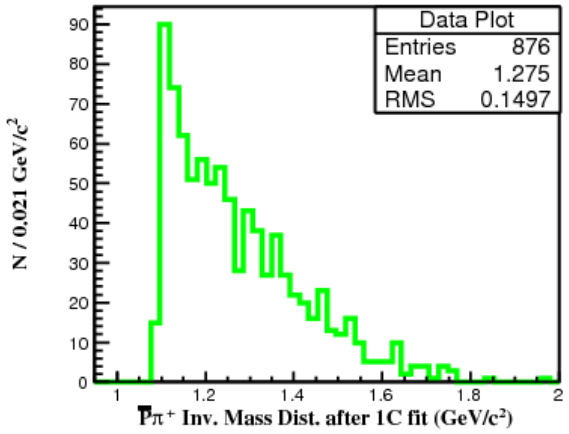

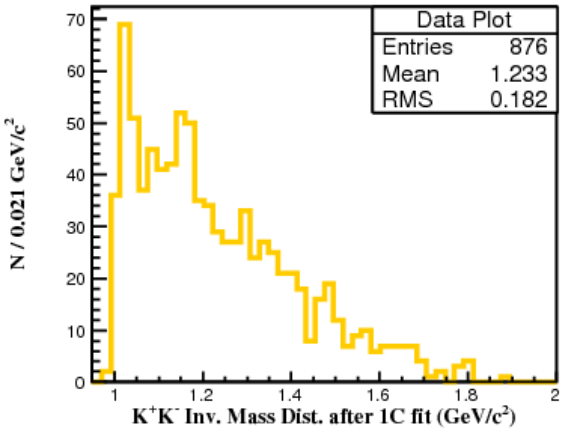

Invariant mass distribution of $p\pi^-$, $\bar{p}\pi^+$ and K^+K^- for (MC and DATA) of 4237 MEV energy after 4C and 1C kinematic fit and without mass, χ^2_{4c} and χ^2_{1c} cuts

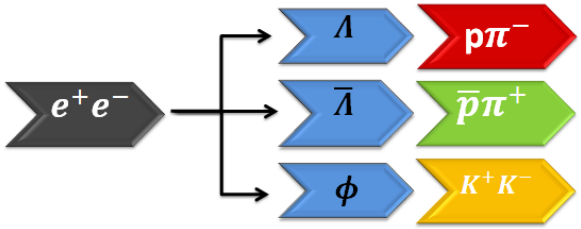

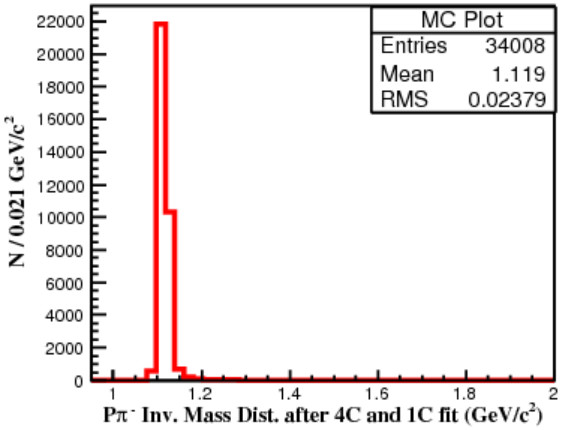

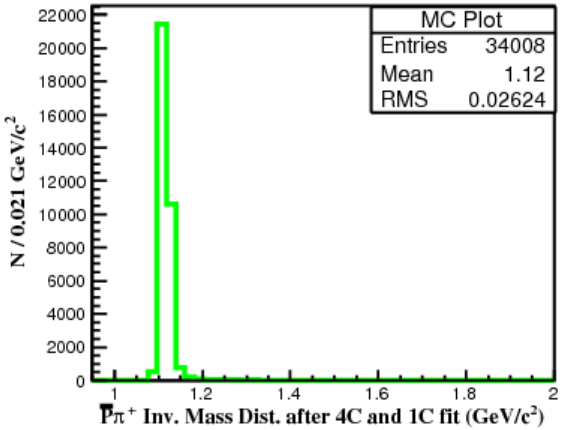

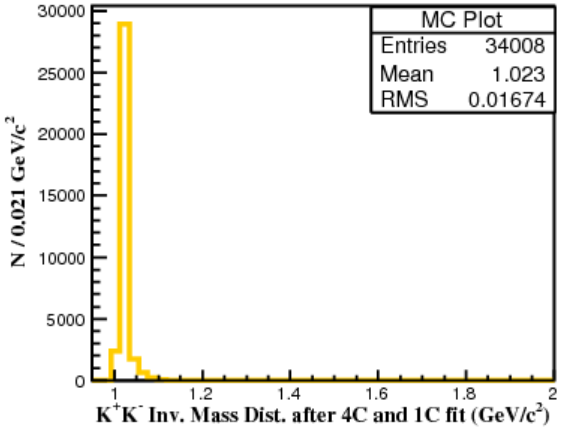

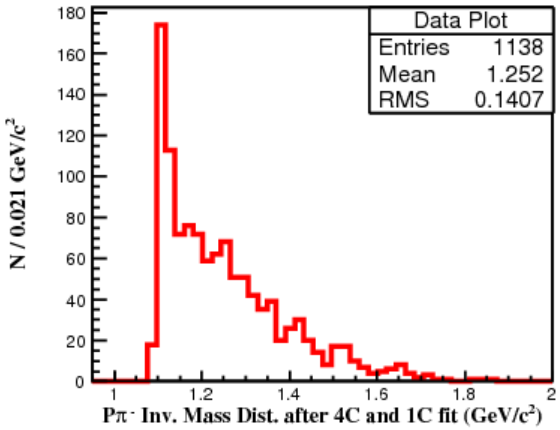

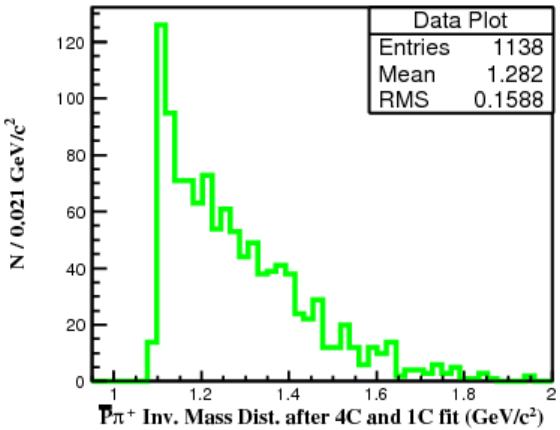

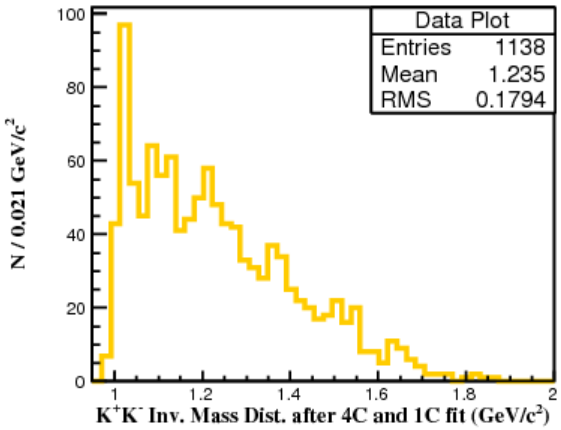

Invariant mass distribution of $p\pi^-$, $\bar{p}\pi^+$ and K^+K^- for (MC and DATA) of 4237 MEV energy after 4C kinematic fit and without mass, χ^2_{4c} and χ^2_{1c} cuts

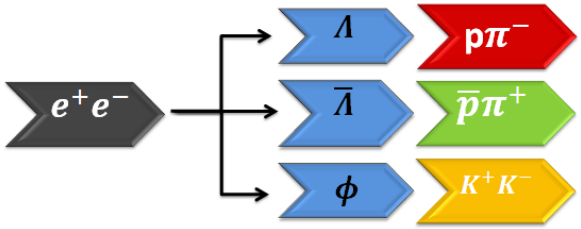

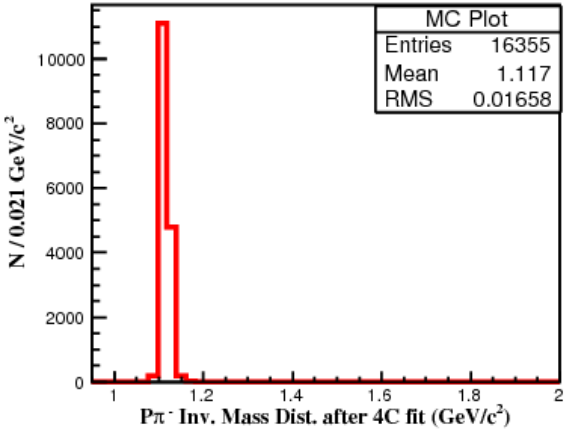

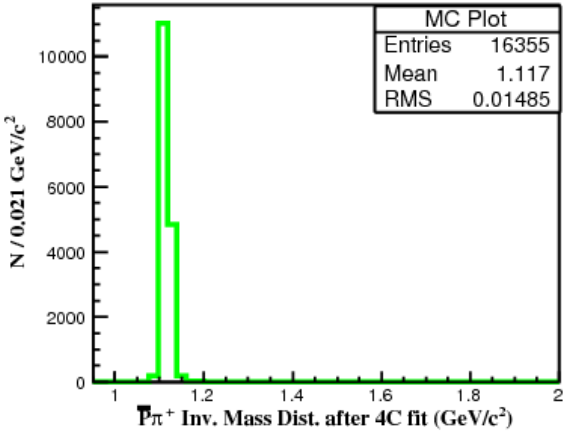

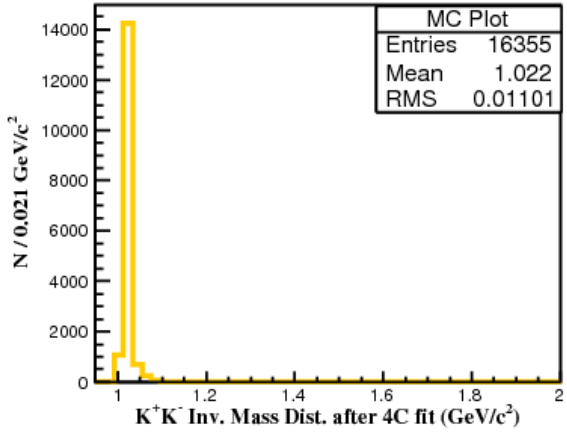

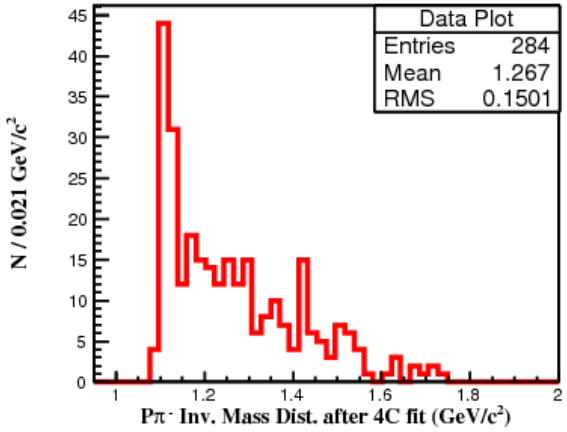

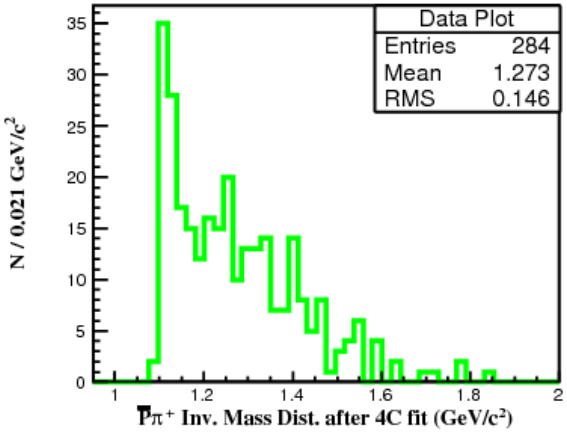

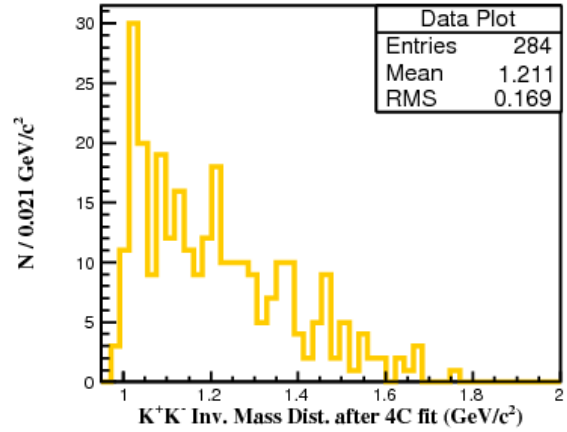

Invariant mass distribution of $p\pi^-$, $\bar{p}\pi^+$ and K^+K^- for (MC and DATA) of 4237 MEV energy after 1C kinematic fit and without mass, χ^2_{4c} and χ^2_{1c} cuts

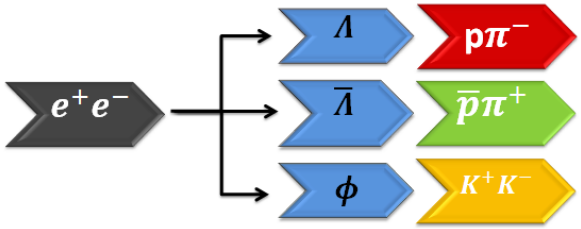

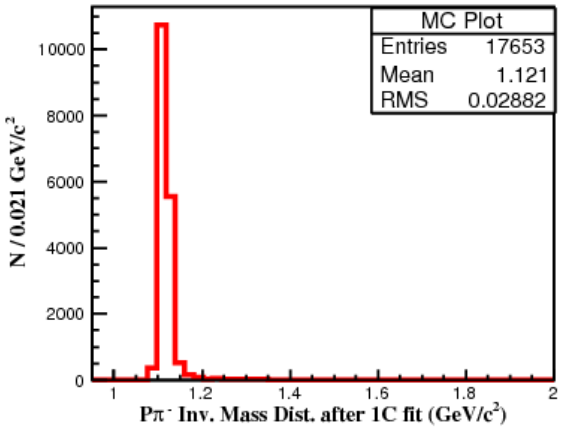

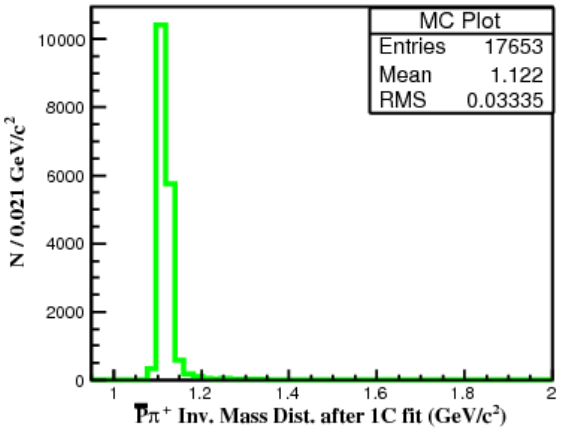

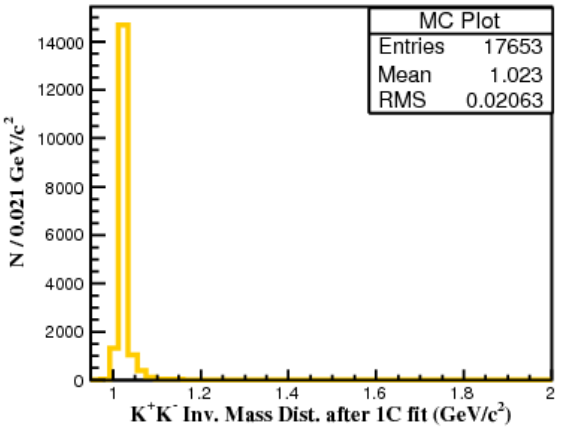

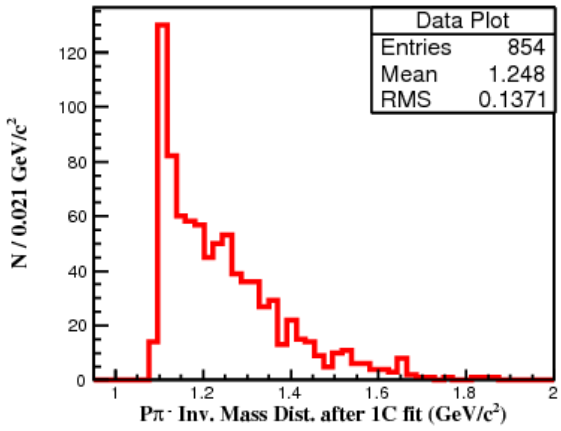

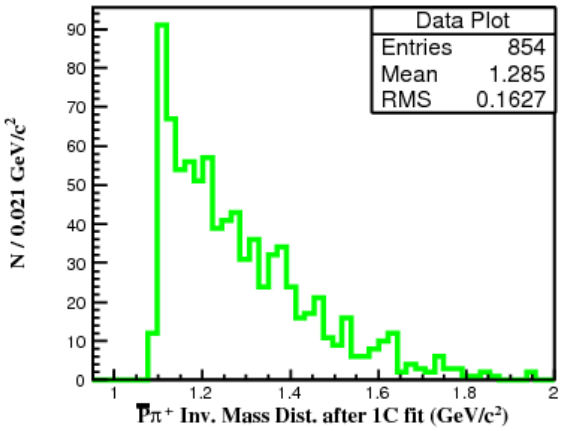

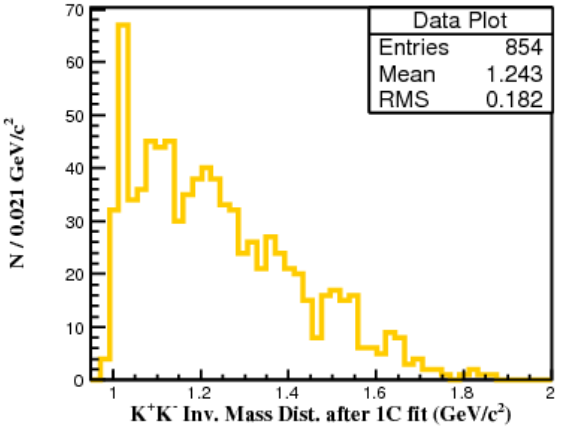

Invariant mass distribution of $p\pi^-$, $\bar{p}\pi^+$ and K^+K^- for (MC and DATA) of 4246 MEV energy after 4C and 1C kinematic fit and without mass, χ^2_{4c} and χ^2_{1c} cuts

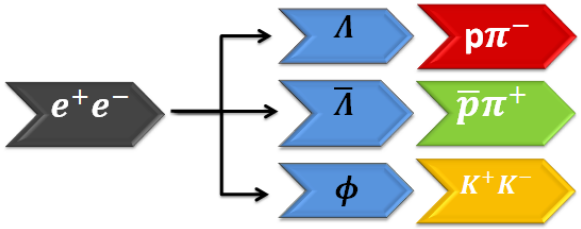

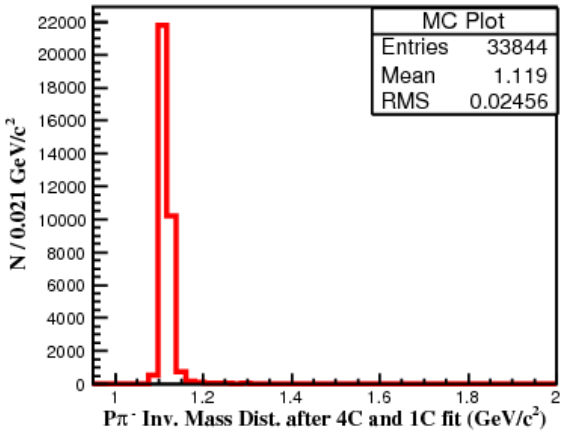

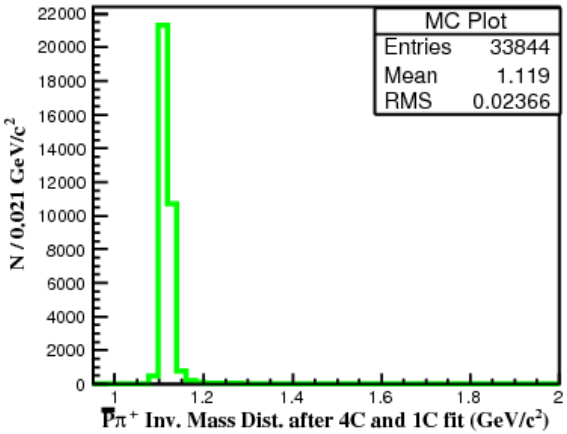

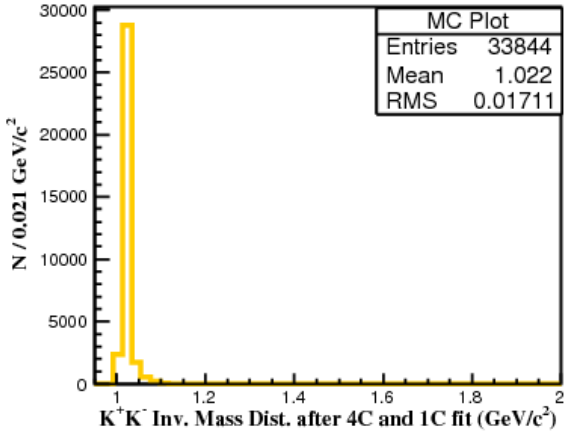

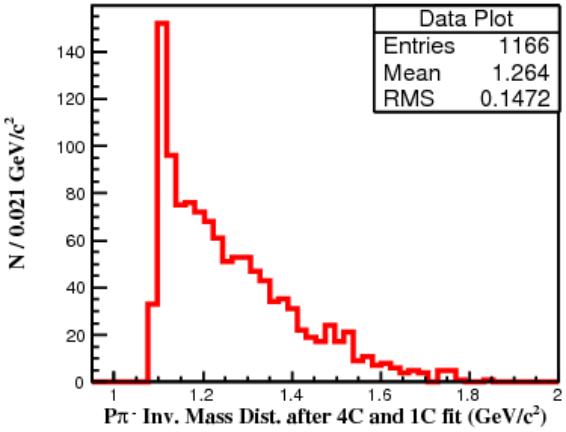

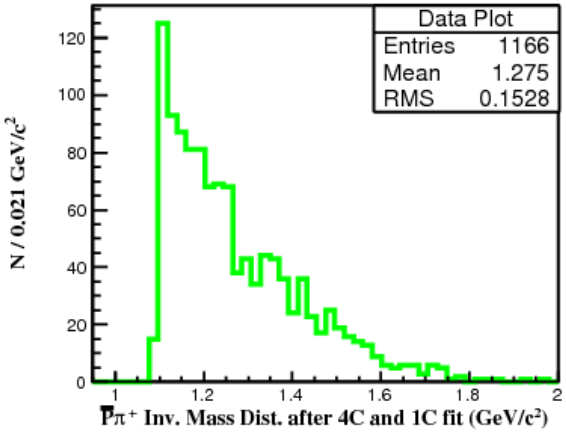

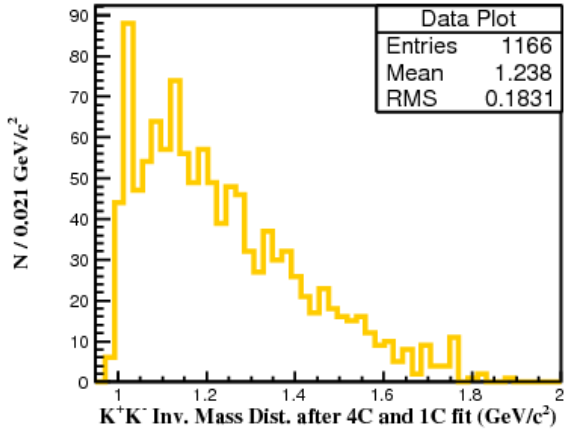

Invariant mass distribution of $p\pi^-$, $\bar{p}\pi^+$ and K^+K^- for (MC and DATA) of 4246 MEV energy after 4C kinematic fit and without mass, χ^2_{4c} and χ^2_{1c} cuts

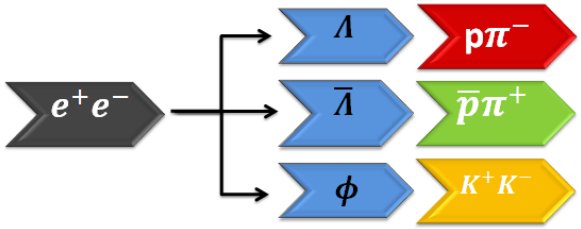

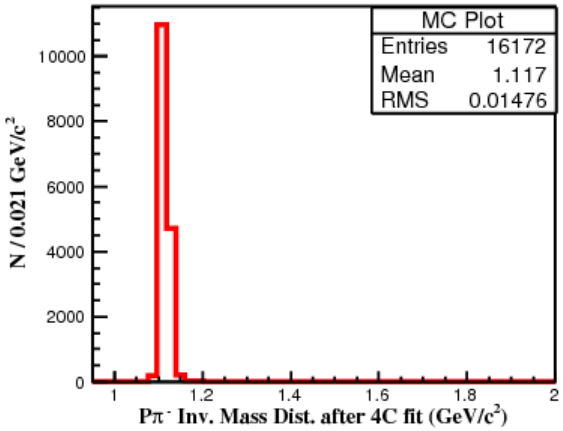

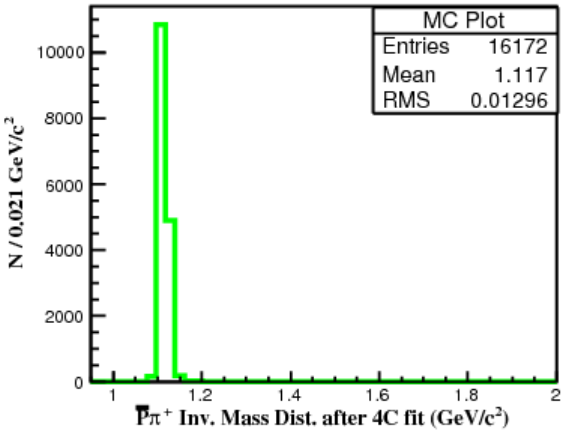

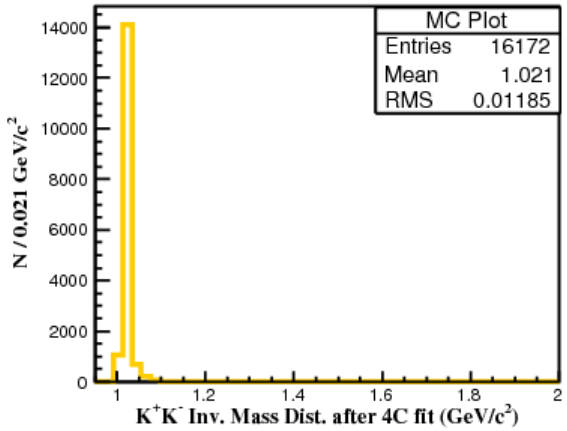

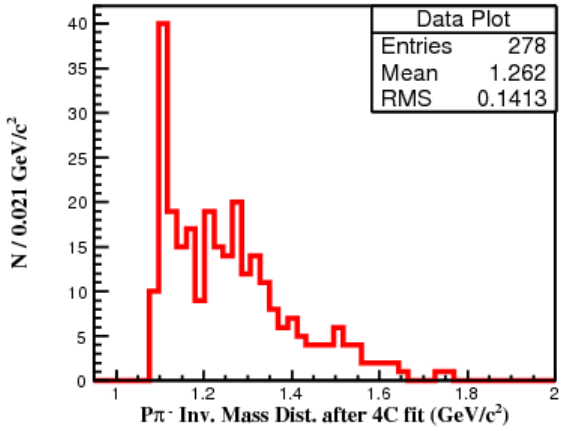

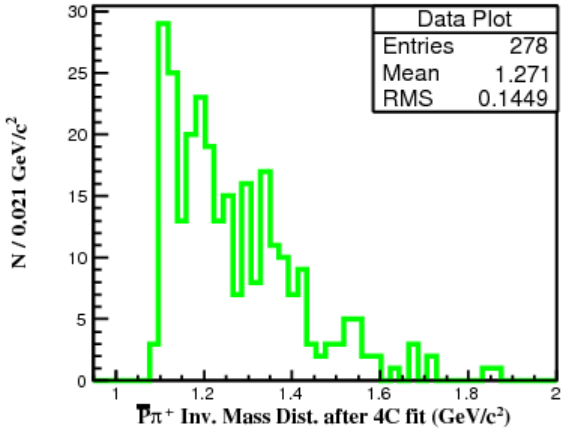

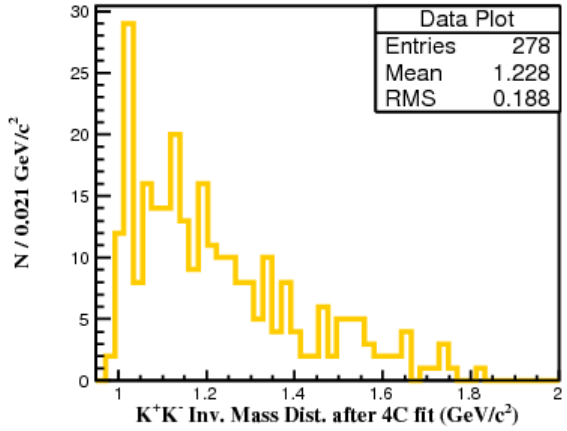

Invariant mass distribution of $p\pi^-$, $\bar{p}\pi^+$ and K^+K^- for (MC and DATA) of 4246 MEV energy after 1C kinematic fit and without mass, χ^2_{4c} and χ^2_{1c} cuts

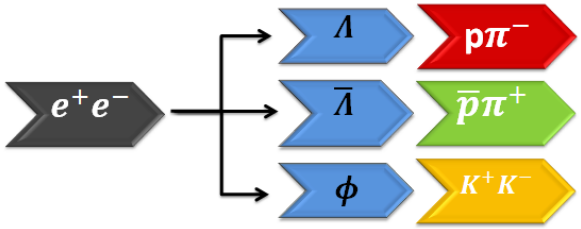

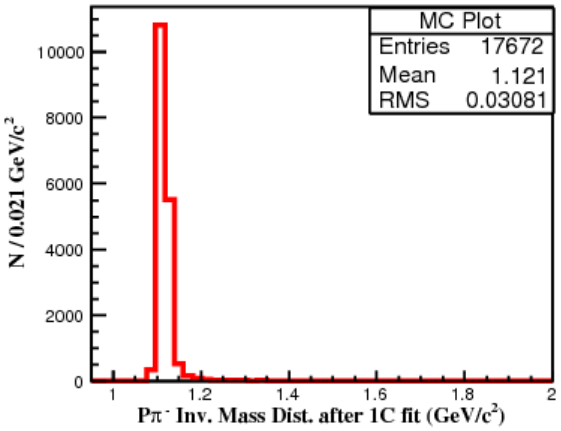

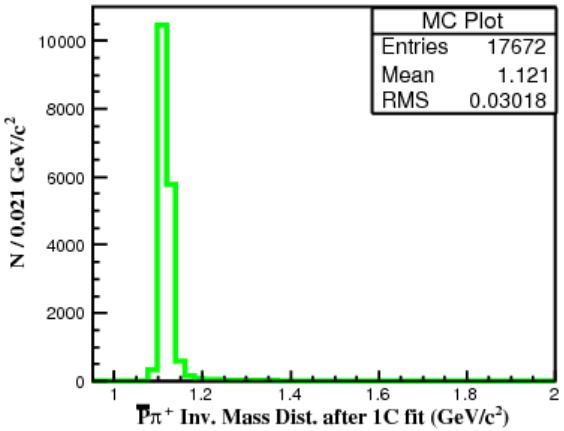

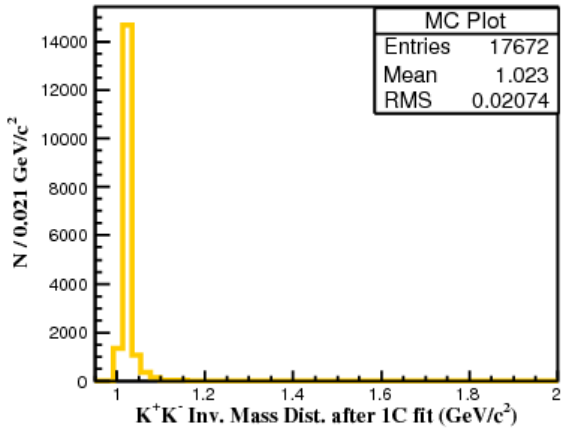

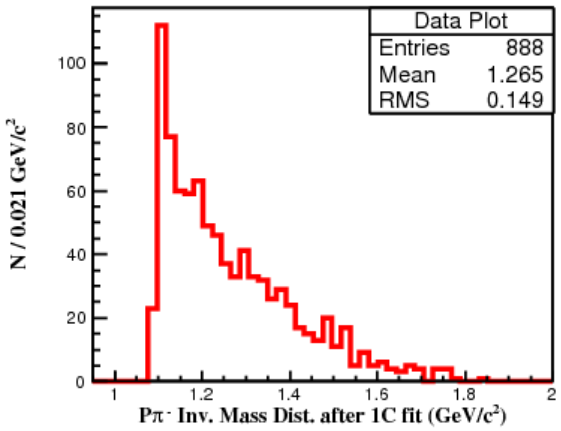

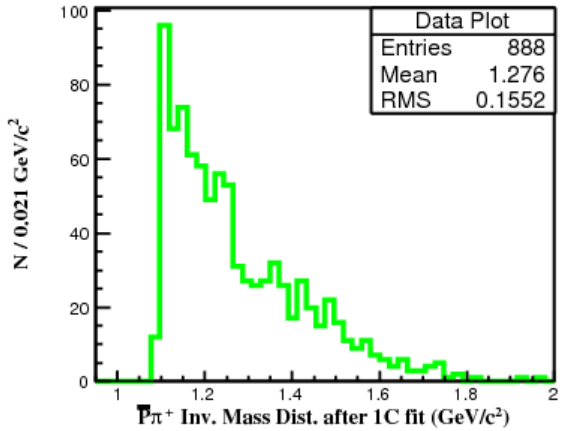

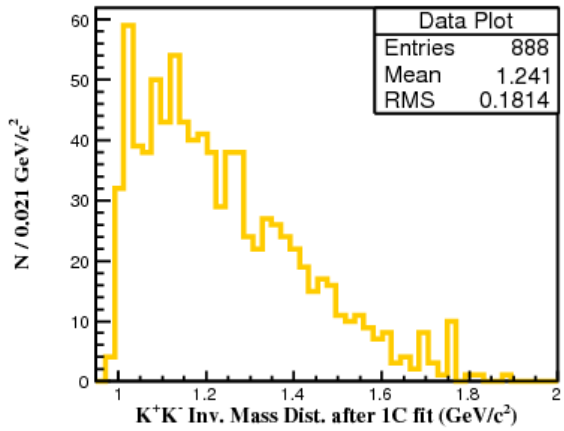

Invariant mass distribution of $p\pi^-$, $\bar{p}\pi^+$ and K^+K^- for (MC and DATA) of 4260 MEV energy after 4C and 1C kinematic fit and without mass, χ^2_{4c} and χ^2_{1c} cuts

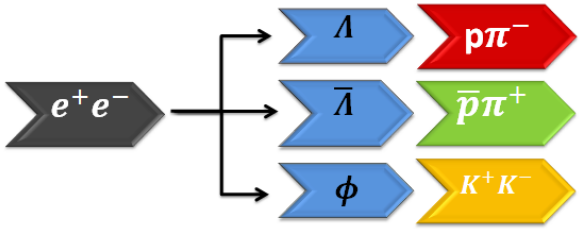

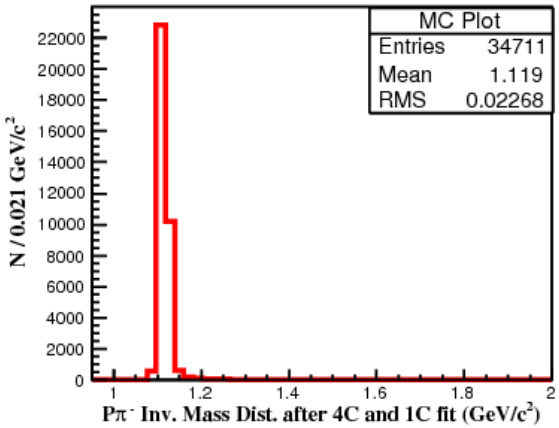

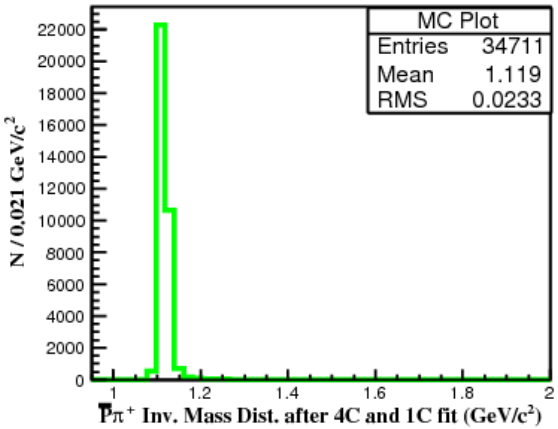

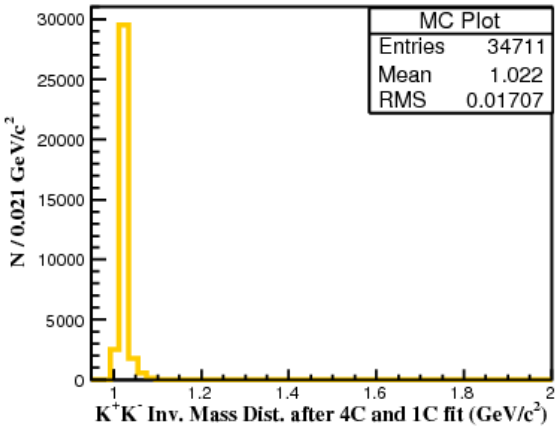

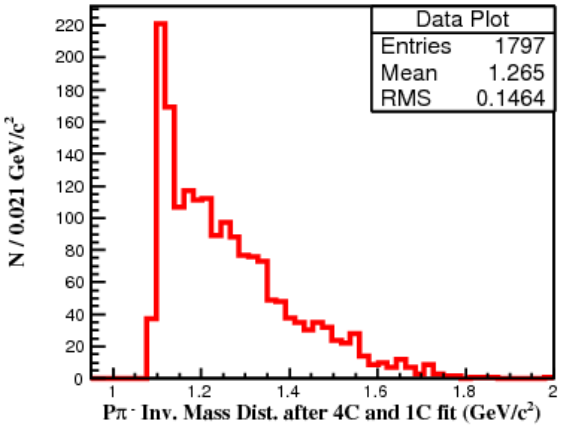

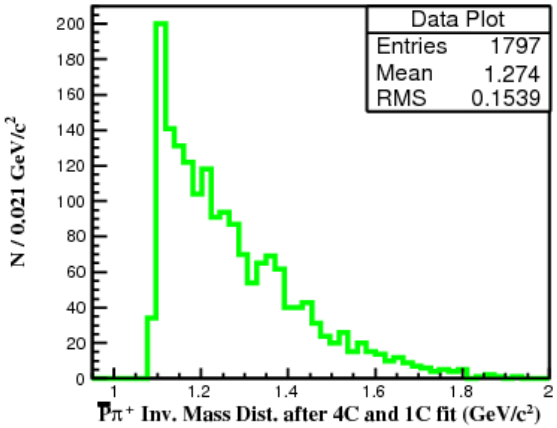

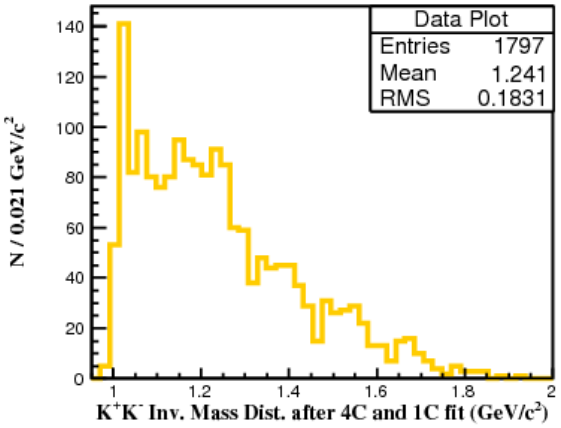

Invariant mass distribution of $p\pi^-$, $\bar{p}\pi^+$ and K^+K^- for (MC and DATA) of 4260 MEV energy after 4C kinematic fit and without mass, χ^2_{4c} and χ^2_{1c} cuts

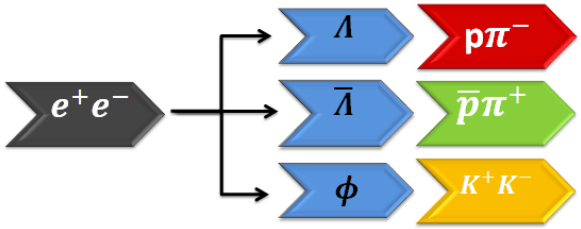

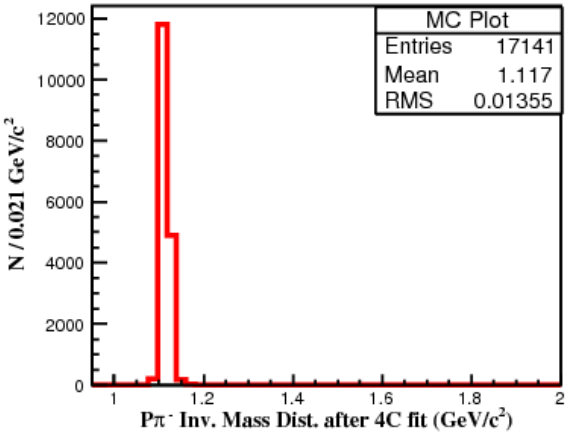

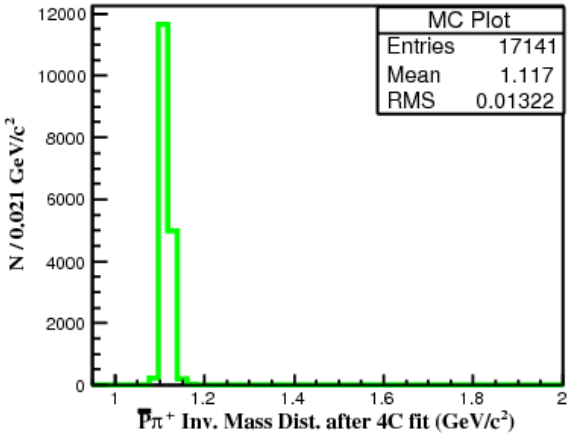

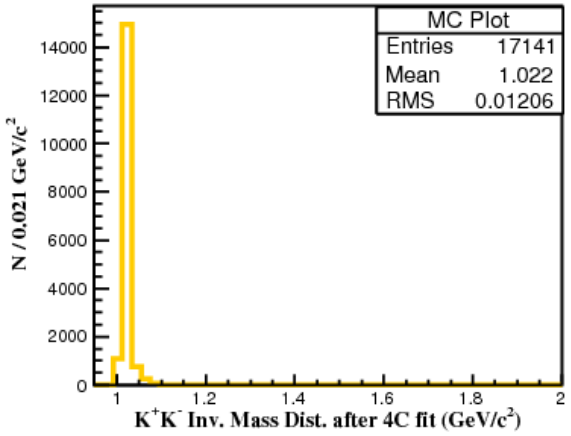

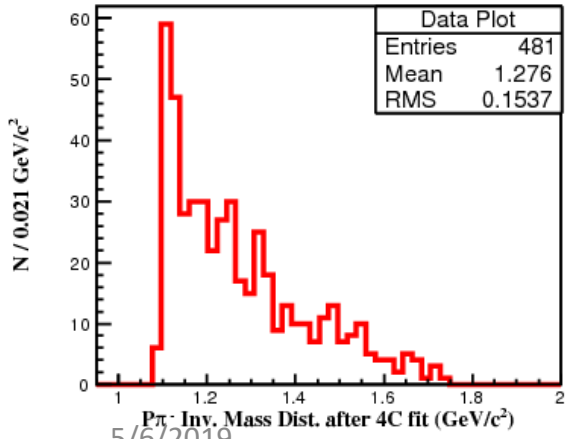

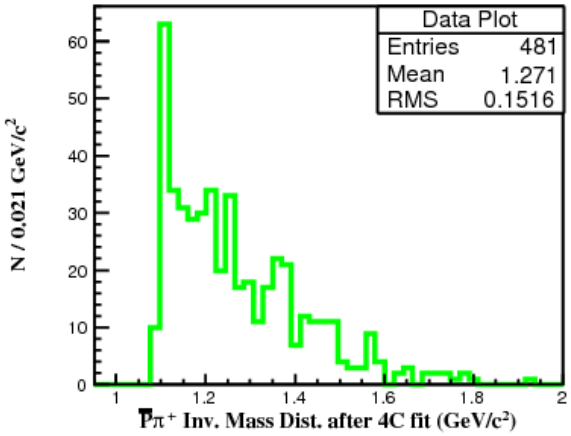

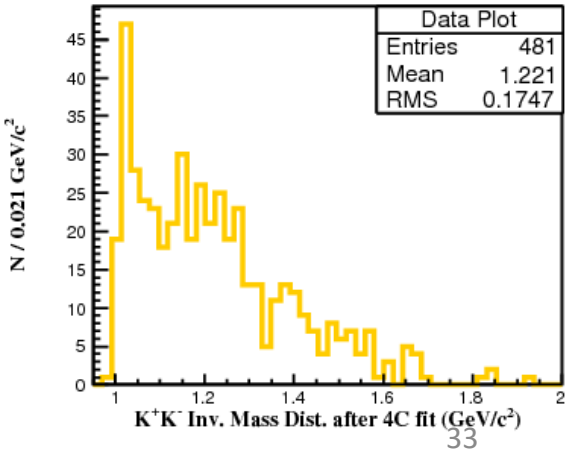

Invariant mass distribution of $p\pi^-$, $\bar{p}\pi^+$ and K^+K^- for (MC and DATA) of 4260 MEV energy after 1C kinematic fit and without mass, χ^2_{4c} and χ^2_{1c} cuts

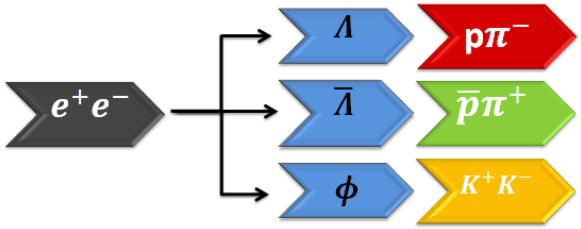

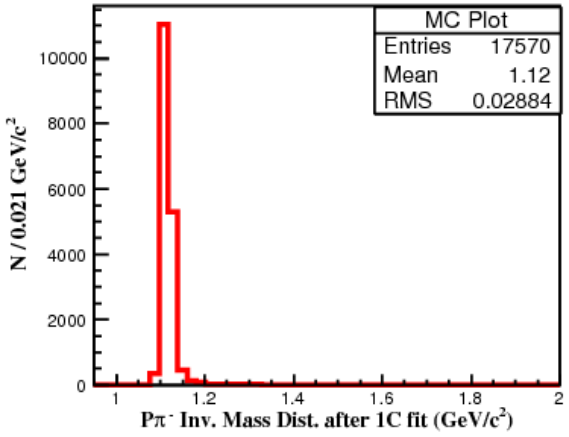

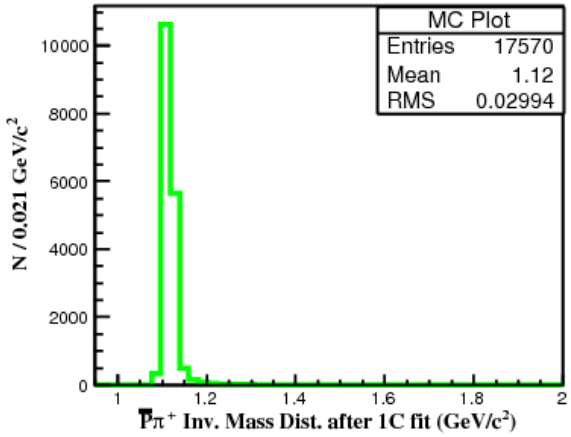

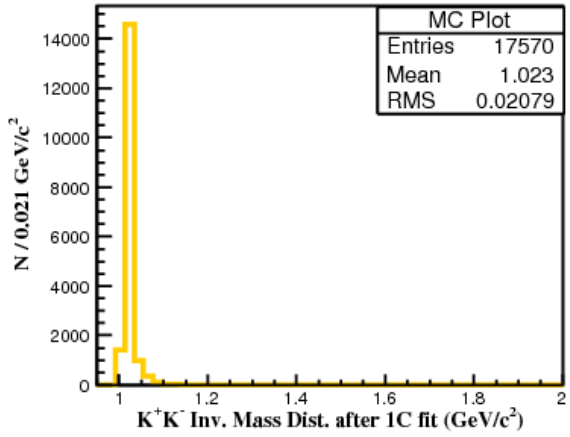

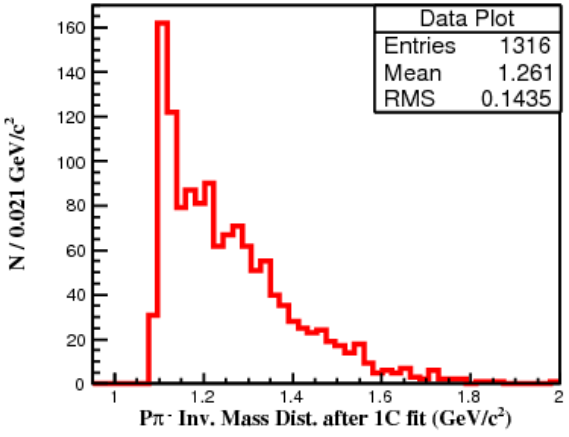

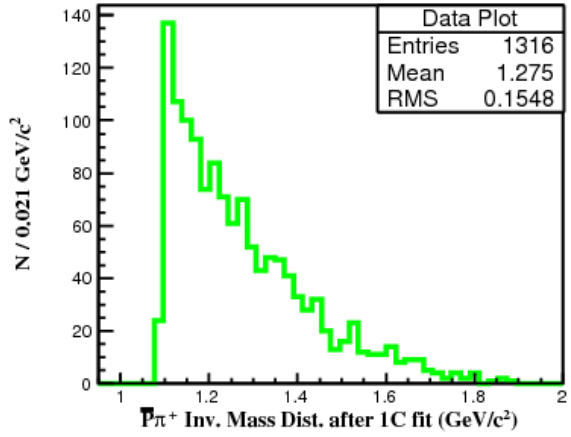

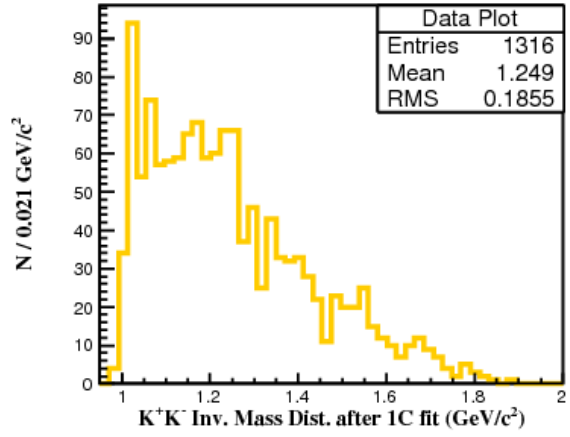

Invariant mass distribution of $p\pi^-$, $\bar{p}\pi^+$ and K^+K^- for (MC and DATA) of 4270 MEV energy after 4C and 1C kinematic fit and without mass, χ^2_{4c} and χ^2_{1c} cuts

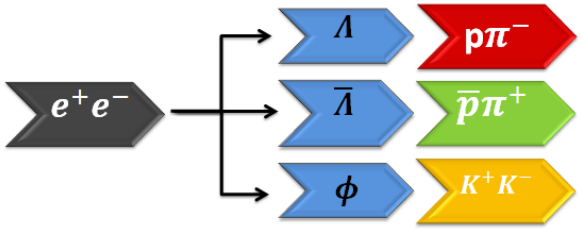

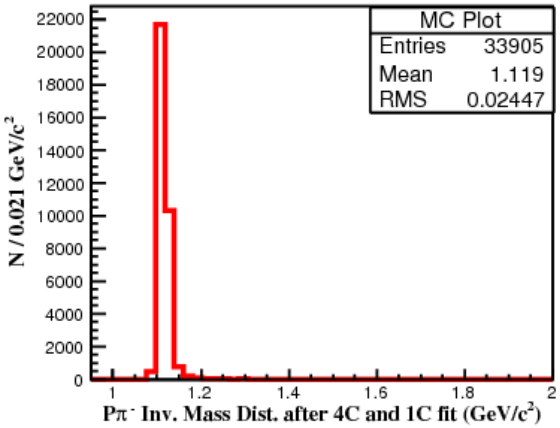

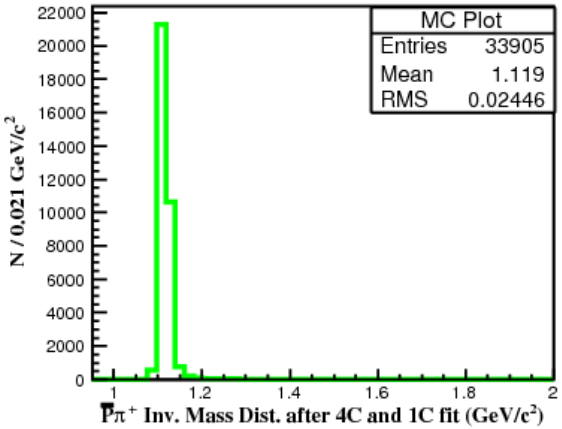

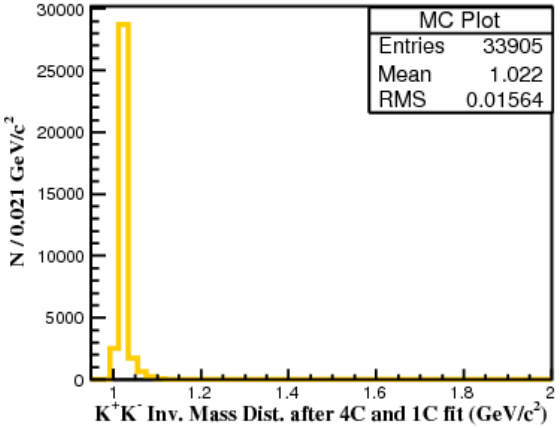

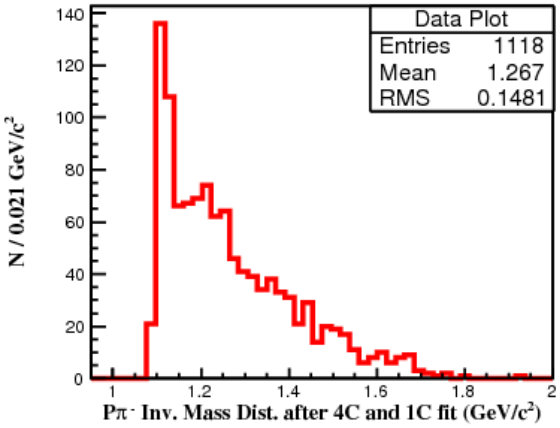

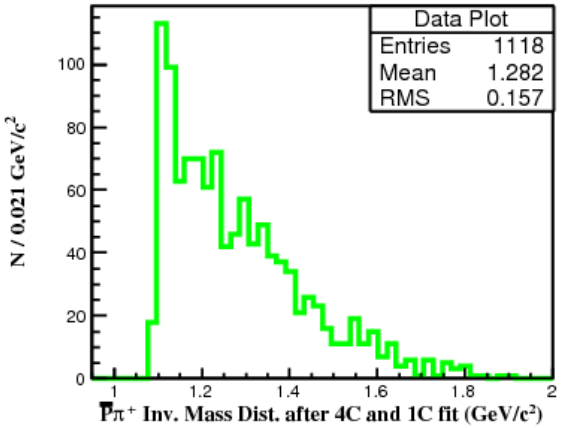

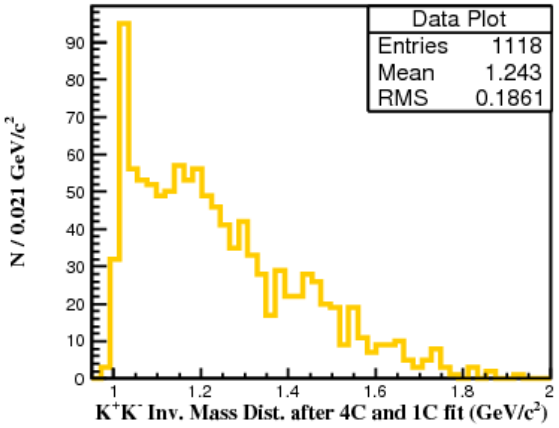

Invariant mass distribution of $p\pi^-$, $\bar{p}\pi^+$ and K^+K^- for (MC and DATA) of 4270 MEV energy after 4C kinematic fit and without mass, χ^2_{4c} and χ^2_{1c} cuts

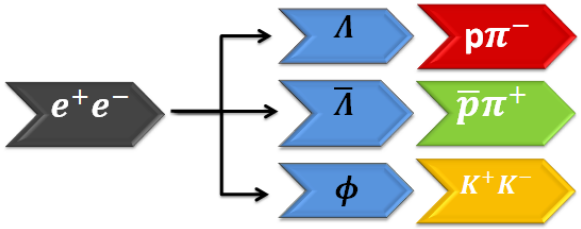

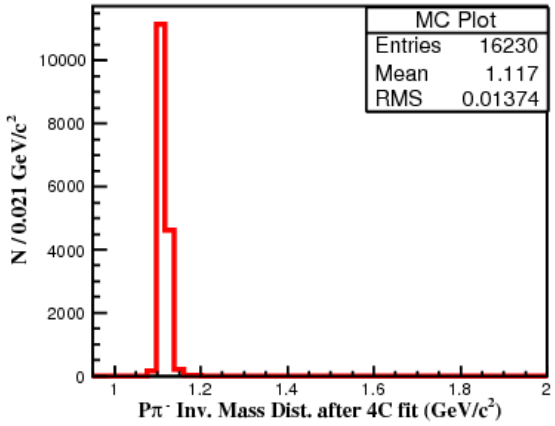

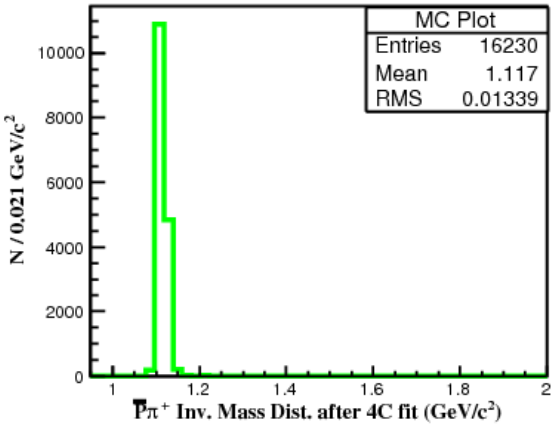

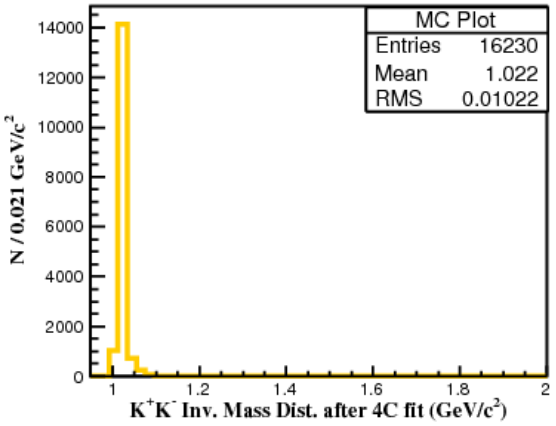

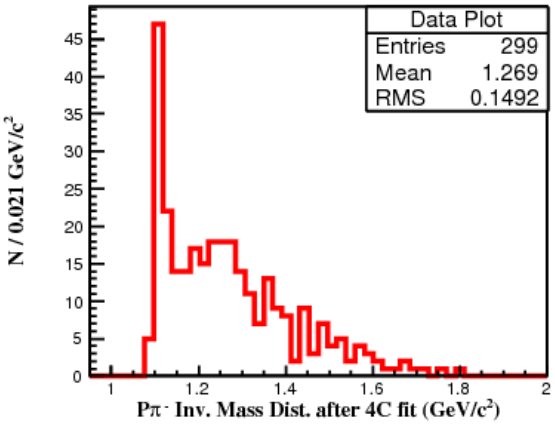

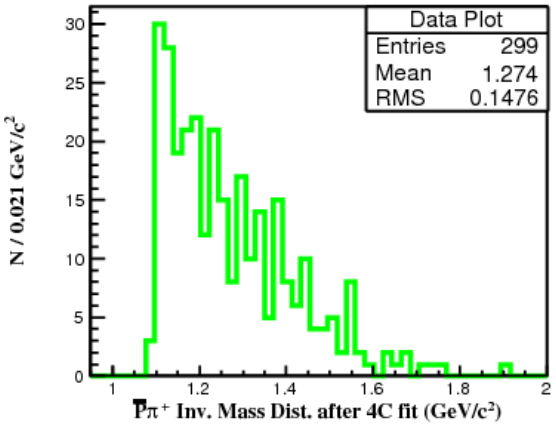

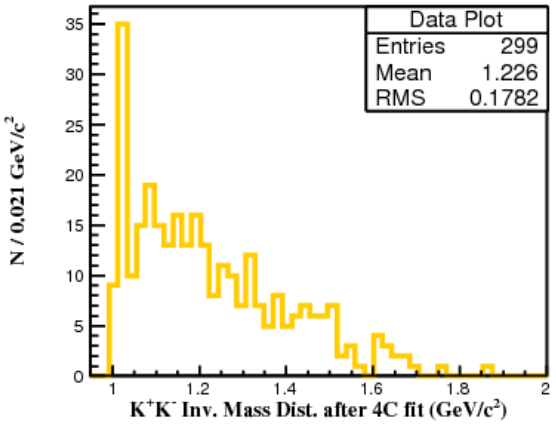

Invariant mass distribution of $p\pi^-$, $\bar{p}\pi^+$ and K^+K^- for (MC and DATA) of 4270 MEV energy after 1C kinematic fit and without mass, χ^2_{4c} and χ^2_{1c} cuts

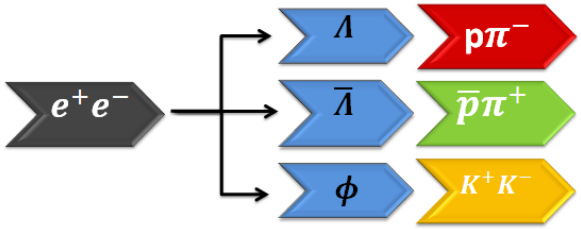

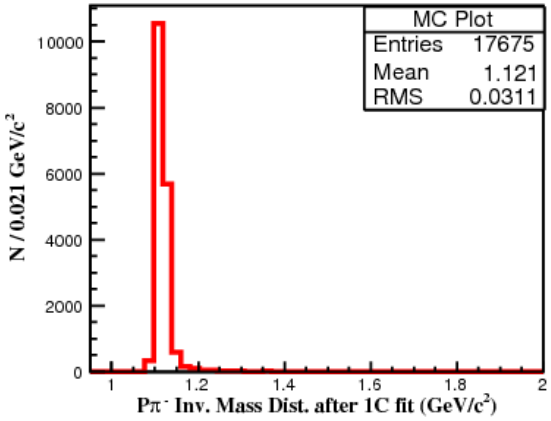

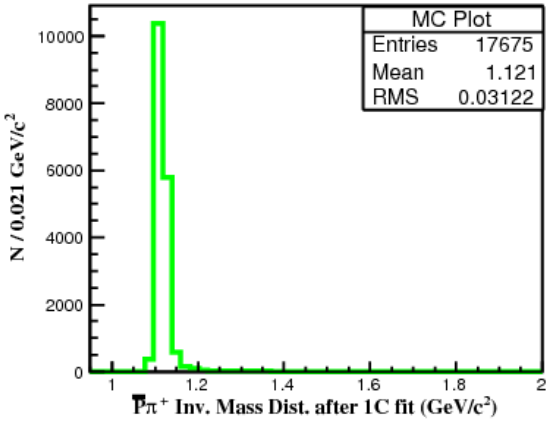

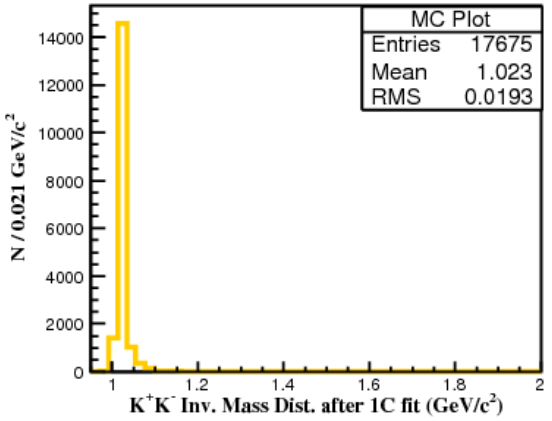

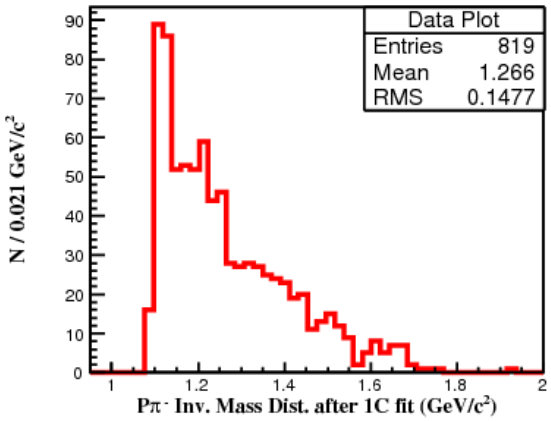

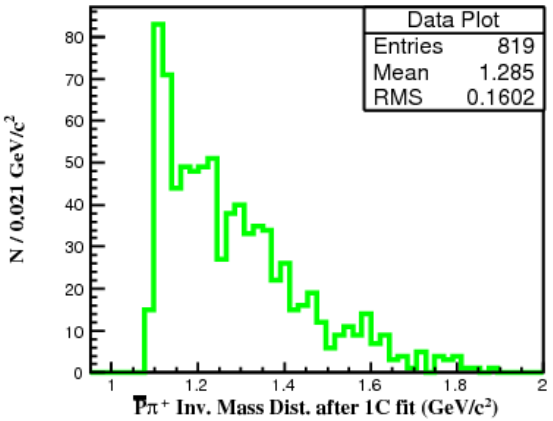

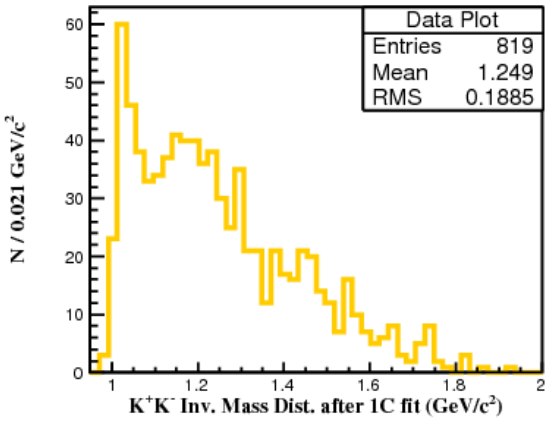

Invariant mass distribution of $p\pi^-$, $\bar{p}\pi^+$ and K^+K^- for (MC and DATA) of 4280 MEV energy after 4C and 1C kinematic fit and without mass, χ^2_{4c} and χ^2_{1c} cuts

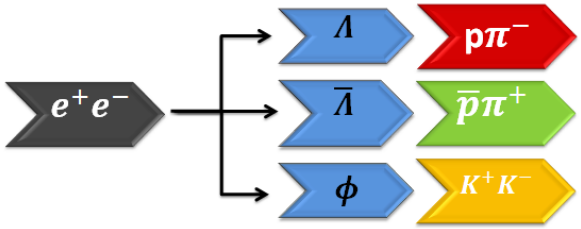

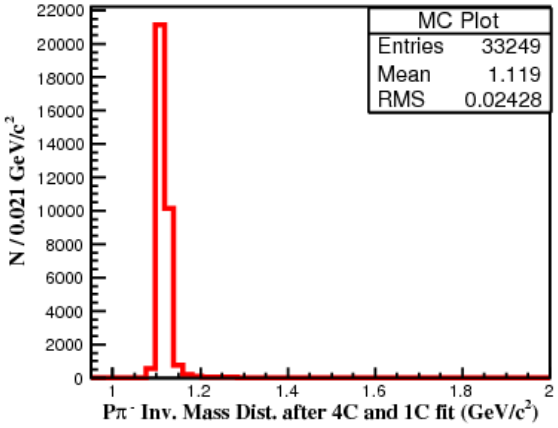

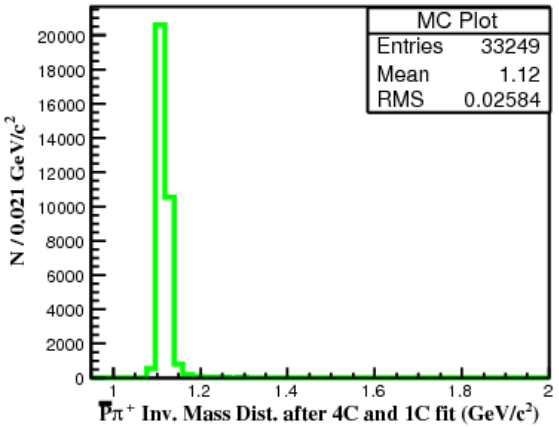

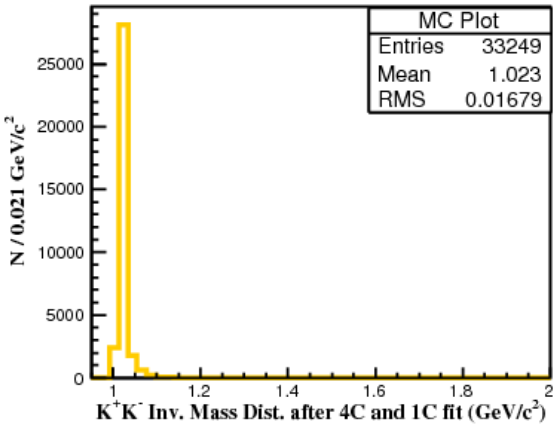

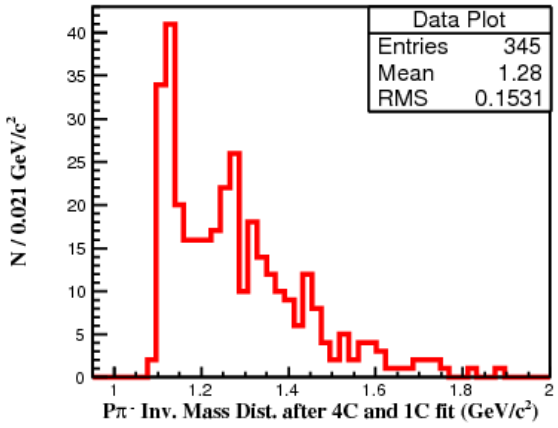

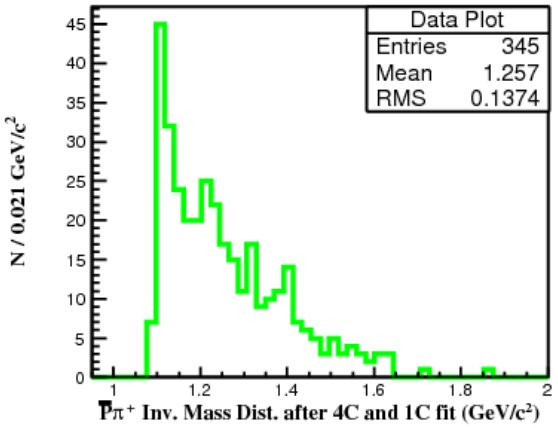

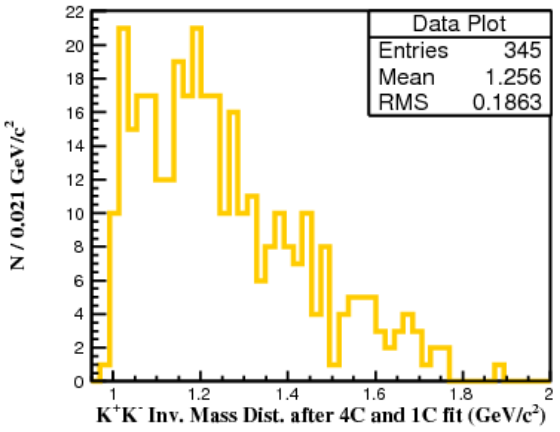

Invariant mass distribution of $p\pi^-$, $\bar{p}\pi^+$ and K^+K^- for (MC and DATA) of 4280 MEV energy after 4C kinematic fit and without mass, χ^2_{4c} and χ^2_{1c} cuts

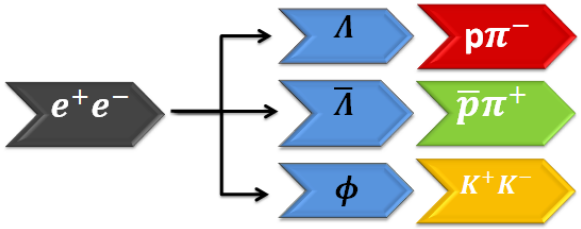

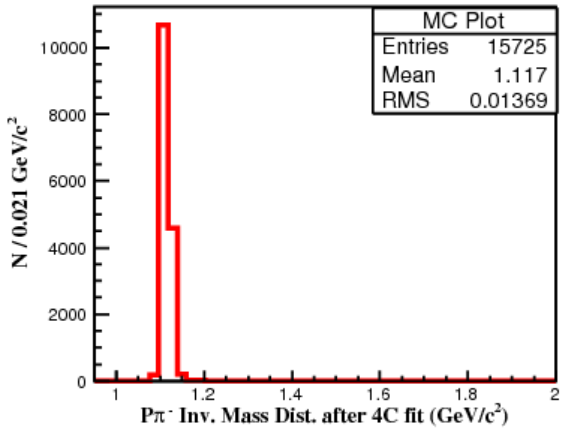

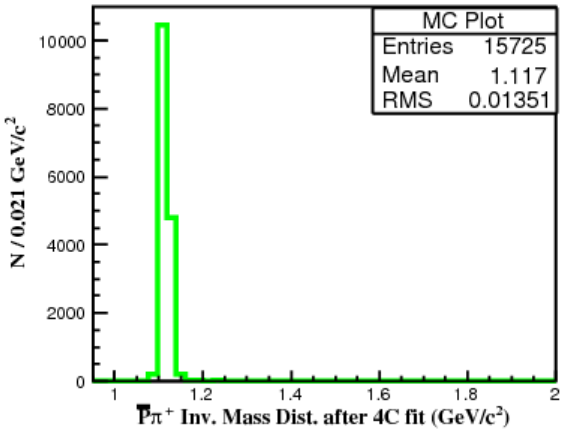

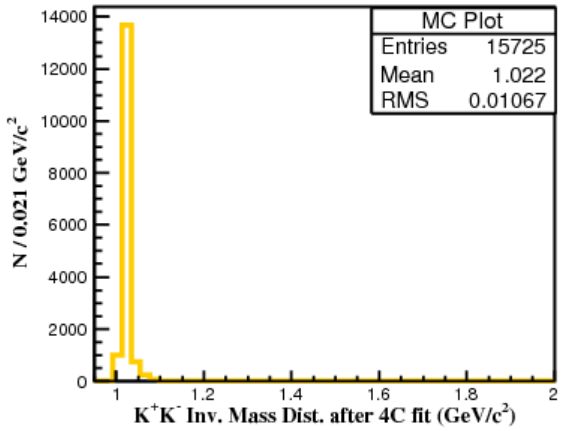

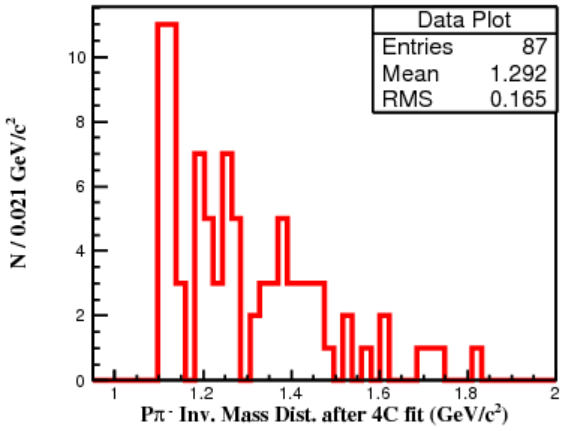

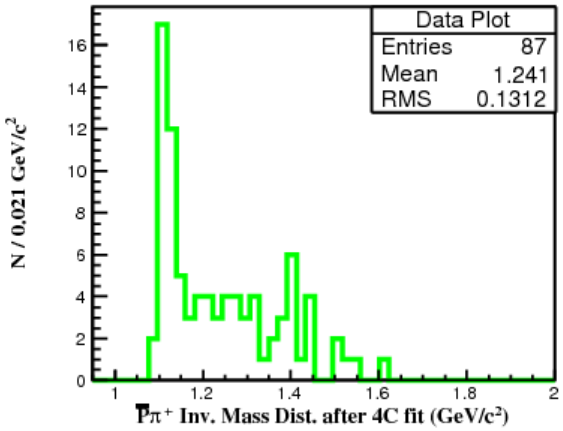

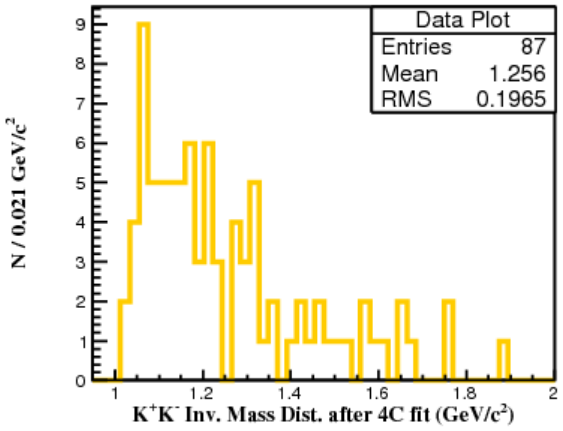

Invariant mass distribution of $p\pi^-$, $\bar{p}\pi^+$ and K^+K^- for (MC and DATA) of 4280 MEV energy after 1C kinematic fit and without mass, χ^2_{4c} and χ^2_{1c} cuts

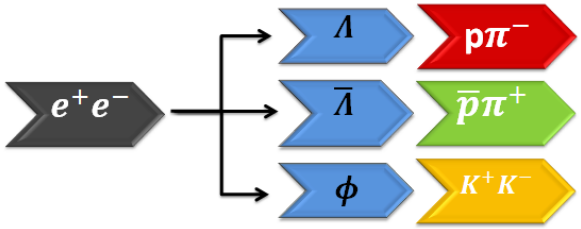

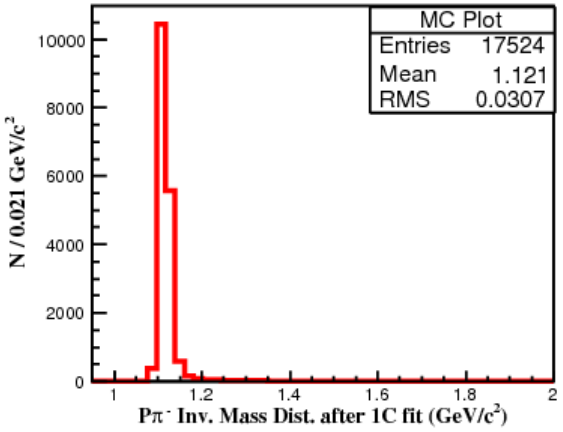

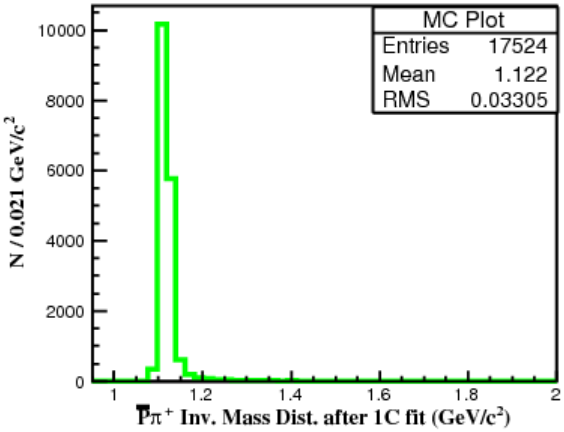

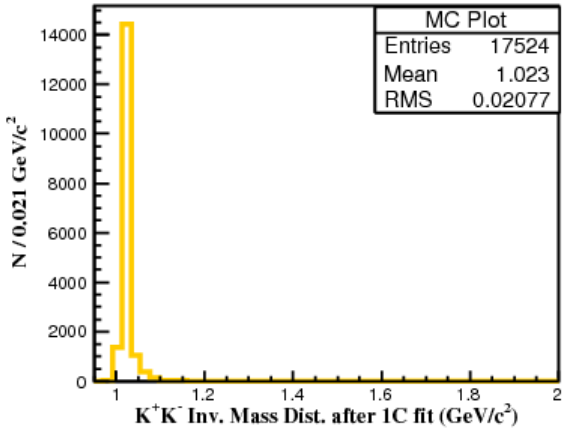

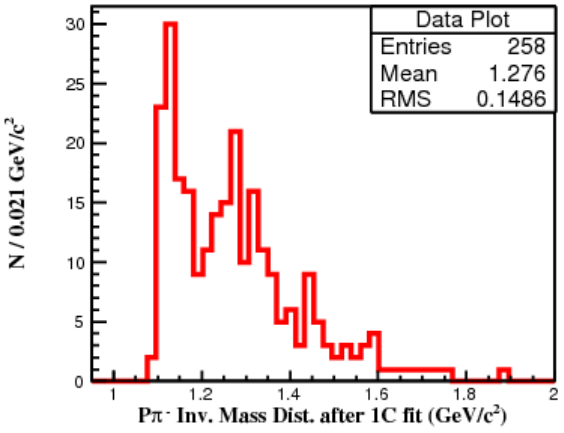

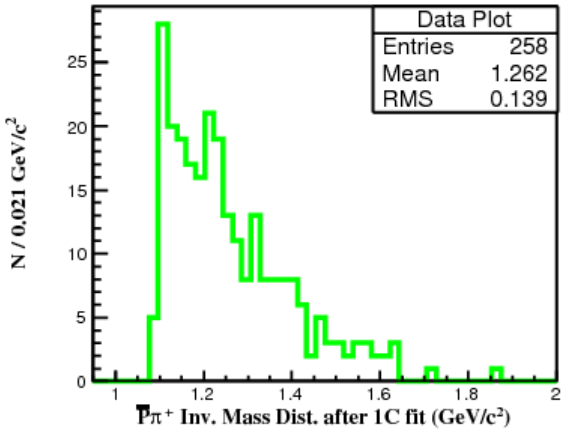

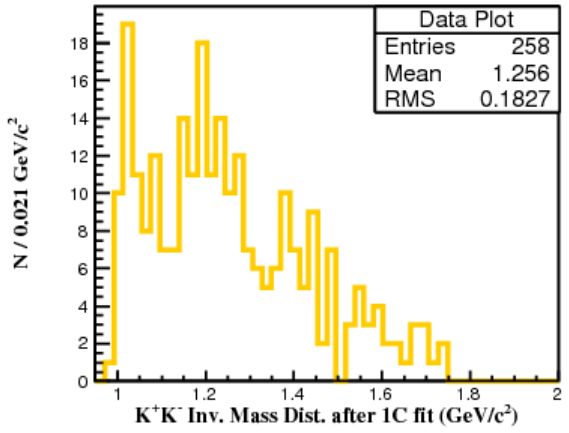

Summary of Events coming from MC and Data

Energy Points	Monte Carlo			Real		
	4C and 1C	4C	1C	4C and 1C	4C	1C
4190	32410	15048	17362	1166	252	914
4200	32838	15612	17226	1161	245	916
4210	32485	15181	17304	1191	289	902
4220	32750	15445	17305	1139	263	876
4237	34008	16355	17653	1138	284	854
4246	33844	16172	17672	1166	278	888
4260	34711	17141	17570	1797	481	1316
4270	33905	16230	17675	1118	299	819
4280	33249	15725	17524	345	87	258
All (9) energy points	300200	142909	157291	10221	2478	7743

Invariant mass distribution of $p\pi^-$ (MC and DATA) of all 9 energy points after 4C and 1C kinematic fit and without mass, χ^2_{4c} and χ^2_{1c} cuts

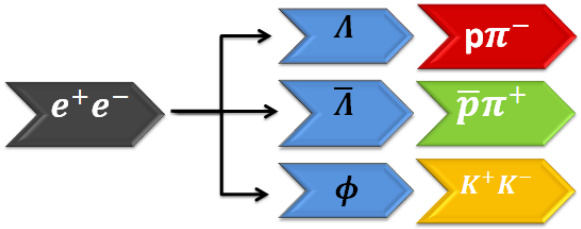

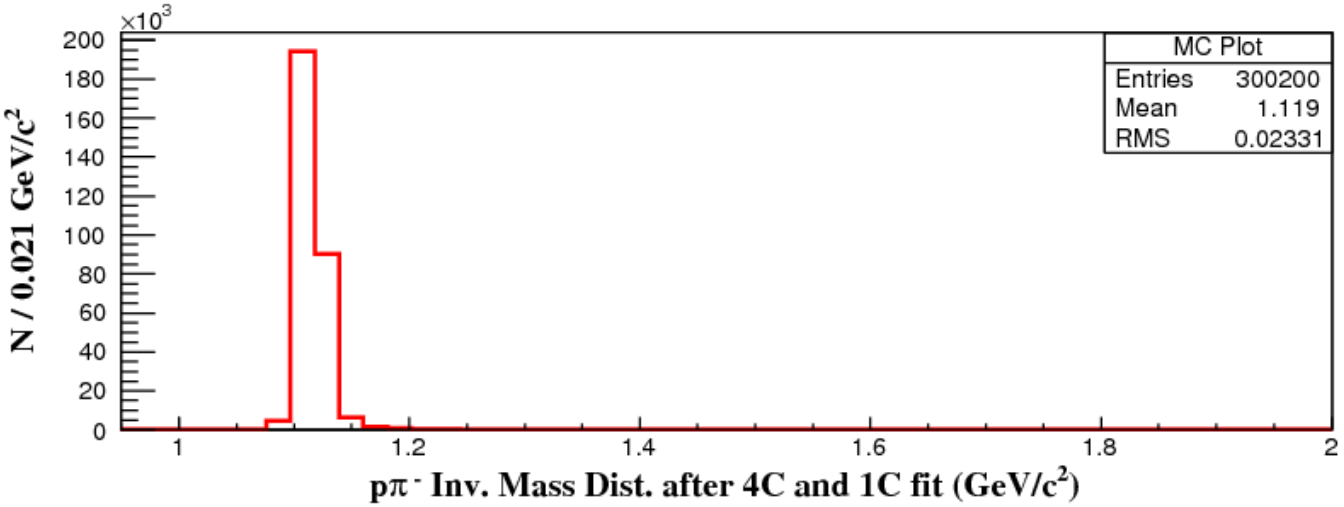

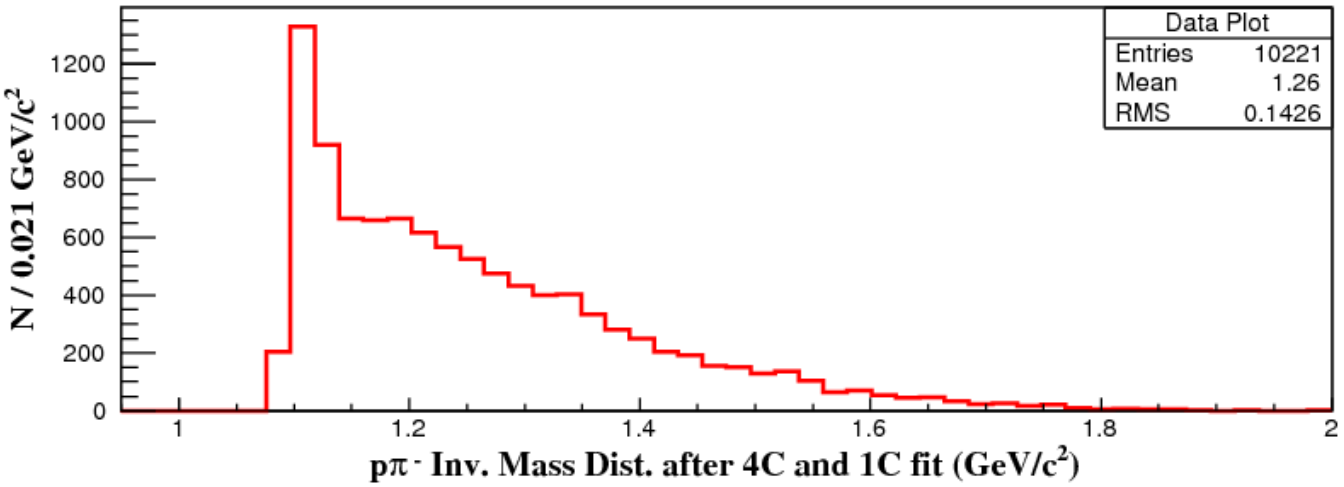

Invariant mass distribution of $p\pi^-$ (MC and DATA) of all 9 energy points after 4C kinematic fit and without mass, χ^2_{4c} and χ^2_{1c} cuts

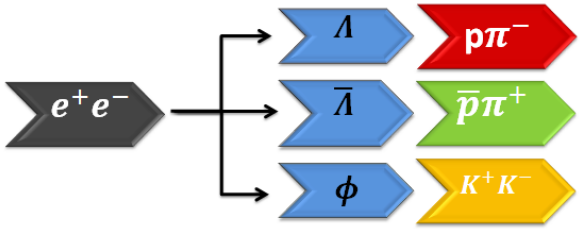

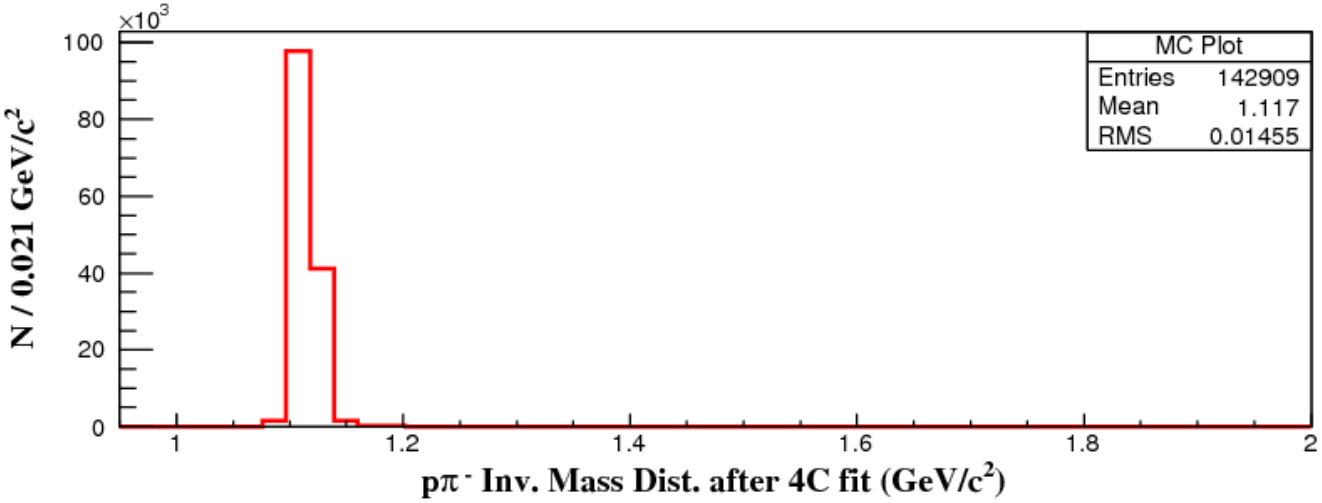

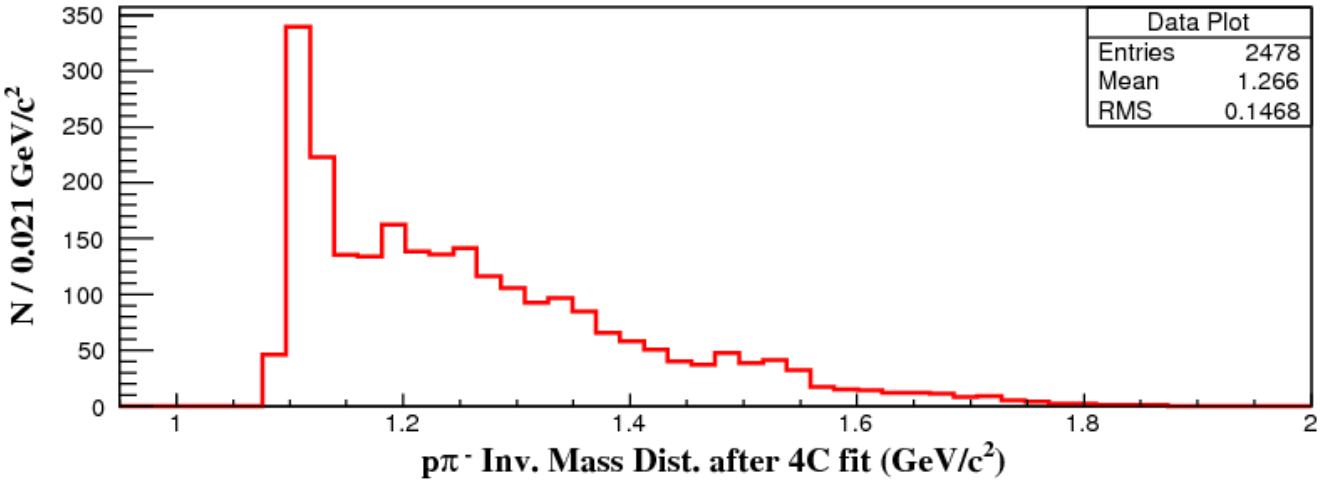

Invariant mass distribution of $p\pi^-$ (MC and DATA) of all 9 energy points after 1C kinematic fit and without mass, χ^2_{4c} and χ^2_{1c} cuts

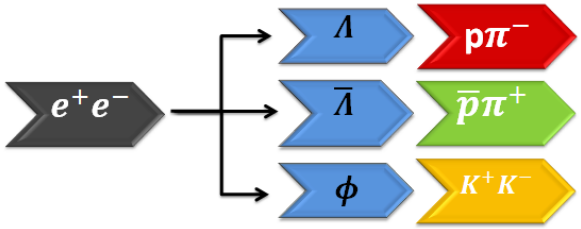

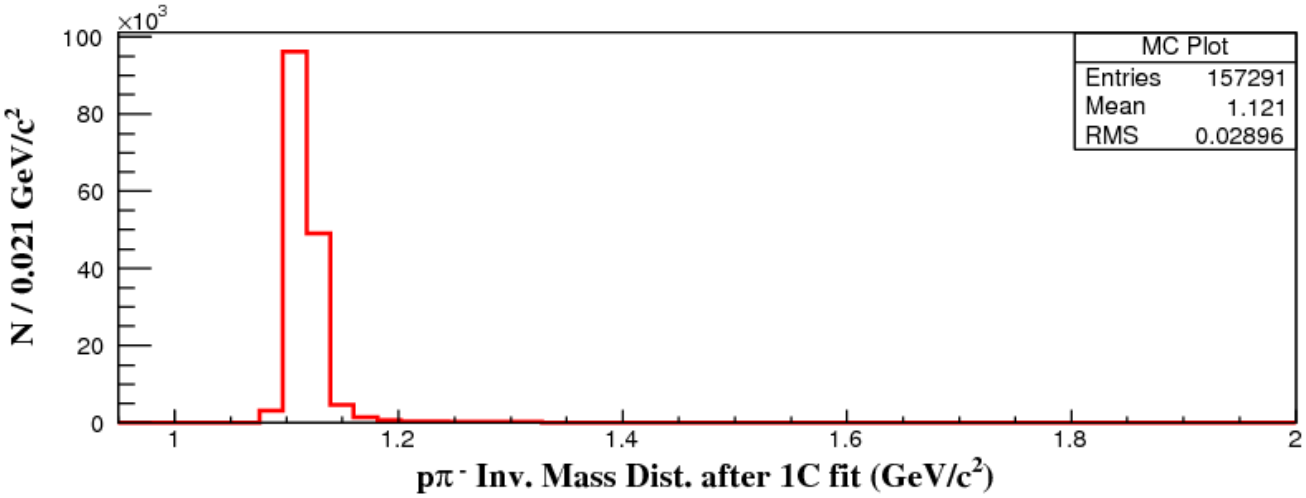

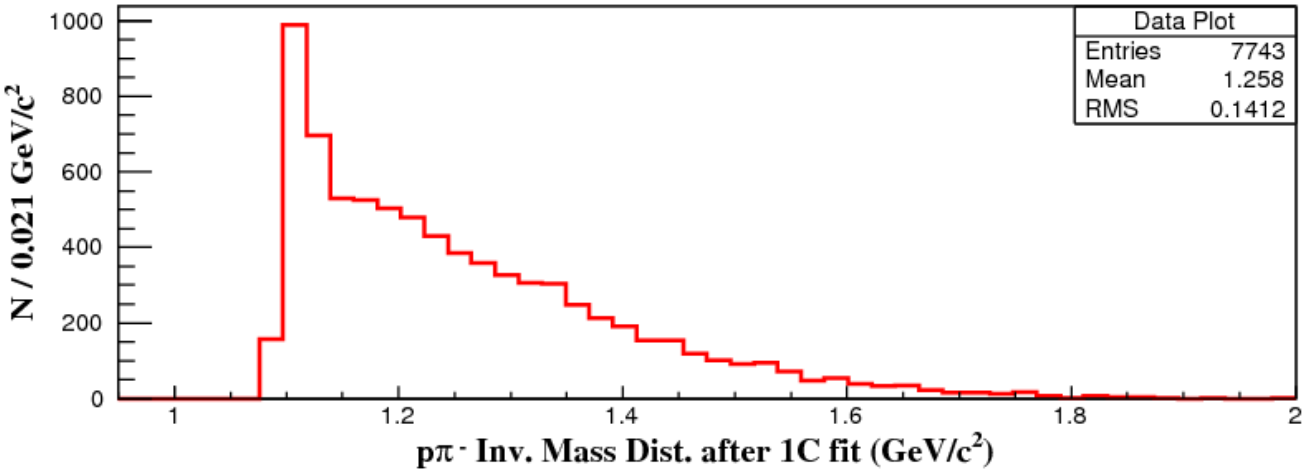

Invariant mass distribution of $\bar{p}\pi^+$ (MC and DATA) of all 9 energy points after 4C and 1C kinematic fit and without mass, χ^2_{4c} and χ^2_{1c} cuts

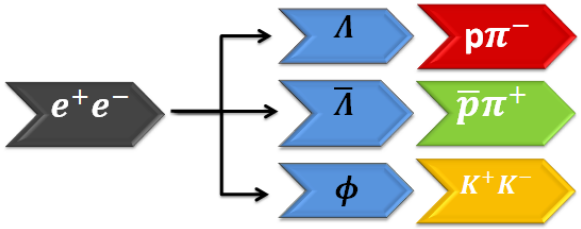

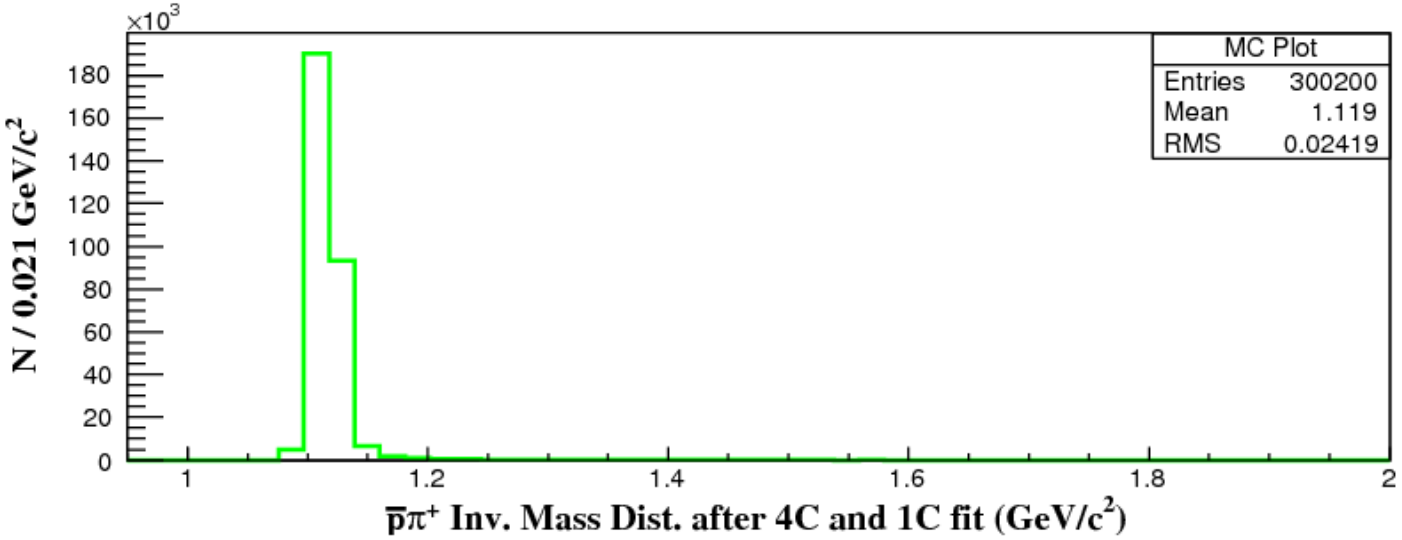

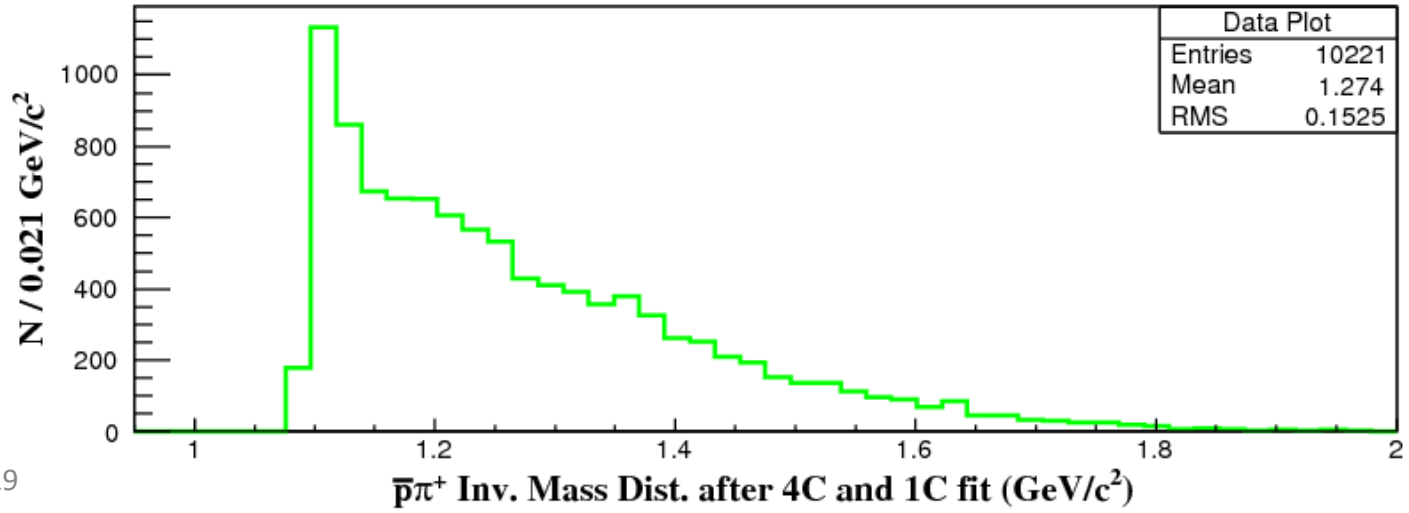

Invariant mass distribution of $\bar{p}\pi^+$ (MC and DATA) of all 9 energy points after 4C kinematic fit and without mass, χ^2_{4c} and χ^2_{1c} cuts

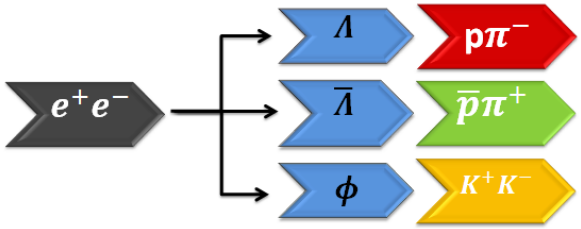

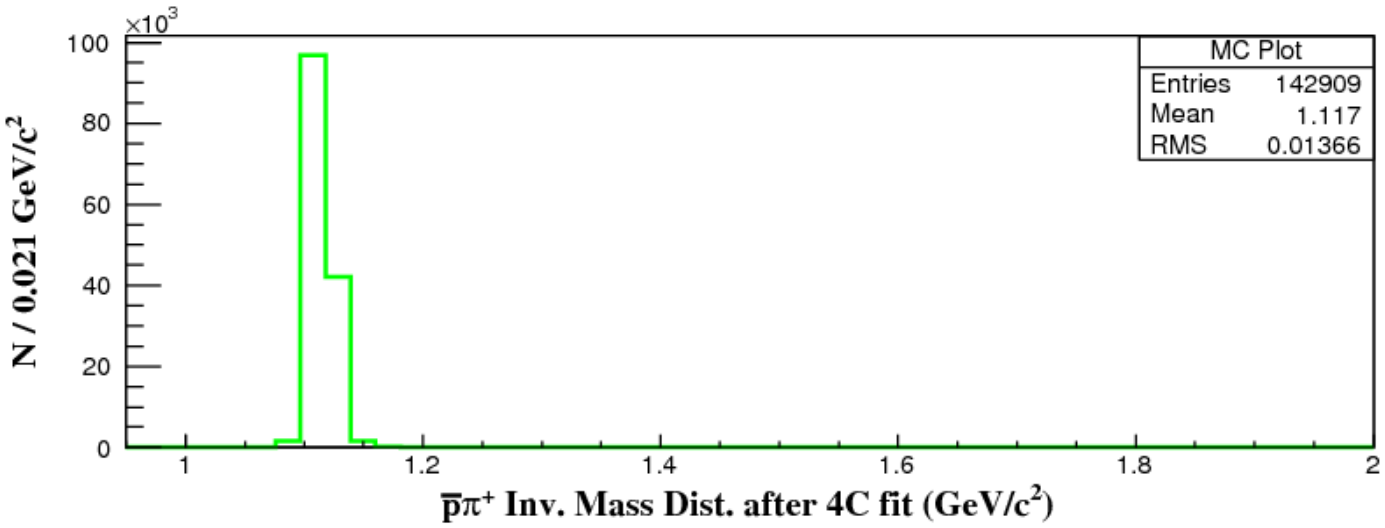

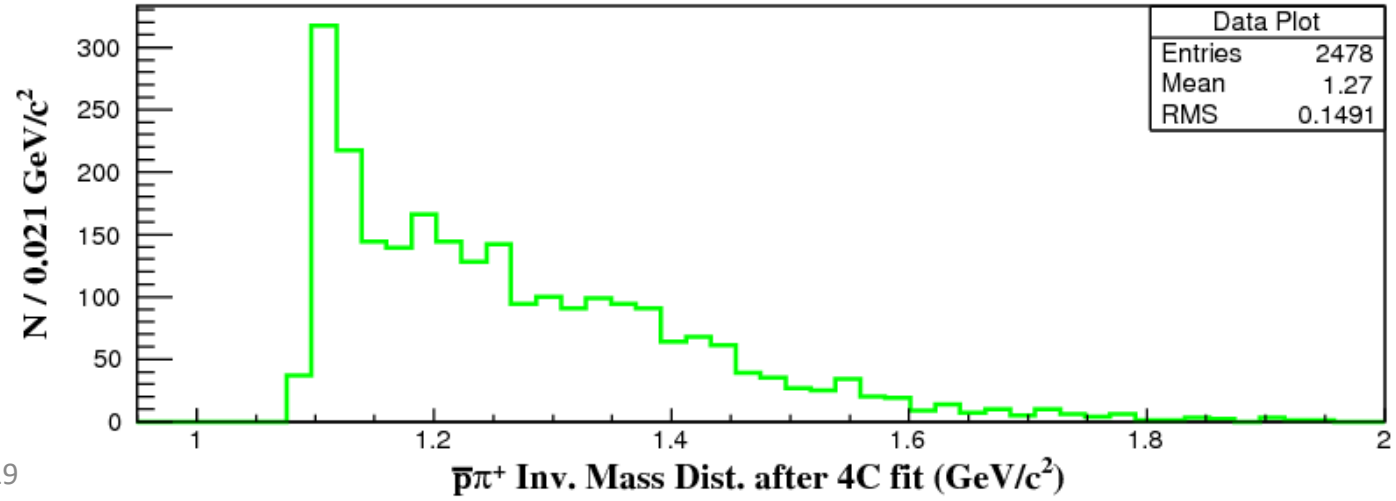

Invariant mass distribution of $\bar{p}\pi^+$ (MC and DATA) of all 9 energy points after 1C kinematic fit and without mass, χ^2_{4c} and χ^2_{1c} cuts

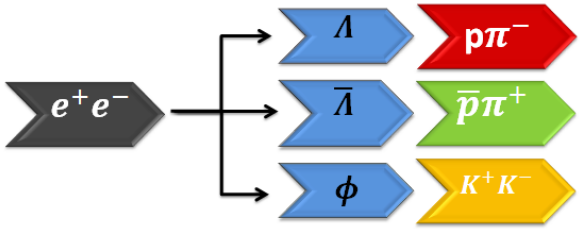

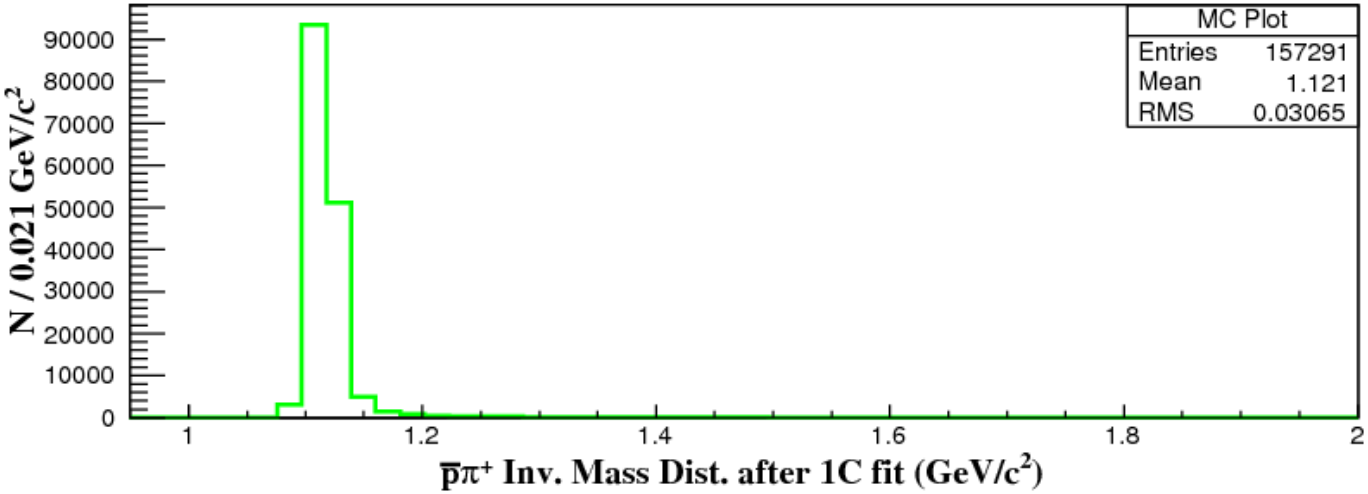

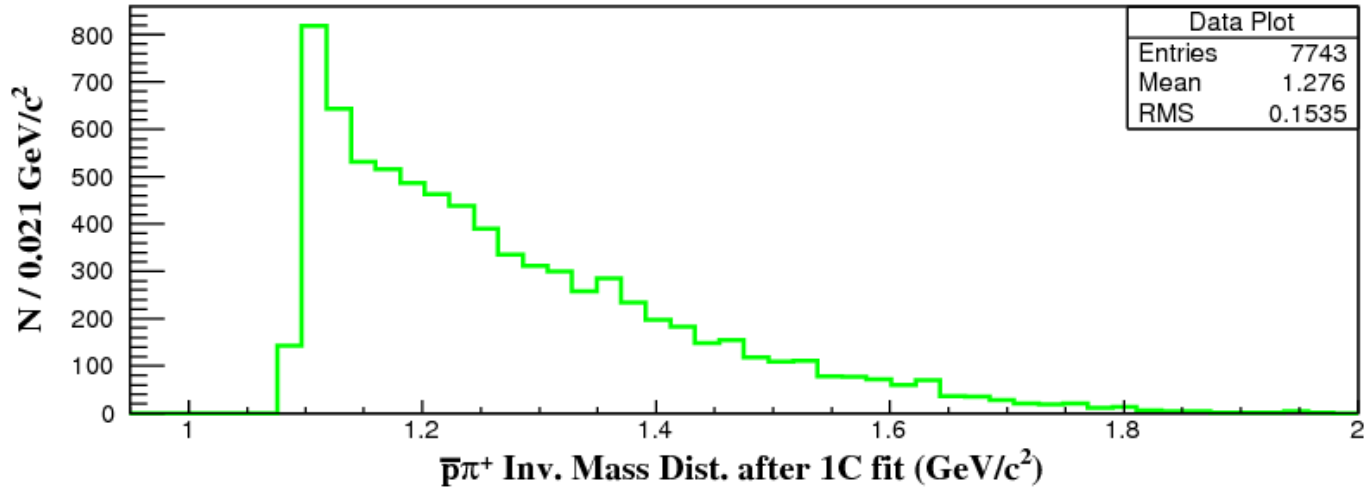

Invariant mass distribution of K^+K^- (MC and DATA) of all 9 energy points after 4C and 1C kinematic fit and without mass, χ^2_{4c} and χ^2_{1c} cuts

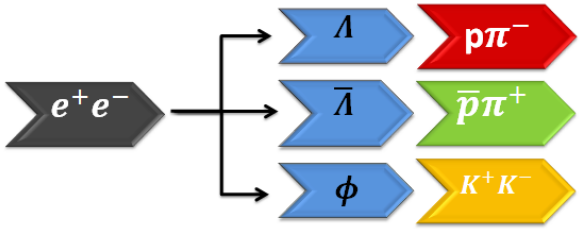

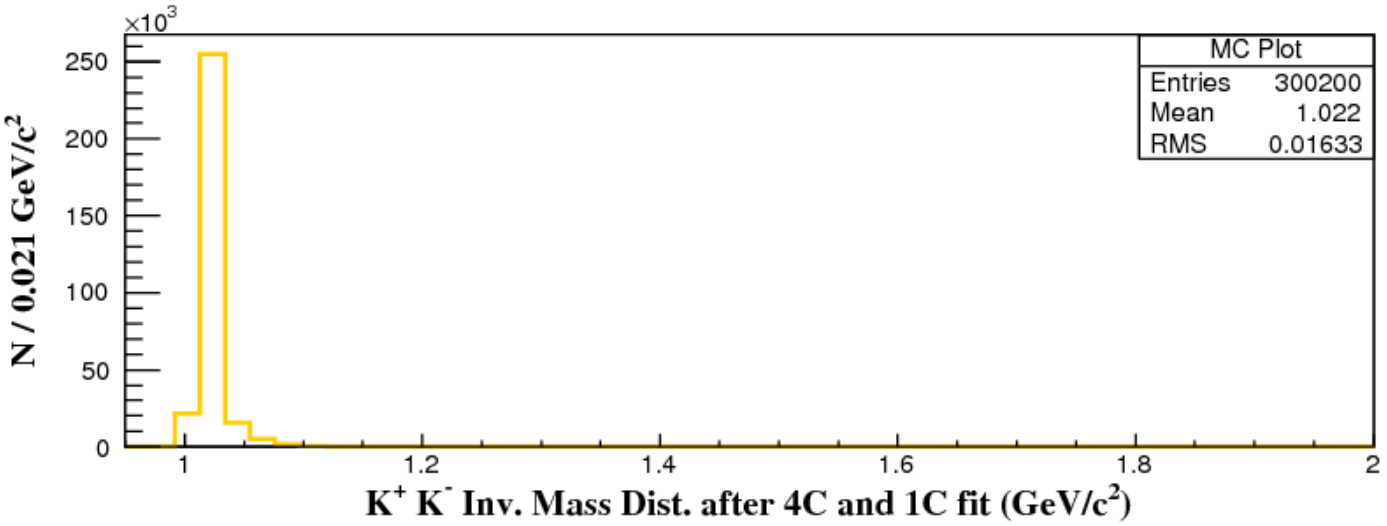

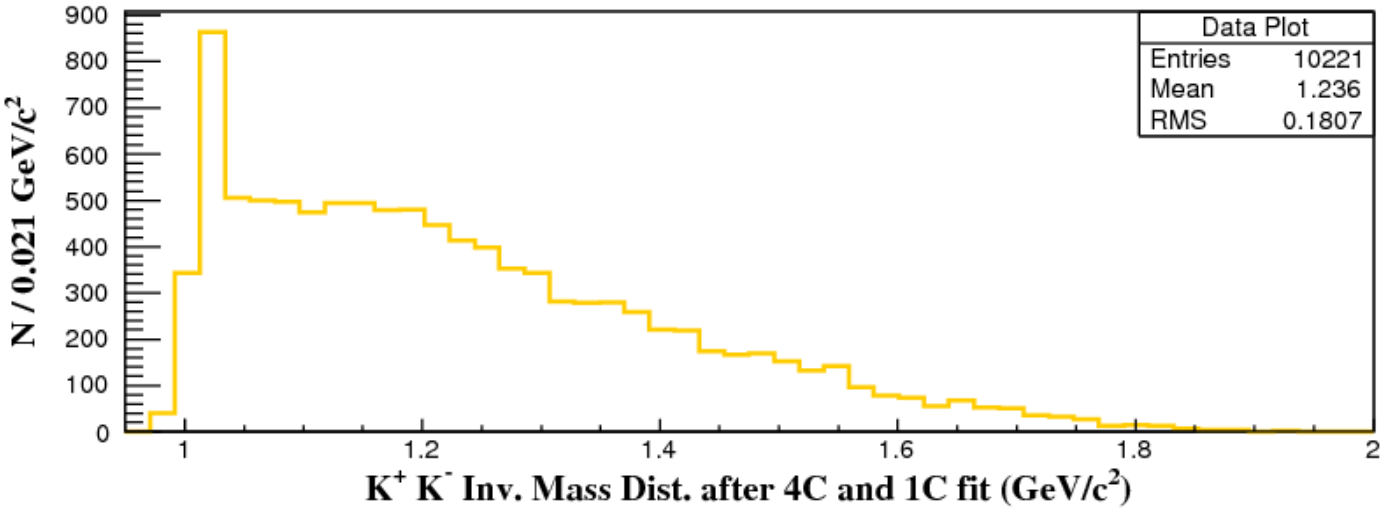

Invariant mass distribution of K^+K^- (MC and DATA) of all 9 energy points after 4C kinematic fit and without mass, χ^2_{4c} and χ^2_{1c} cuts

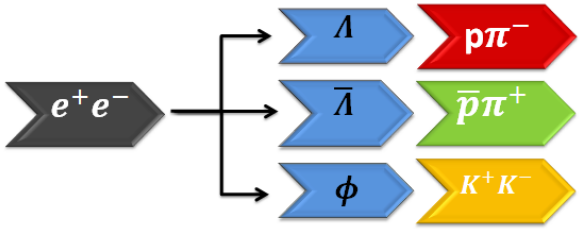

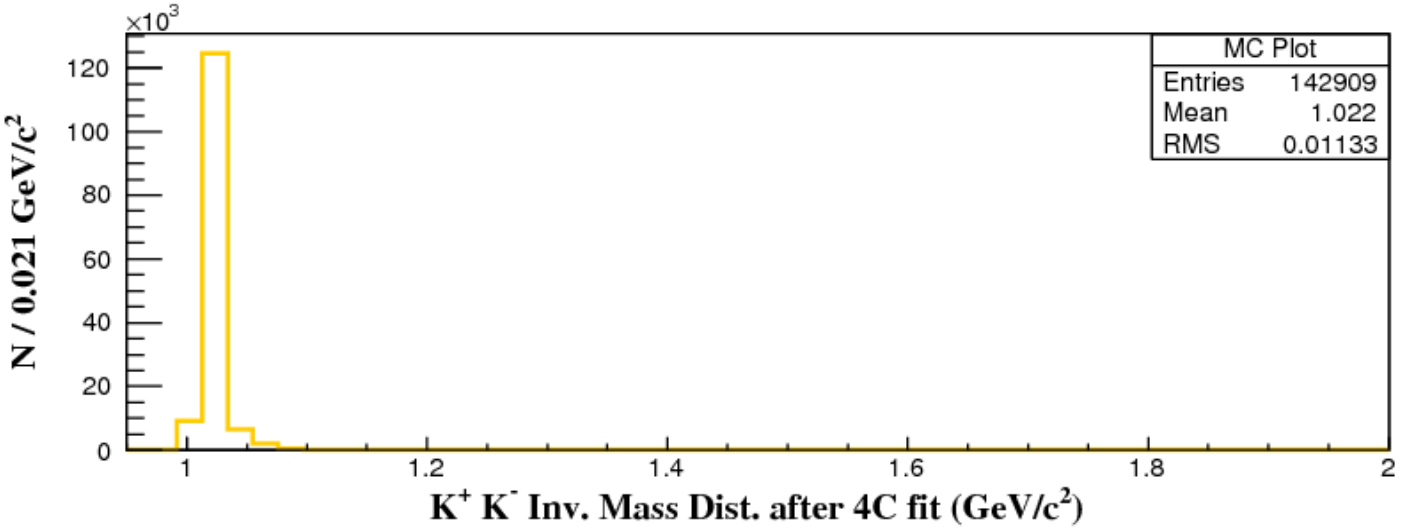

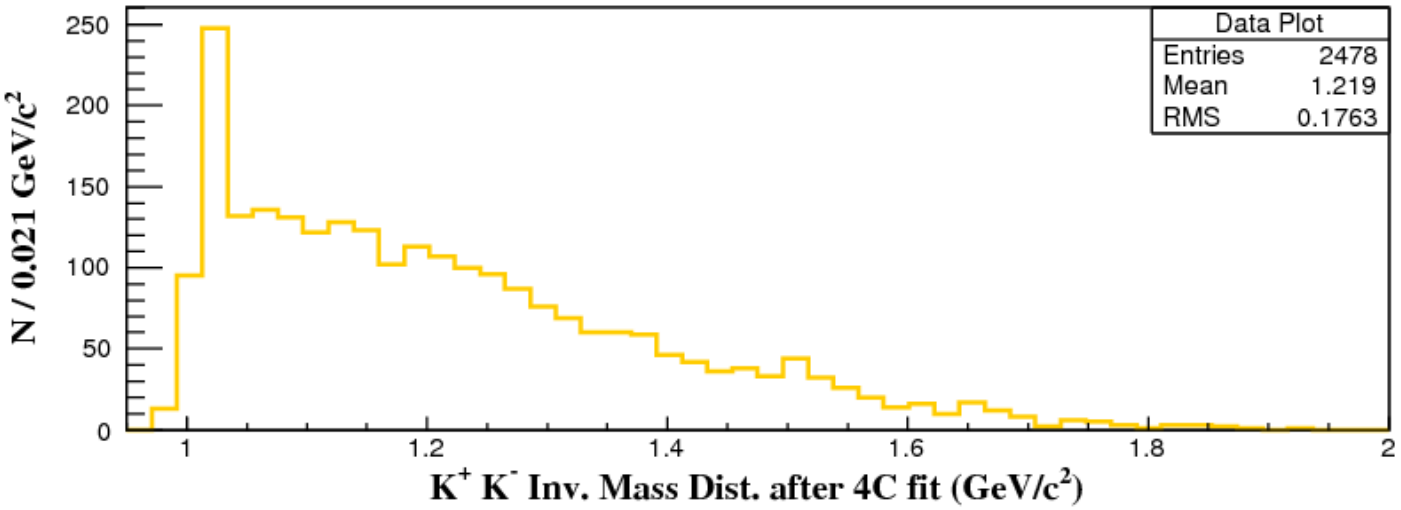

Invariant mass distribution of K^+K^- (MC and DATA) of all 9 energy points after 1C kinematic fit and without mass, χ^2_{4c} and χ^2_{1c} cuts

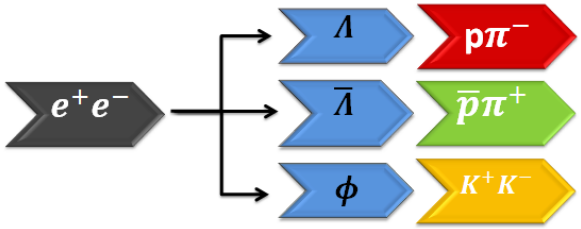

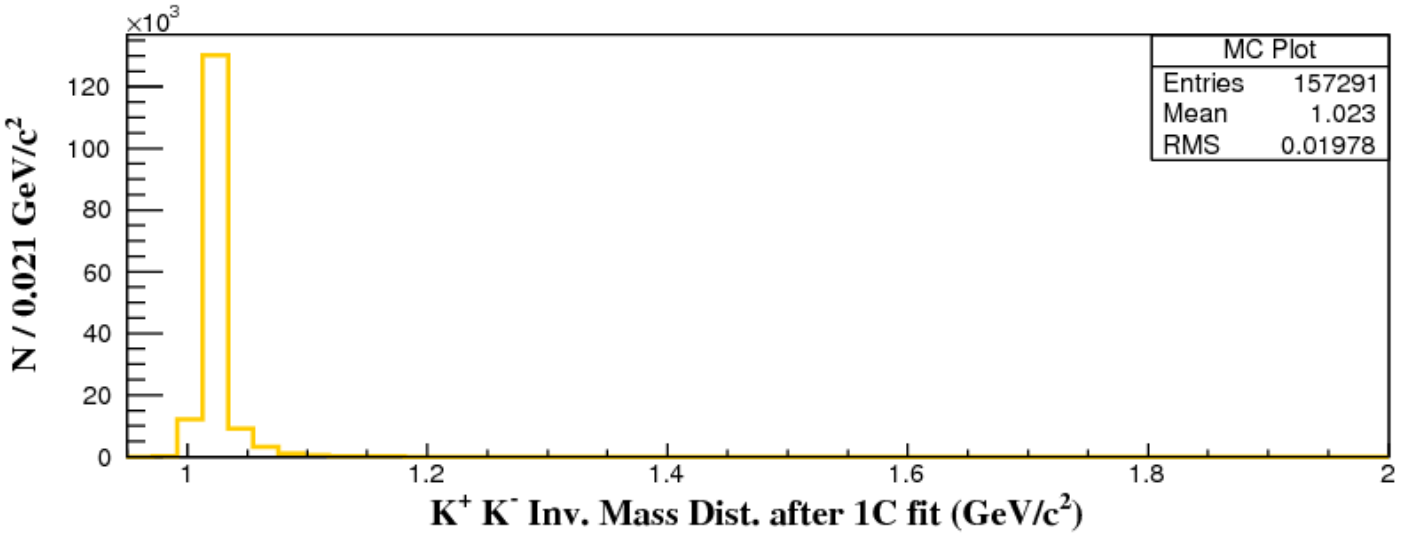

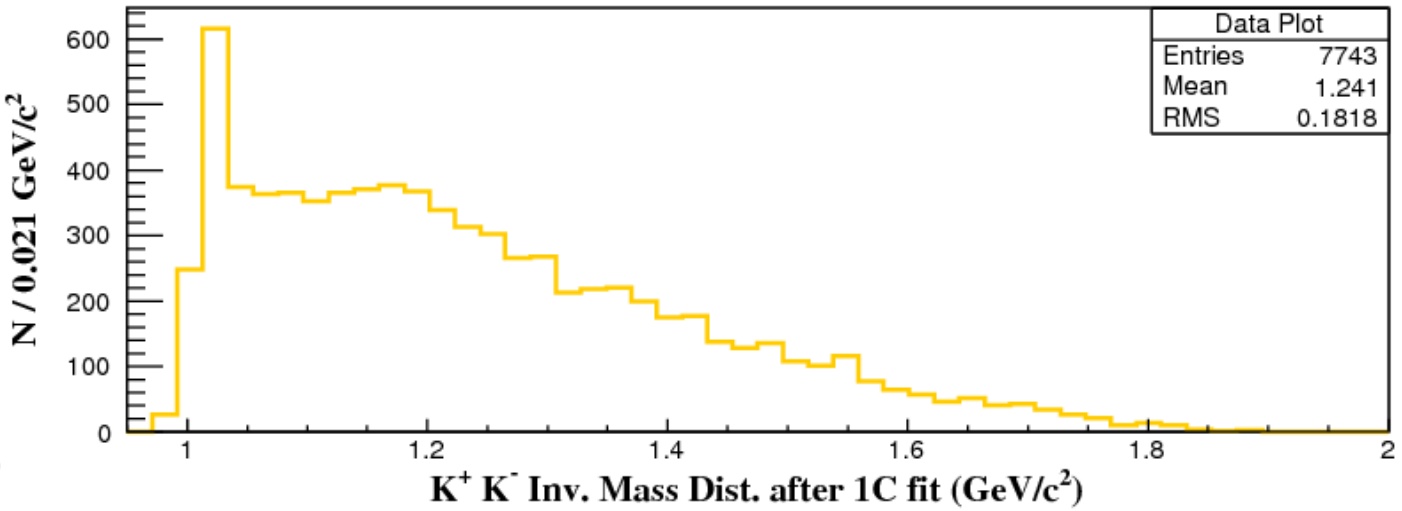

Proper time distribution of $p\pi^-$, $\bar{p}\pi^+$ and K^+K^- (MC and DATA) of all 9 energy points after 4C kinematic fit and without mass, χ^2_{4c} and χ^2_{1c} cuts

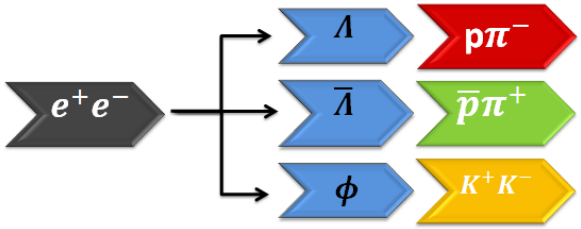

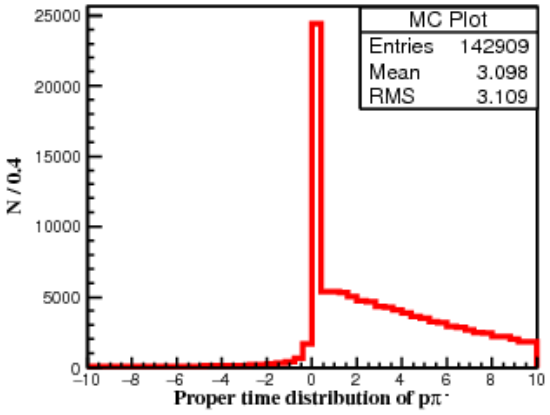

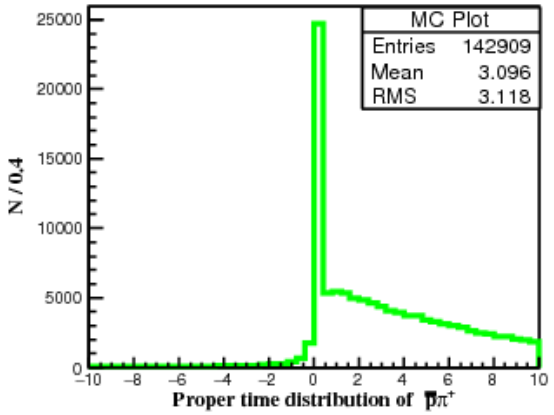

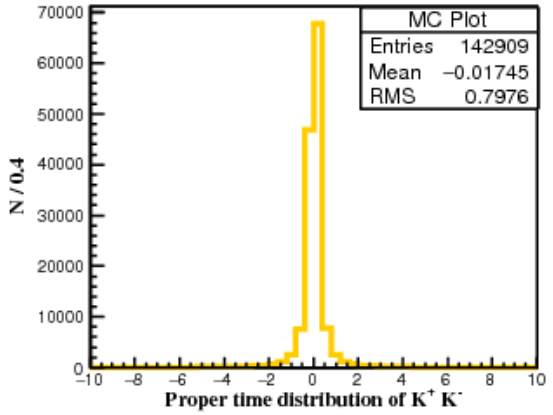

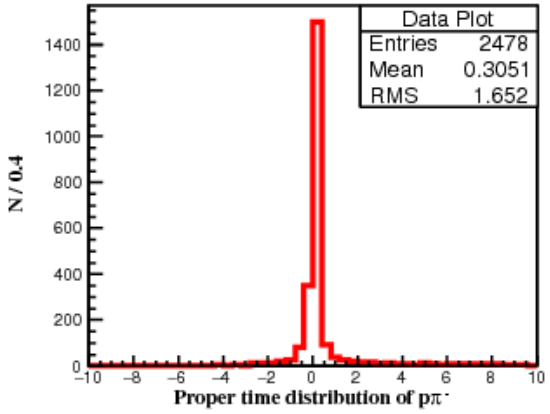

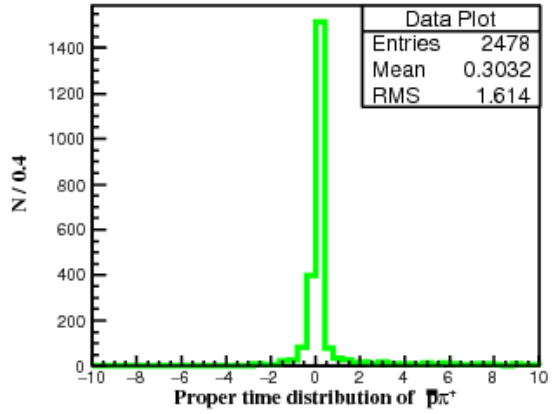

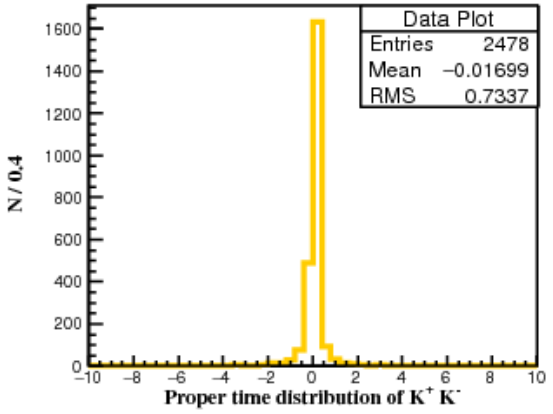

Invariant mass distribution of $p\pi^-$, $\bar{p}\pi^+$ and K^+K^- for (Inclusive MC) after 4C and 1C kinematic fit and without mass, χ^2_{4c} and χ^2_{1c} cuts

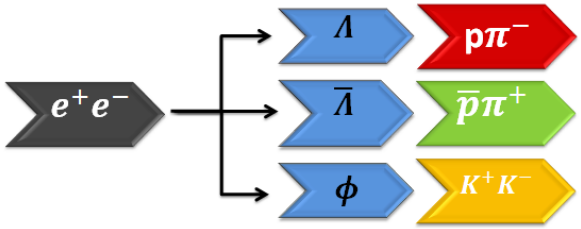

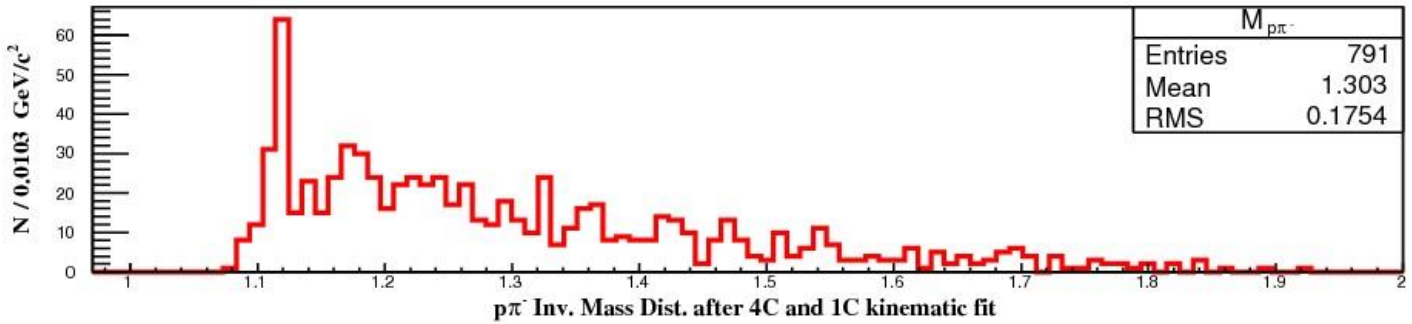

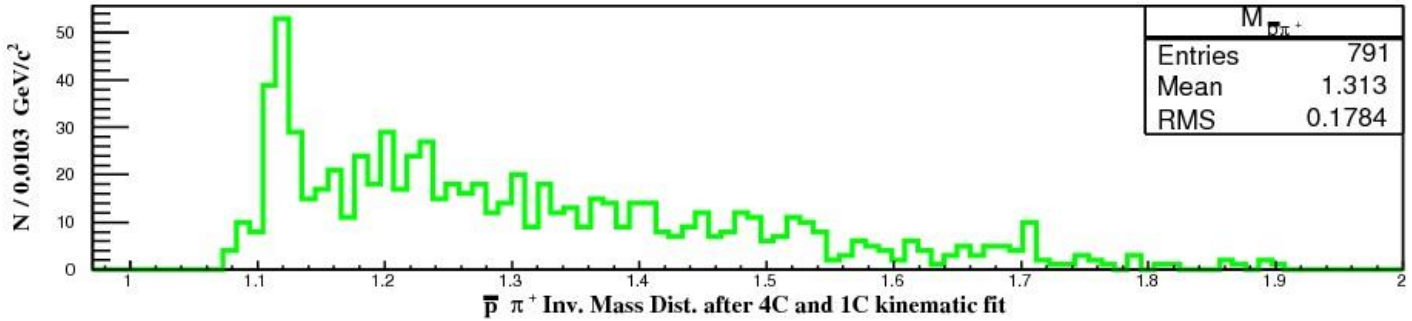

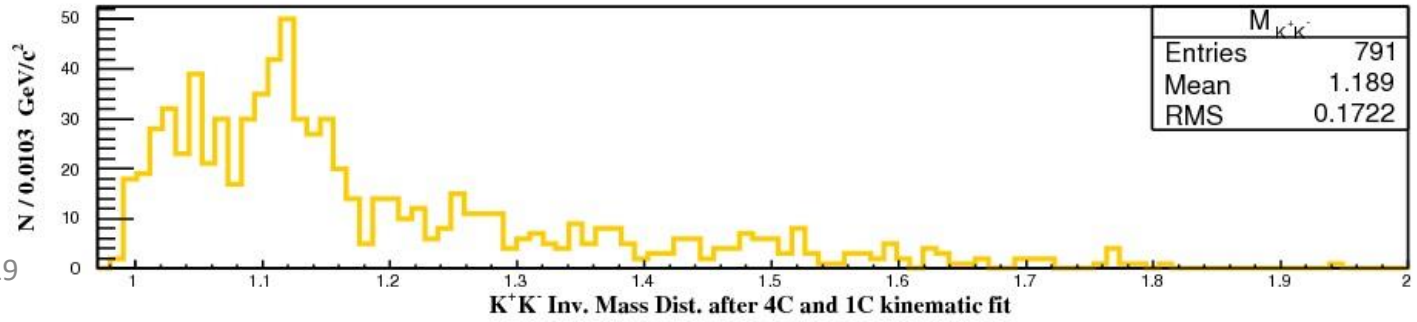

Invariant mass distribution of $p\pi^-$, $\bar{p}\pi^+$ and K^+K^- for (Inclusive MC) after 4C kinematic fit and without mass, χ^2_{4c} and χ^2_{1c} cuts

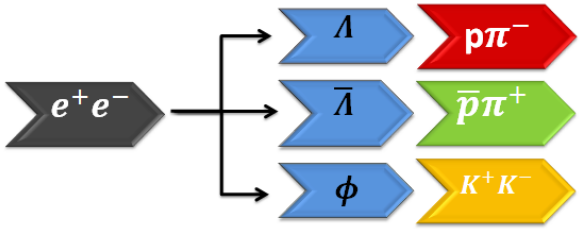

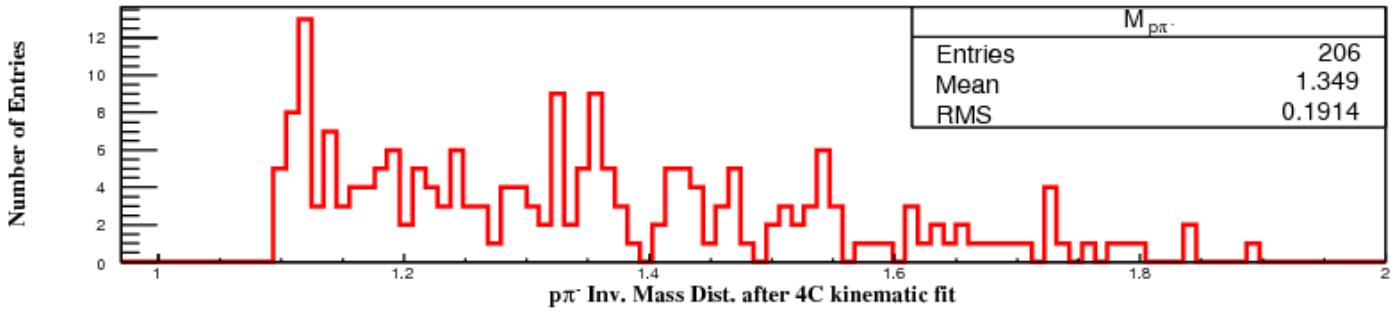

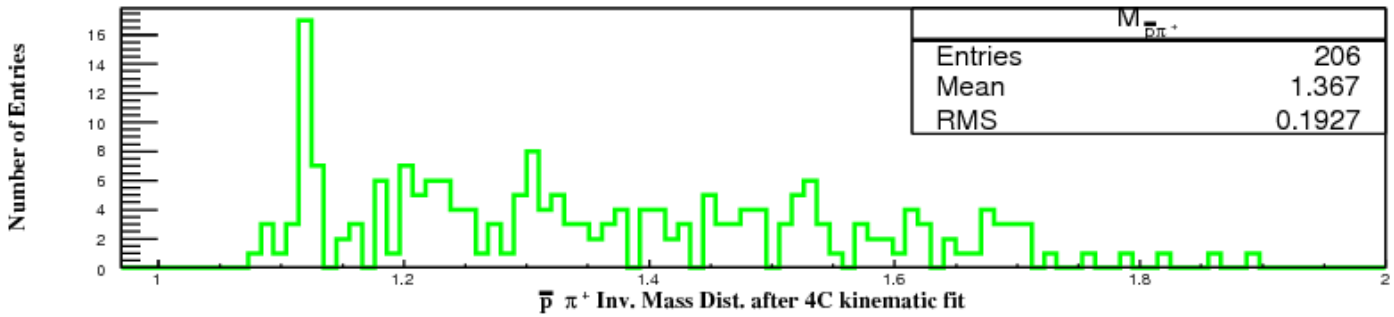

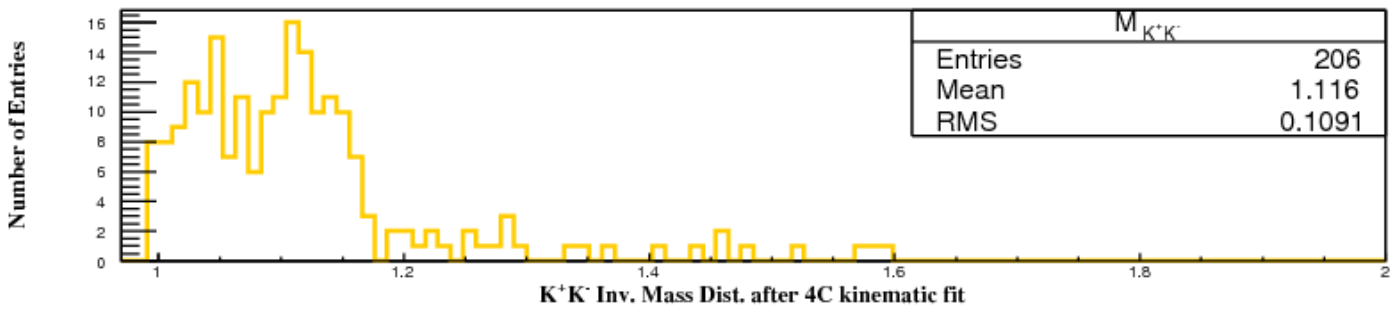

Invariant mass distribution of $p\pi^-$, $\bar{p}\pi^+$ and K^+K^- for (Inclusive MC) after 1C kinematic fit and without mass, χ^2_{4c} and χ^2_{1c} cuts

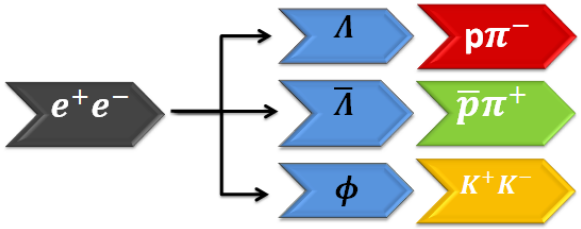

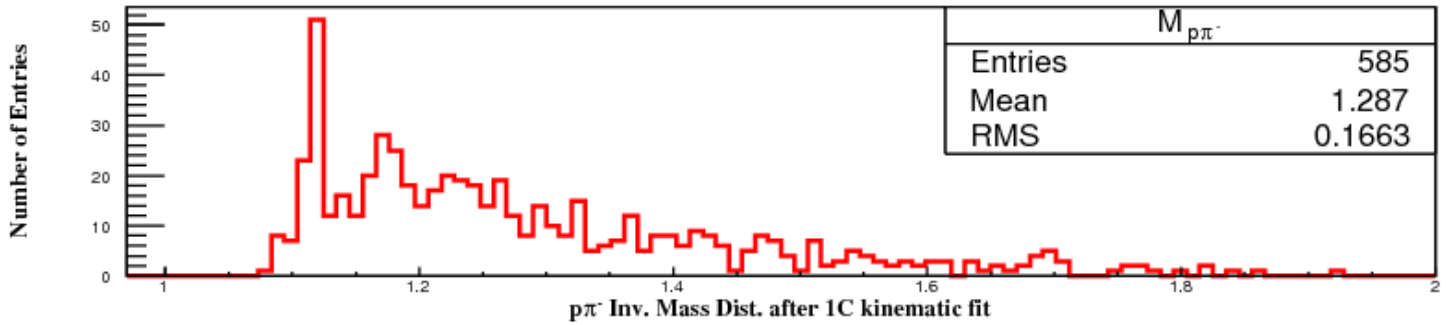

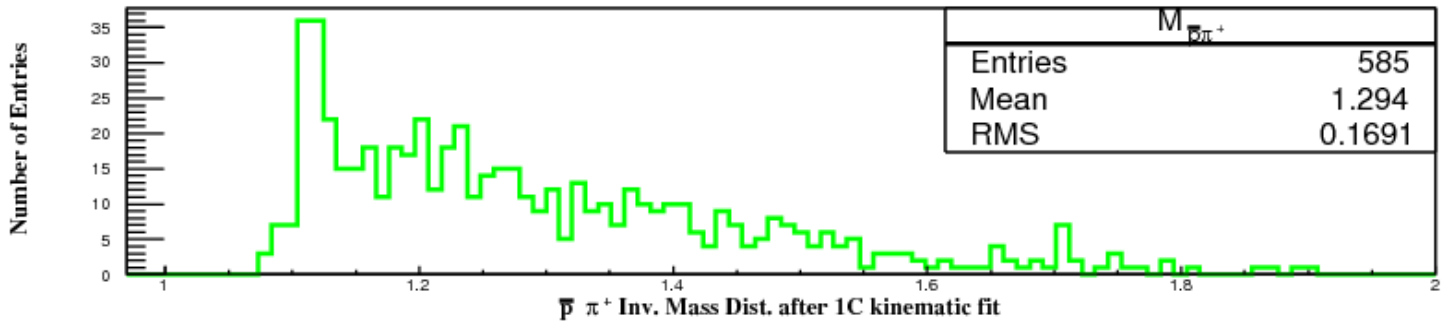

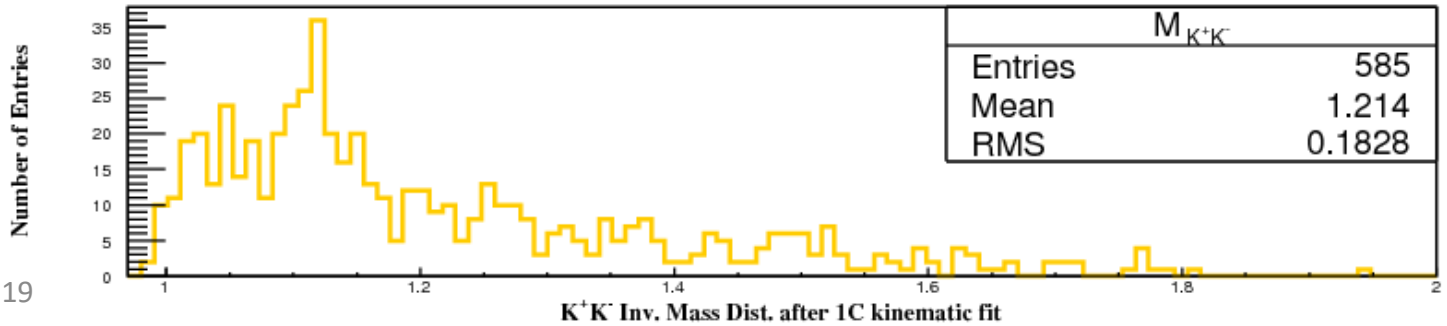

Gaussian fit to invariant mass of $M_{p\pi^-}$, $M_{\bar{p}\pi^+}$ and $M_{K^+K^-}$ for Λ, $\bar{\Lambda}$ and ϕ Resolution after 4C and 1C kinematic fit (MC)

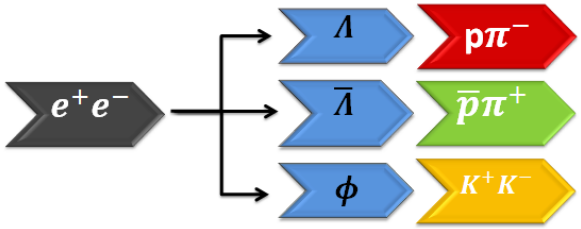

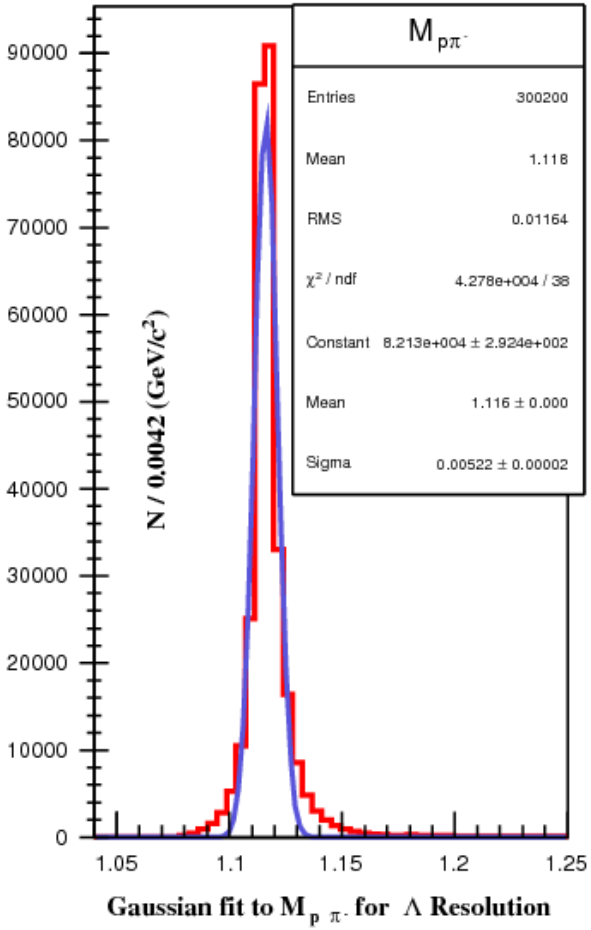

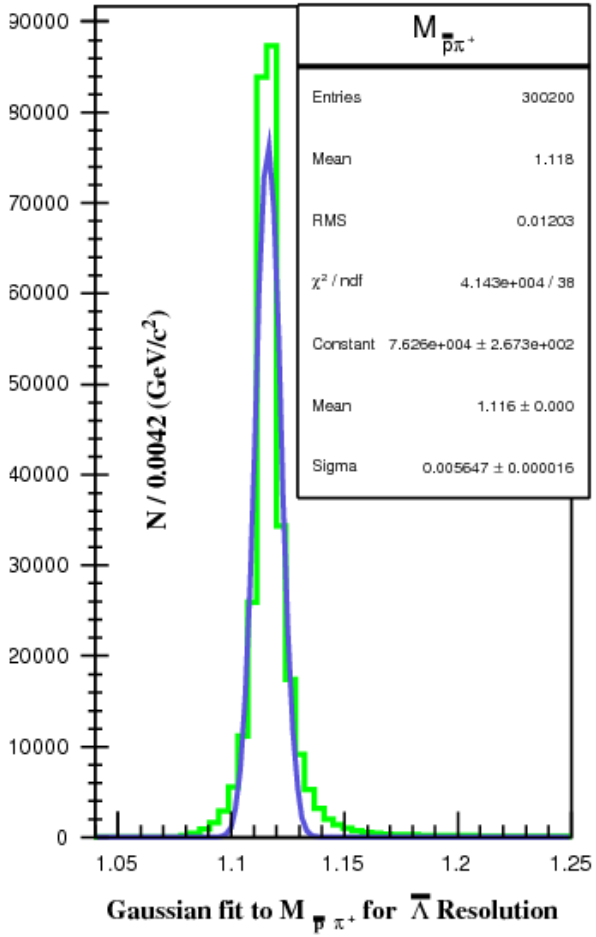

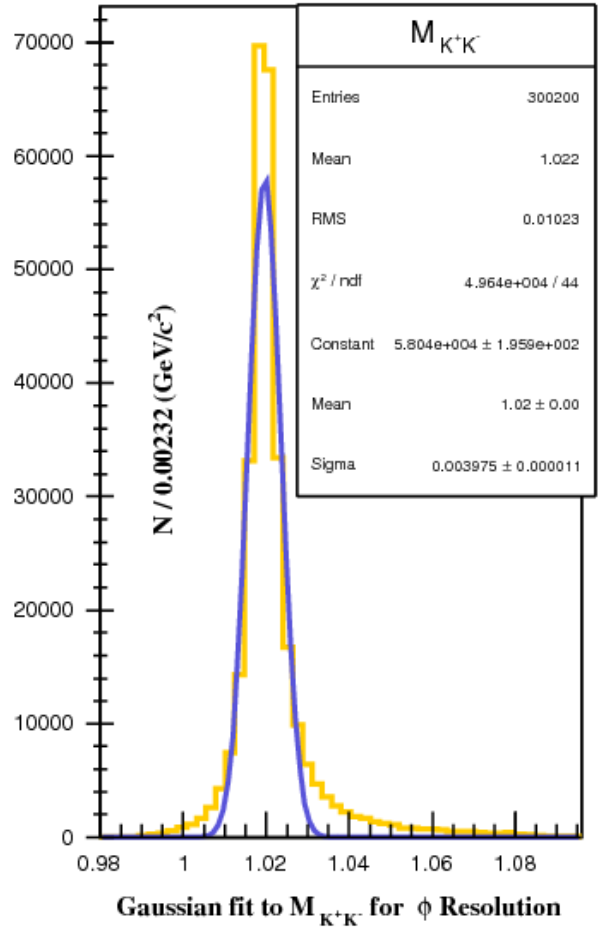

Gaussian fit to invariant mass of $M_{p\pi^-}$, $M_{\bar{p}\pi^+}$ and $M_{K^+K^-}$ for Λ, $\bar{\Lambda}$ and ϕ Resolution after 4C kinematic fit (MC)

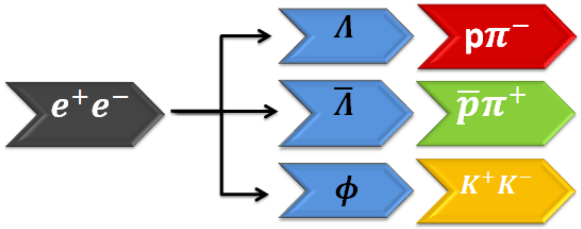

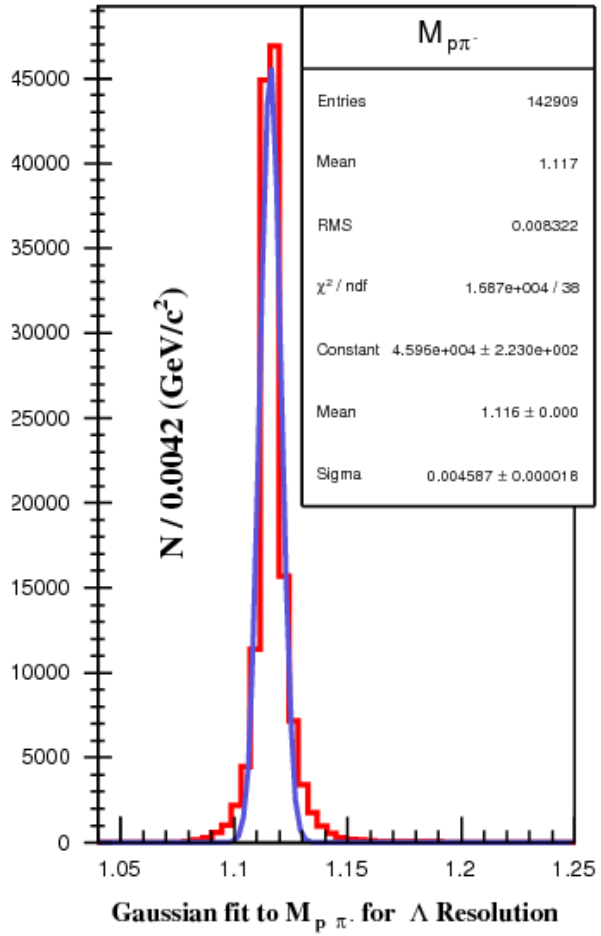

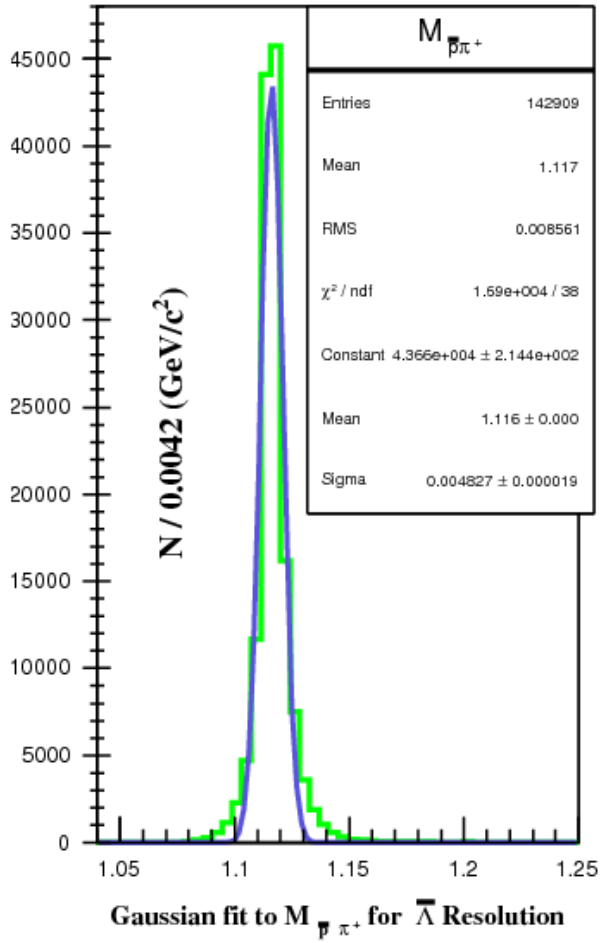

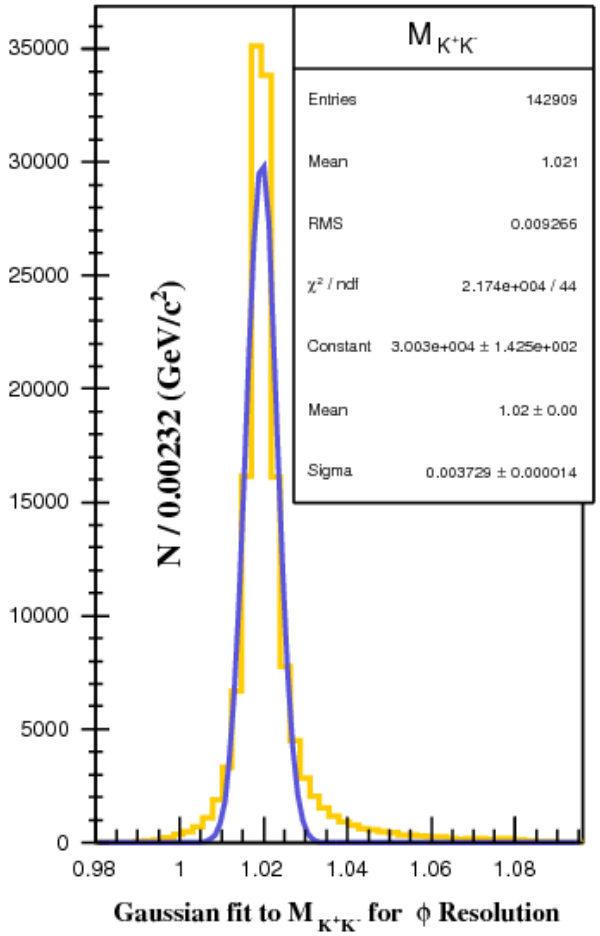

Gaussian fit to invariant mass of $M_{p\pi^-}$, $M_{\bar{p}\pi^+}$ and $M_{K^+K^-}$ for Λ, $\bar{\Lambda}$ and ϕ Resolution after 1C kinematic fit (MC)

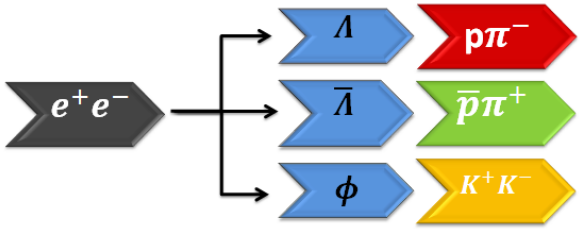

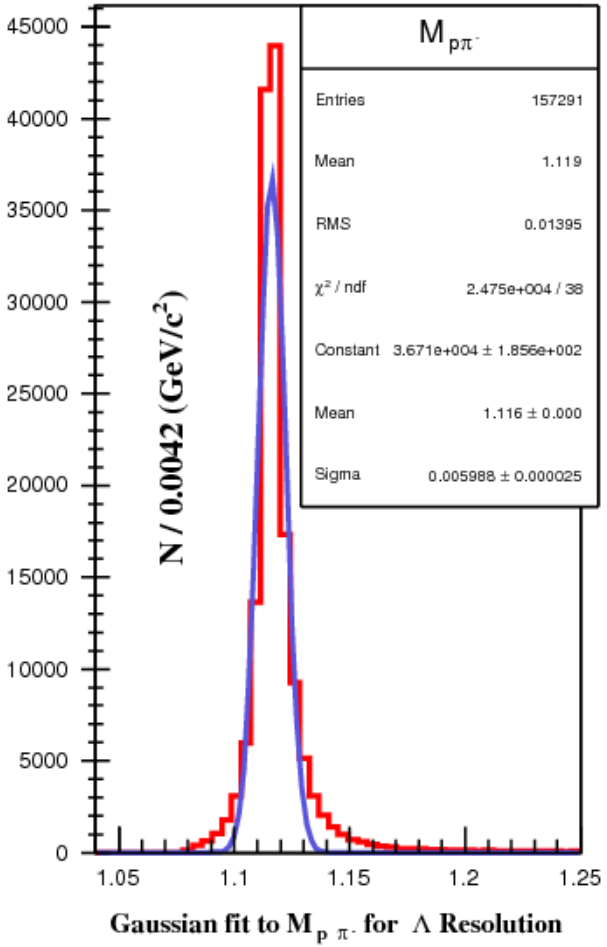

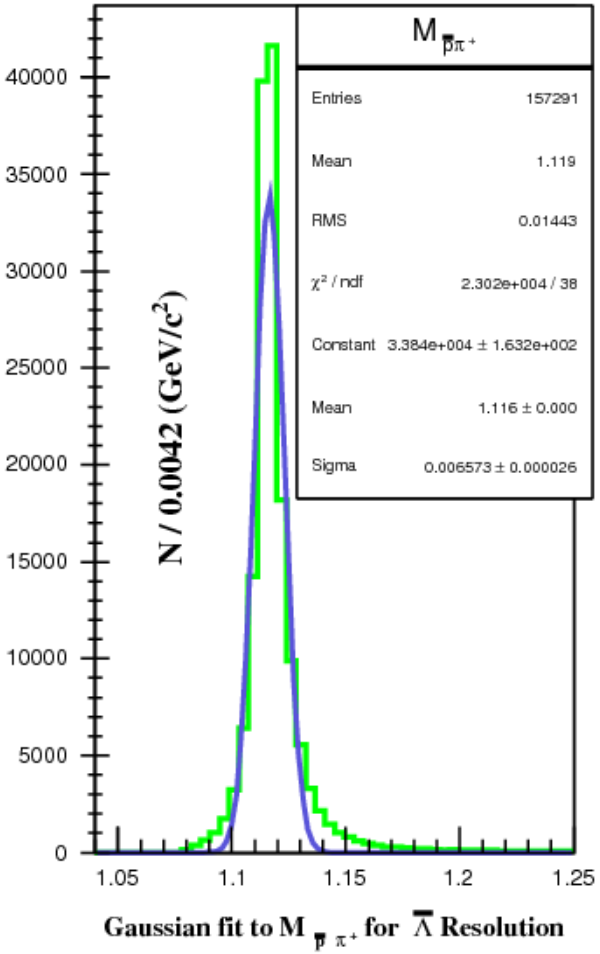

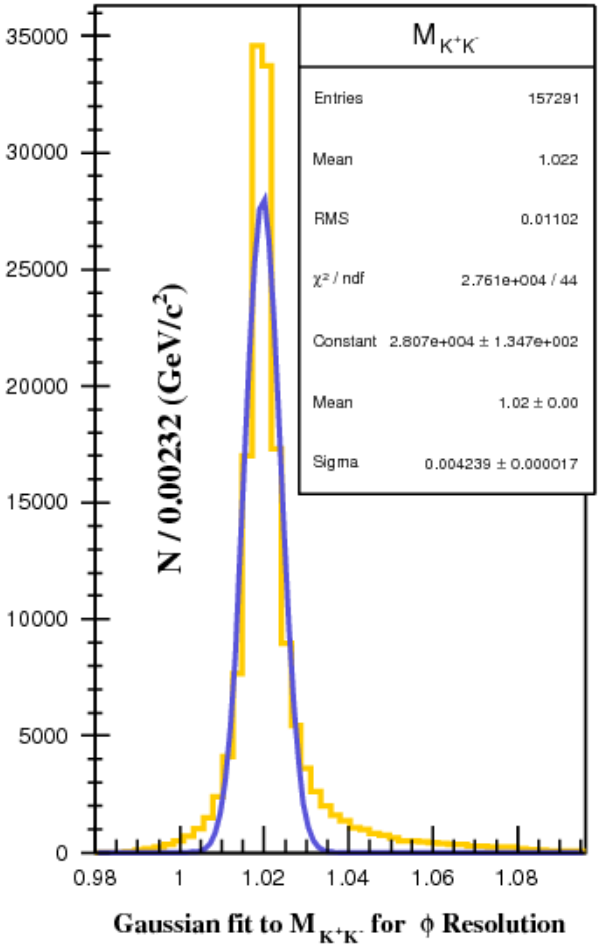

Optimization of χ^2_{4c}

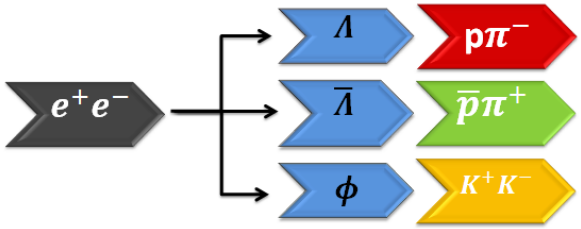

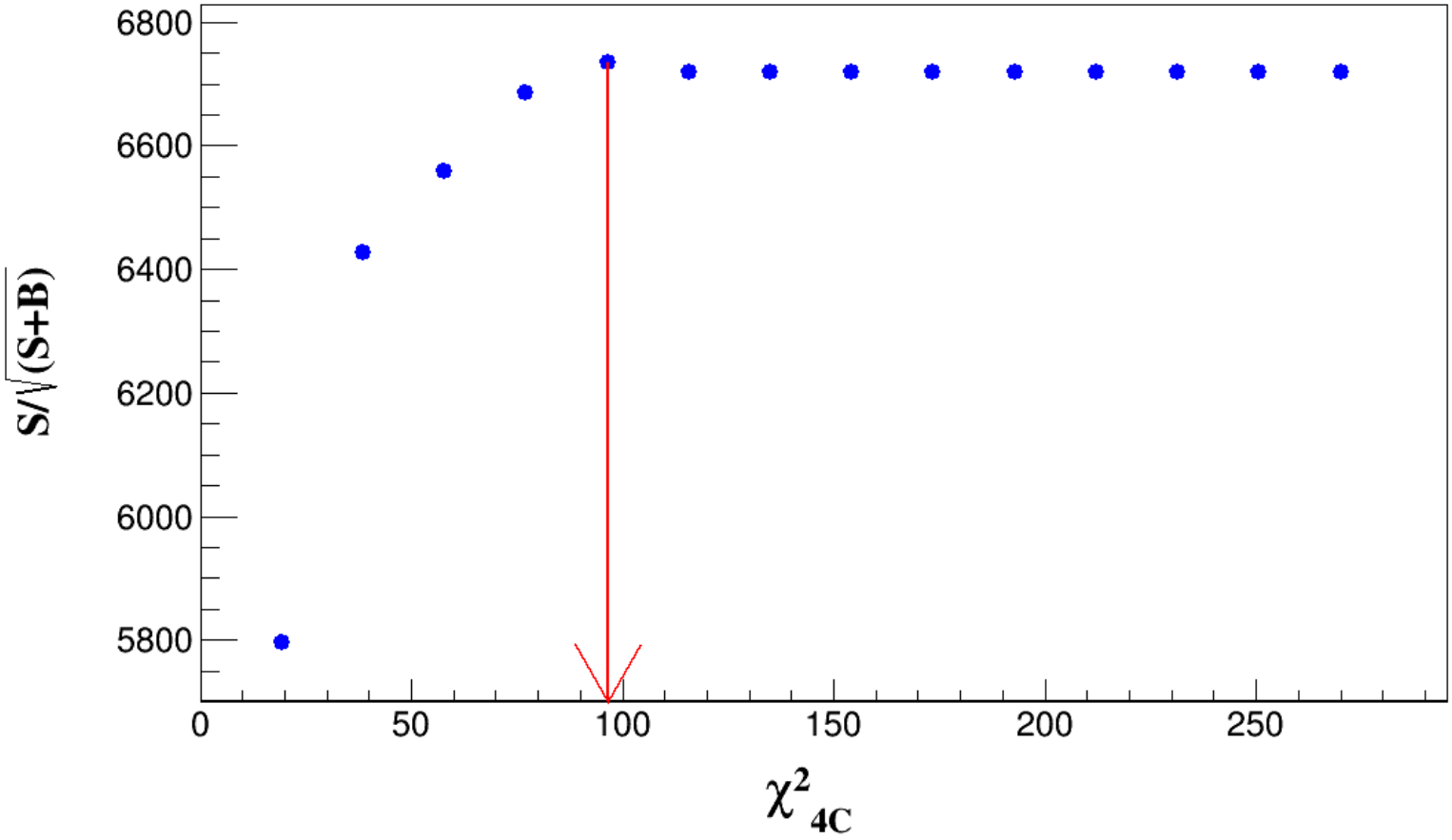

Final Event Selection for 4C and 1C

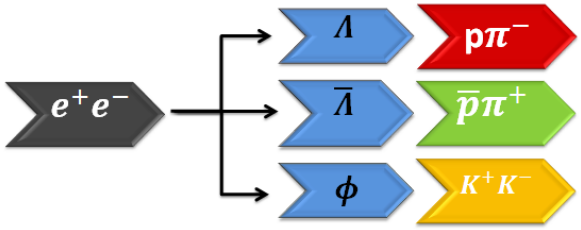

- In $e^+e^- \rightarrow \Lambda\bar{\Lambda}\phi$ study, invariant mass of K^+K^- is plotted here. To look all $\Lambda\bar{\Lambda}\phi$ events, cuts have been applied (within 3σ) on ϕ by fitting the invariant mass of $p\pi^-$ and $\bar{p}\pi^+$ in MC. Fitting suggested the σ value to be 0.004GeV . To suppress the background some other cuts have also been applied including $\chi^2_{4c\text{ and }1c}$. All the cuts with their range that are applied to plot invariant mass of K^+K^- is given below.

- Following inclusive cuts of $p\pi^-$, $\bar{p}\pi^+$ and $\chi^2_{4c\ and\ 1c}$ are used:
  $|M_{p\pi^-} - M_{\Lambda}| < 0.0156$,
  $|M_{\bar{p}\pi^+} - M_{\bar{\Lambda}}| < 0.01694$ and
  $\chi^2_{4c\ and\ 1c} < 80$

- Following exclusive cuts of $p\pi^-K^-$, $\bar{p}\pi^+K^+$ and $p\bar{p}\pi^-\pi^+$ are used:
  $|M_{p\pi^-K^-} - M_{\Omega}| > 0.023$,
  $|M_{\bar{p}\,\pi^+K^+} - M_{\bar{\Omega}}| > 0.023$ and
  $|M_{p\bar{p}\,\pi^-\pi^+} - M_{J/\psi}| > 0.00889$

Final Event Selection for 4C

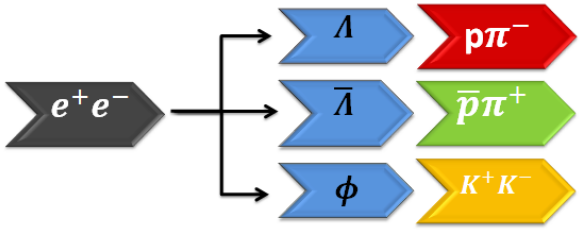

- Following inclusive cuts of $p\pi^-$, $\bar{p}\pi^+$ and χ^2_{4c} are used:
  $|M_{p\pi^-} - M_{\Lambda}| < 0.0137$,
  $|M_{\bar{p}\pi^+} - M_{\bar{\Lambda}}| < 0.0144$ and
  $\chi^2_{4c} < 80$

- Following exclusive cuts of $p\pi^-K^-$, $\bar{p}\pi^+K^+$ and $p\bar{p}\pi^-\pi^+$ are used:
  $|M_{p\pi^-K^-} - M_{\Omega}| > 0.0207$,
  $|M_{\bar{p}\,\pi^+K^+} - M_{\bar{\Omega}}| > 0.0207$ and
  $|M_{p\bar{p}\,\pi^-\pi^+} - M_{J/\psi}| > 0.00796$

Final Event Selection for 1C

- Following inclusive cuts of $p\pi^-$, $\bar{p}\pi^+$ and χ^2_{1c} are used:
  $|M_{p\pi^-} - M_{\Lambda}| < 0.01796$,
  $|M_{\bar{p}\pi^+} - M_{\bar{\Lambda}}| < 0.01972$ and
  $\chi^2_{1c} < 80$

- Following exclusive cuts of $p\pi^-K^-$, $\bar{p}\pi^+K^+$ and $p\bar{p}\pi^-\pi^+$ are used:
  $|M_{p\pi^-K^-} - M_{\Omega}| > 0.025$,
  $|M_{\bar{p}\,\pi^+K^+} - M_{\bar{\Omega}}| > 0.025$ and
  $|M_{p\bar{p}\,\pi^-\pi^+} - M_{J/\psi}| > 0.010$

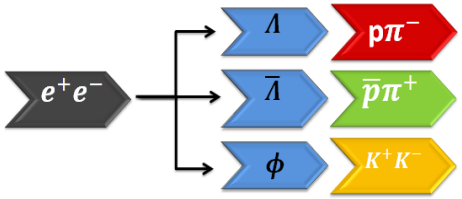

K^+K^- Invariant mass distribution of data of All 9 energy points after 4C and 1C kinematic fit under $|M_{p\pi^-} - M_{\Lambda}| < 0.01566$, $|M_{\bar{p}\pi^+} - M_{\bar{\Lambda}}| < 0.01694$, $\chi^2_{4c\text{ and }1c} < 80$, $|M_{p\pi^-K^-} - M_{\Omega}| > 0.023$, $|M_{\bar{p}\pi^+K^+} - M_{\bar{\Omega}}| > 0.023$ and $|M_{p\bar{p}\pi^-\pi^+} - M_{J/\psi}| > 0.00889$ cuts

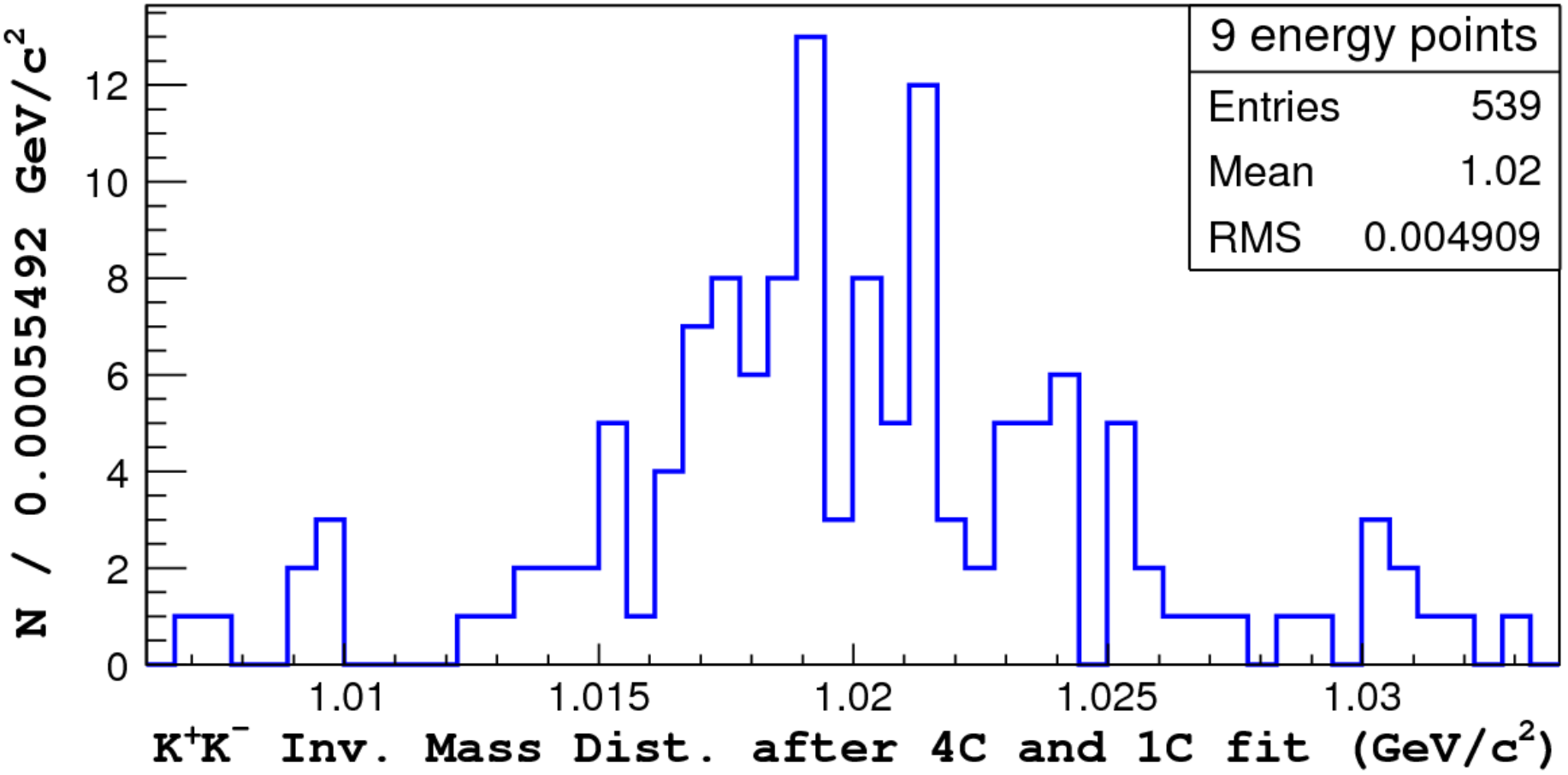

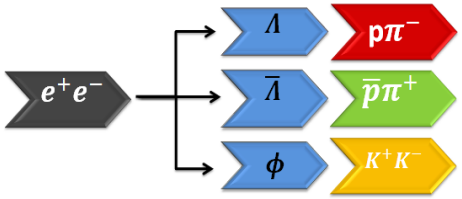

K^+K^- Invariant mass distribution of data of All 9 energy points after 4C kinematic fit under $|M_{p\pi^-} - M_{\Lambda}| < 0.0137$, $|M_{\bar{p}\pi^+} - M_{\bar{\Lambda}}| < 0.0144$, $\chi^2_{4c} < 80$, $|M_{p\pi^-K^-} - M_{\Omega}| > 0.0207$, $|M_{\bar{p}\pi^+K^+} - M_{\bar{\Omega}}| > 0.0207$ and $|M_{p\bar{p}\pi^-\pi^+} - M_{J/\psi}| > 0.00796$ cuts

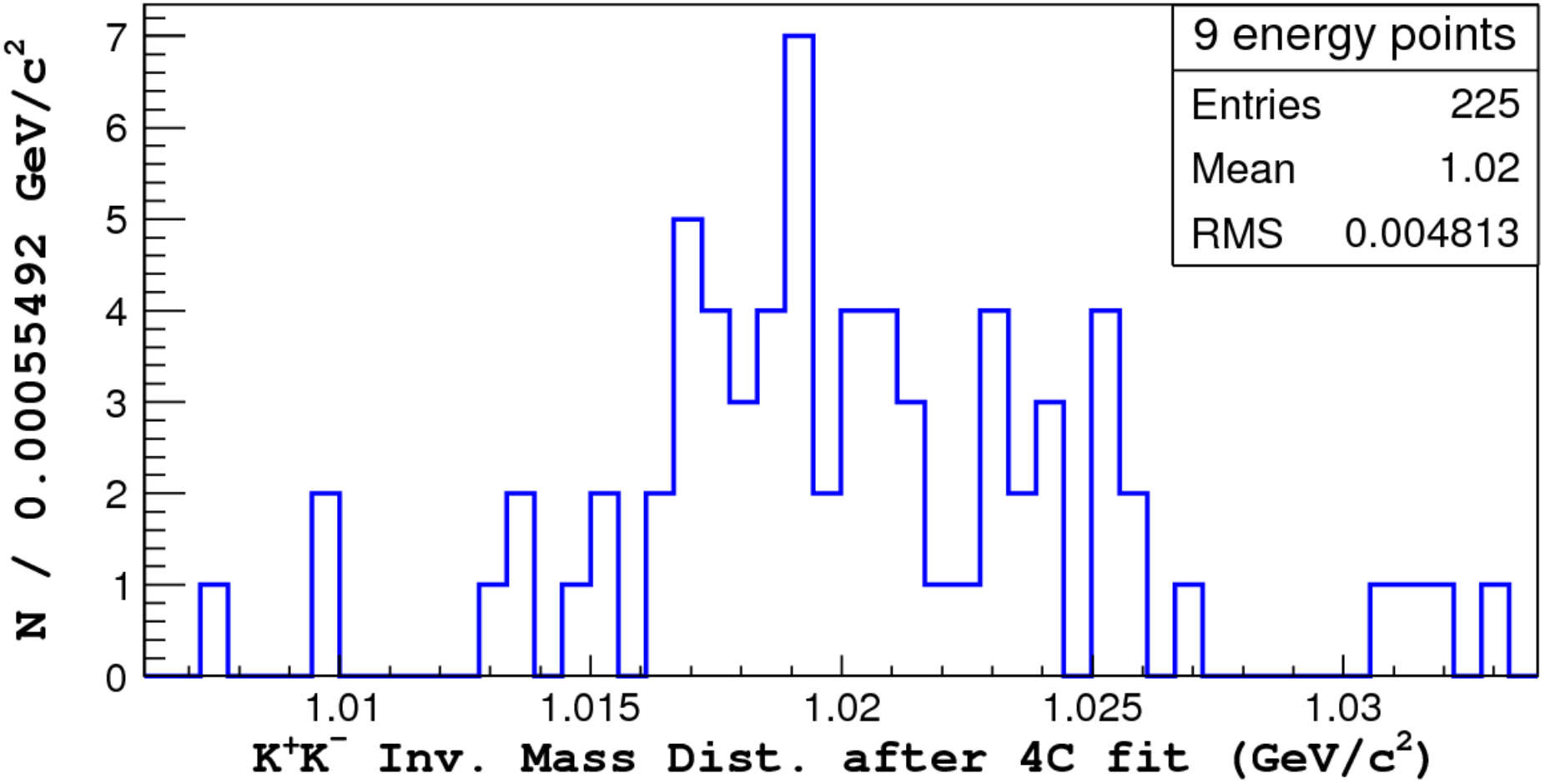

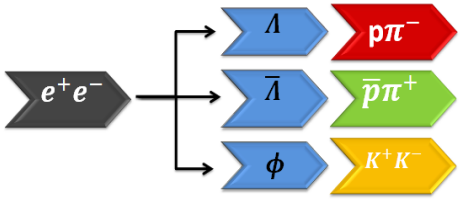

K^+K^- Invariant mass distribution of data of All 9 energy points after 1C kinematic fit under $|M_{p\pi^-} - M_{\Lambda}| < 0.01796$, $|M_{\bar{p}\pi^+} - M_{\bar{\Lambda}}| < 0.01972$, $\chi^2_{1c} < 80$, $|M_{p\pi^-K^-} - M_{\Omega}| > 0.025$, $|M_{\bar{p}\pi^+K^+} - M_{\bar{\Omega}}| > 0.025$ and $|M_{p\bar{p}\pi^-\pi^+} - M_{J/\psi}| > 0.010$ cuts

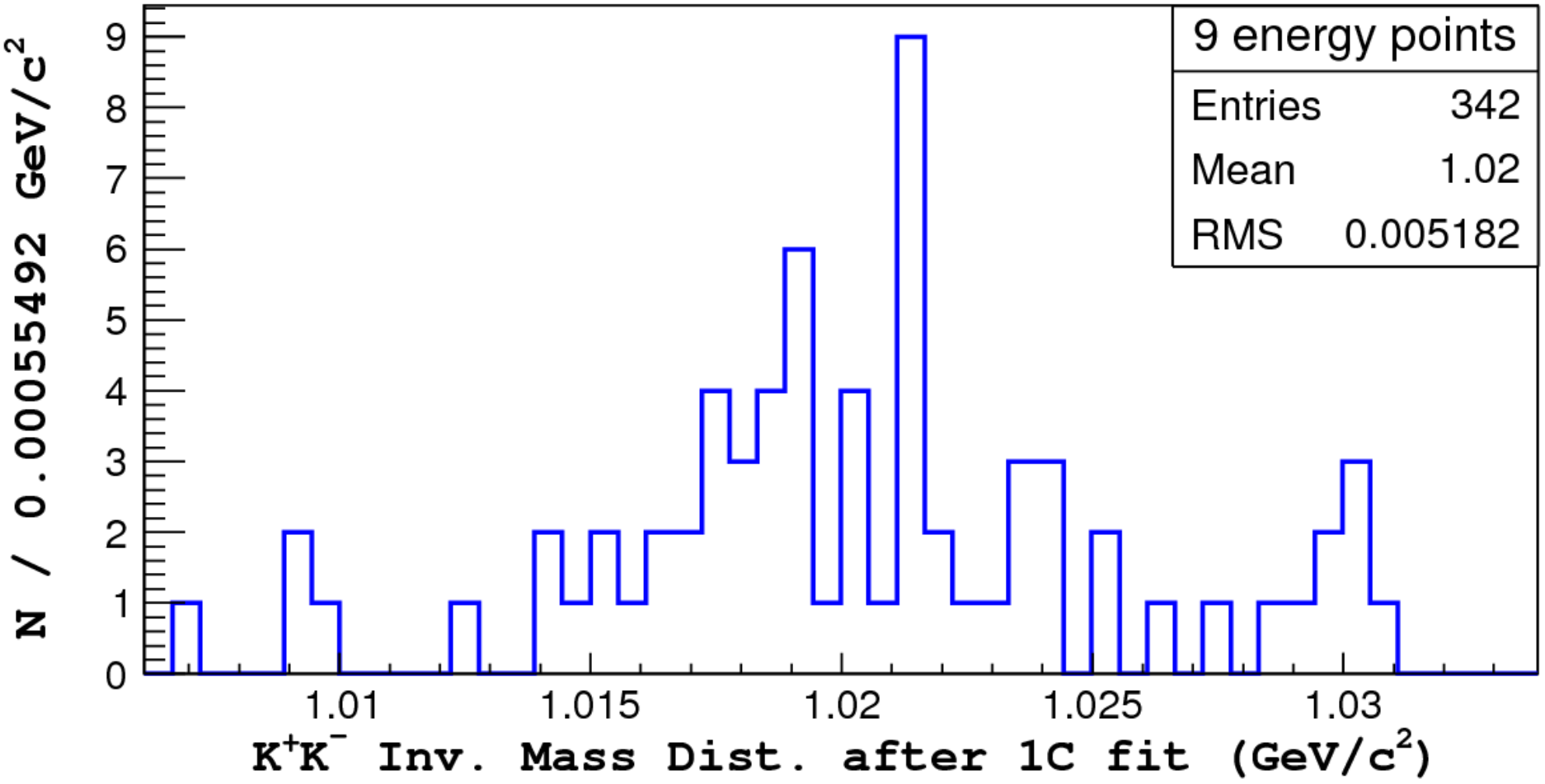

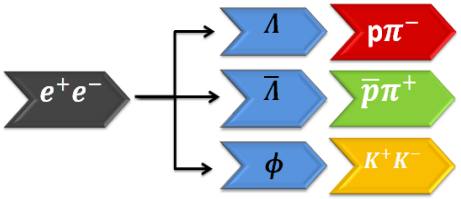

K^+K^- Invariant mass distribution of data of each energy point after 4C and 1C kinematic fit under $|M_{p\pi^-} - M_{\Lambda}| < 0.01566$, $|M_{\bar{p}\pi^+} - M_{\bar{\Lambda}}| < 0.01694$, $\chi^2_{4c\text{ and }1c} < 80$, $|M_{p\pi^-K^-} - M_{\Omega}| > 0.023$, $|M_{\bar{p}\pi^+K^+} - M_{\bar{\Omega}}| > 0.023$ and $|M_{p\bar{p}\pi^-\pi^+} - M_{J/\psi}| > 0.00889$ cuts

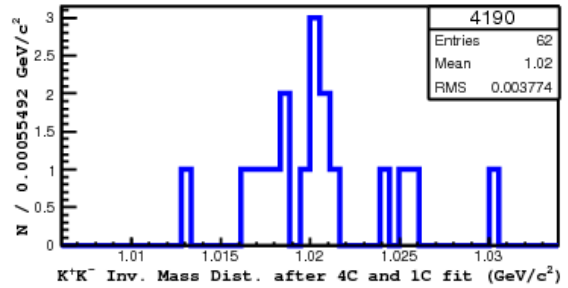

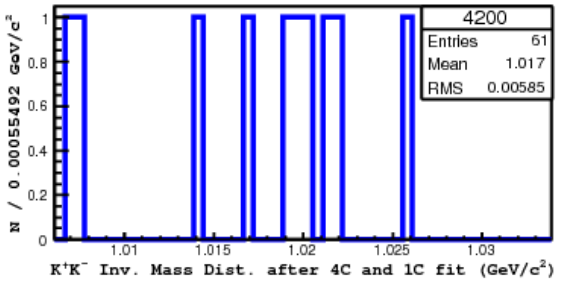

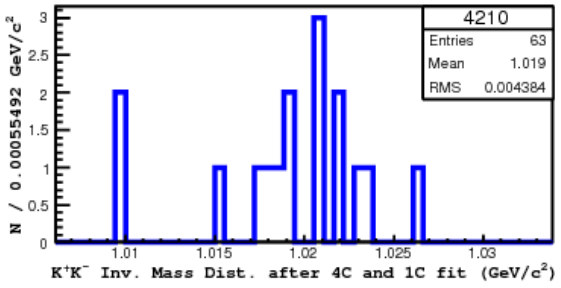

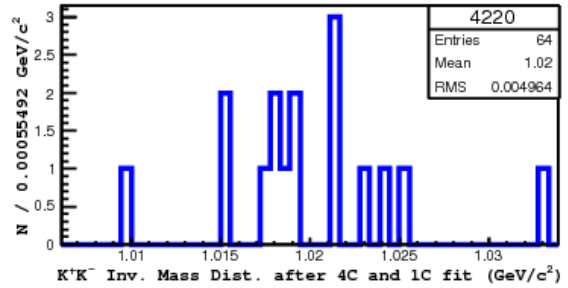

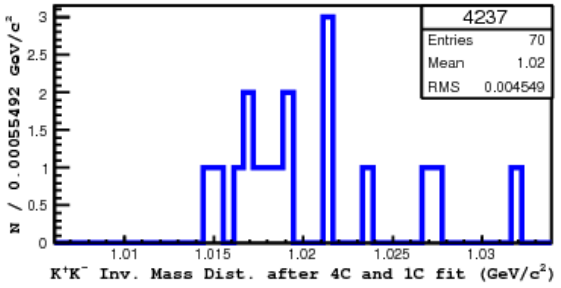

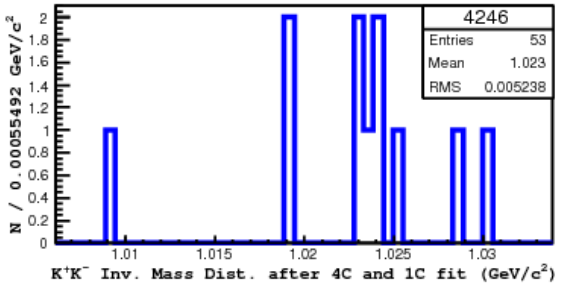

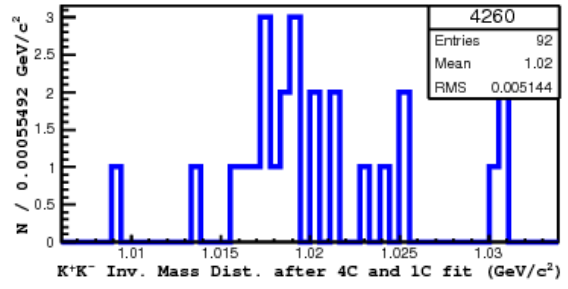

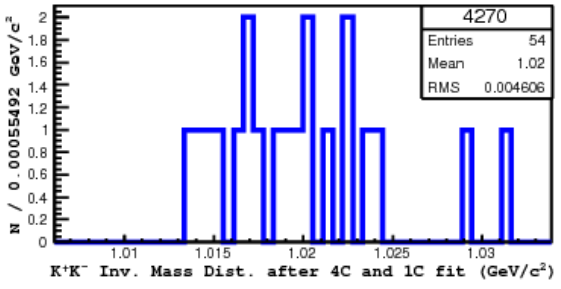

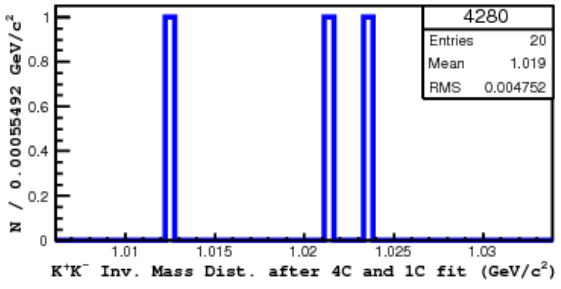

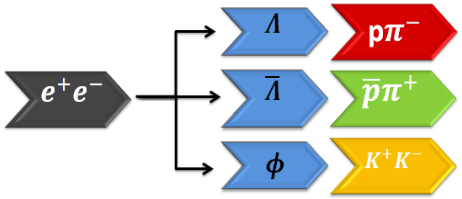

K^+K^- Invariant mass distribution of data of each energy point after 4C kinematic fit under

$|M_{p\pi^-} - M_{\Lambda}| < 0.0137$, $|M_{\bar{p}\pi^+} - M_{\bar{\Lambda}}| < 0.0144$, $\chi^2_{4c} < 80$, $|M_{p\pi^-K^-} - M_{\Omega}| > 0.0207$, $|M_{\bar{p}\pi^+K^+} - M_{\bar{\Omega}}| > 0.0207$ and $|M_{p\bar{p}\pi^-\pi^+} - M_{J/\psi}| > 0.00796$ cuts

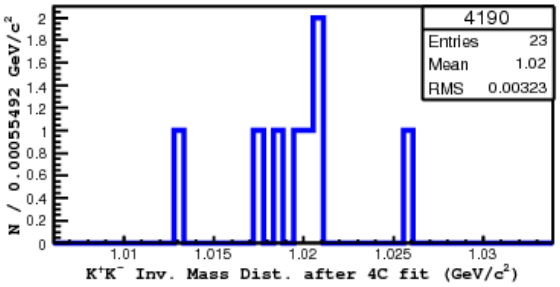

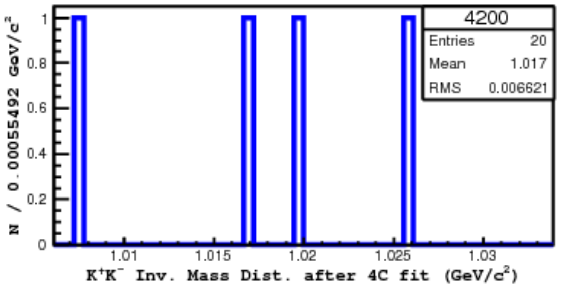

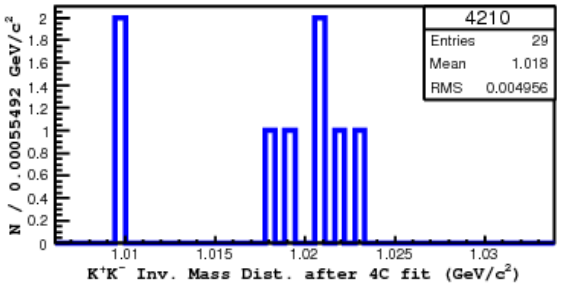

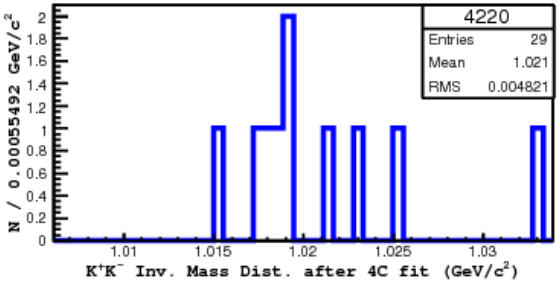

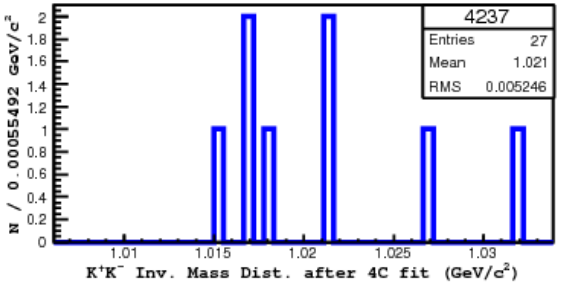

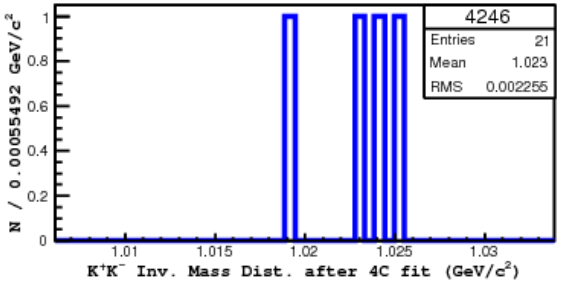

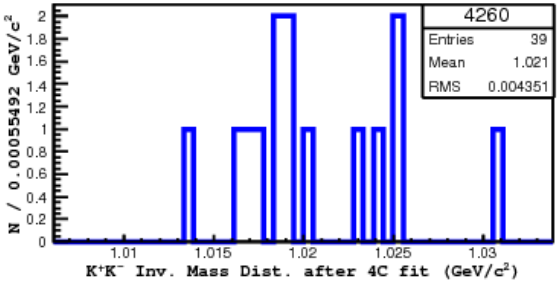

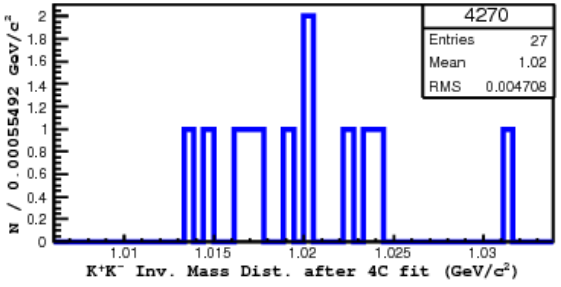

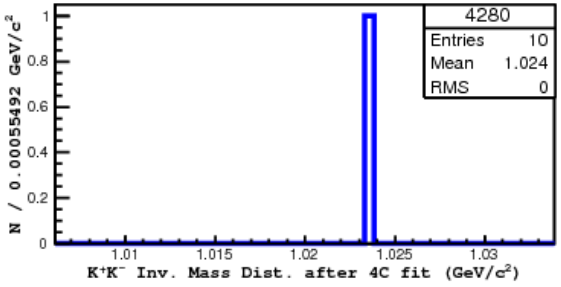

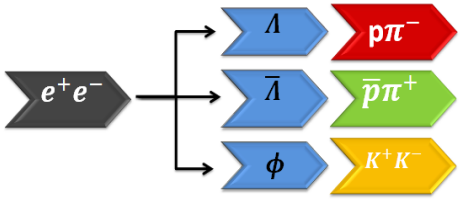

K^+K^- Invariant mass distribution of data of each energy point after 1C kinematic fit under

$|M_{p\pi^-} - M_{\Lambda}| < 0.01796$, $|M_{\bar{p}\pi^+} - M_{\bar{\Lambda}}| < 0.01972$, $\chi^2_{1c} < 80$,

$|M_{p\pi^-K^-} - M_{\Omega}| > 0.025$, $|M_{\bar{p}\pi^+K^+} - M_{\bar{\Omega}}| > 0.025$ and

$|M_{p\bar{p}\pi^-\pi^+} - M_{J/\psi}| > 0.010$ cuts

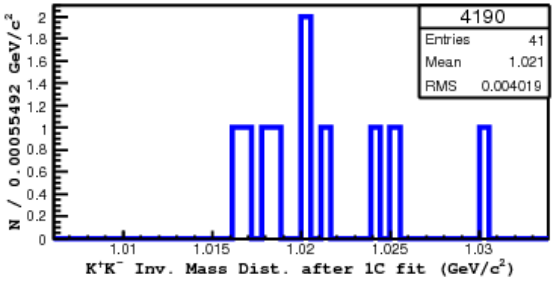

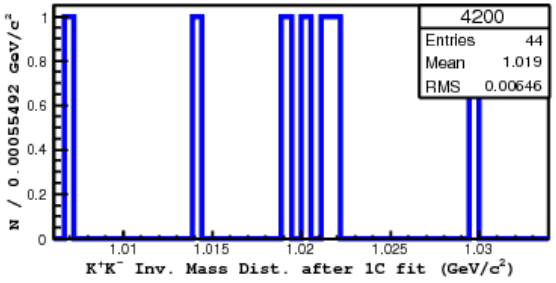

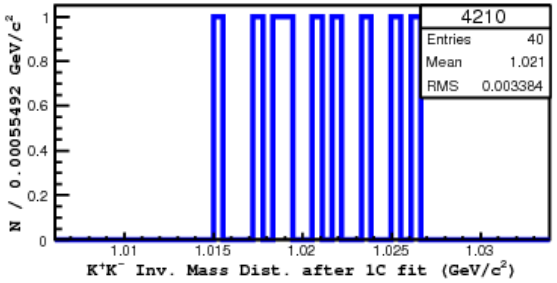

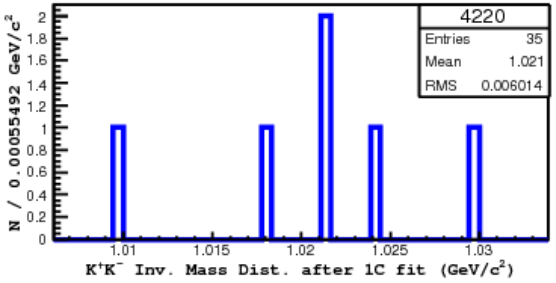

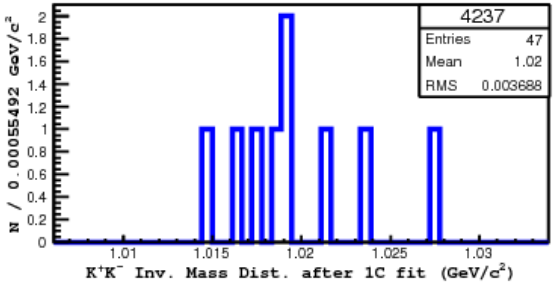

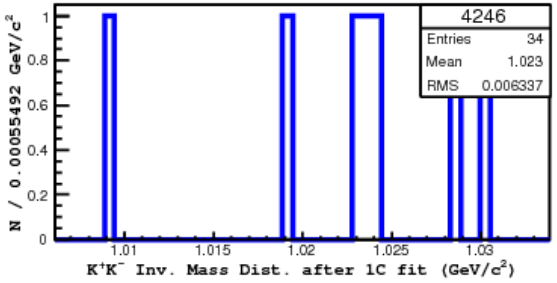

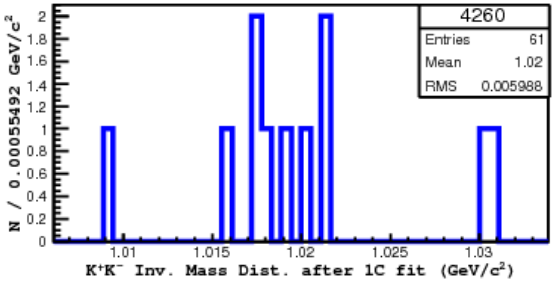

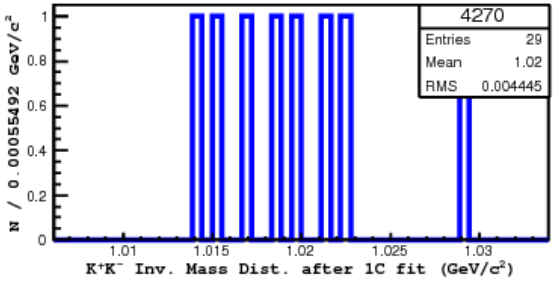

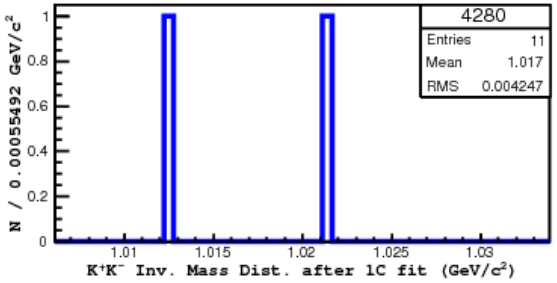

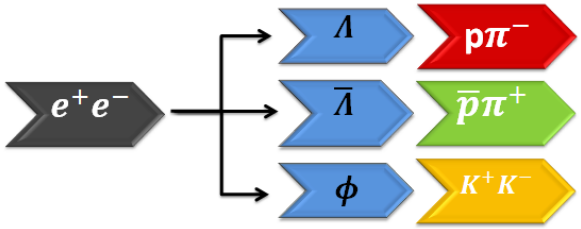

K^+K^- Invariant mass distribution of data after 4C and 1C kinematic fit under $|M_{p\pi^-} - M_{\Lambda}| < 0.01566$, $|M_{\bar{p}\pi^+} - M_{\bar{\Lambda}}| < 0.01694$, $\chi^2_{4c\ and\ 1c} < 80$, $|M_{p\pi^-K^-} - M_{\Omega}| > 0.023$, $|M_{\bar{p}\pi^+K^+} - M_{\bar{\Omega}}| > 0.023$ and $|M_{p\bar{p}\pi^-\pi^+} - M_{J/\psi}| > 0.00889$ cuts

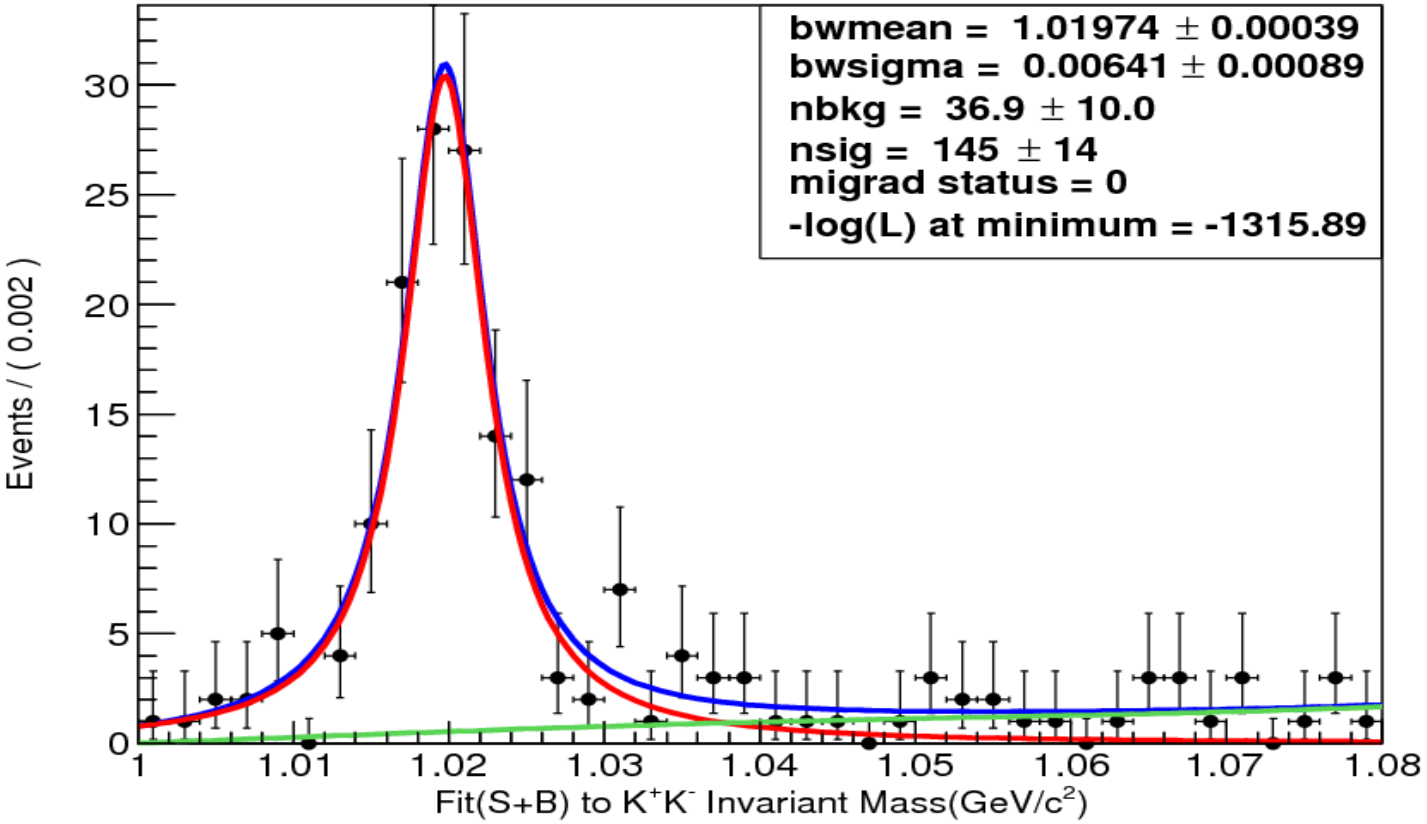

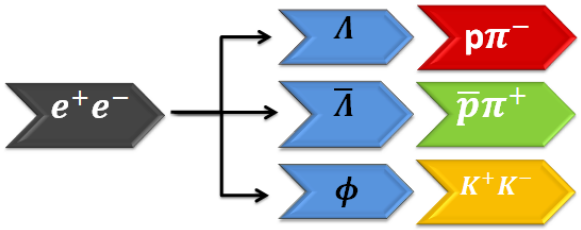

K^+K^- Invariant mass distribution of data after 4C and 1C kinematic fit under $|M_{p\pi^-} - M_{\Lambda}| < 0.01566$, $|M_{\bar{p}\pi^+} - M_{\bar{\Lambda}}| < 0.01694$, $\chi^2_{4c\ and\ 1c} < 80$, $|M_{p\pi^-K^-} - M_{\Omega}| > 0.023$, $|M_{\bar{p}\pi^+K^+} - M_{\bar{\Omega}}| > 0.023$ and $|M_{p\bar{p}\pi^-\pi^+} - M_{J/\psi}| > 0.00889$ cuts

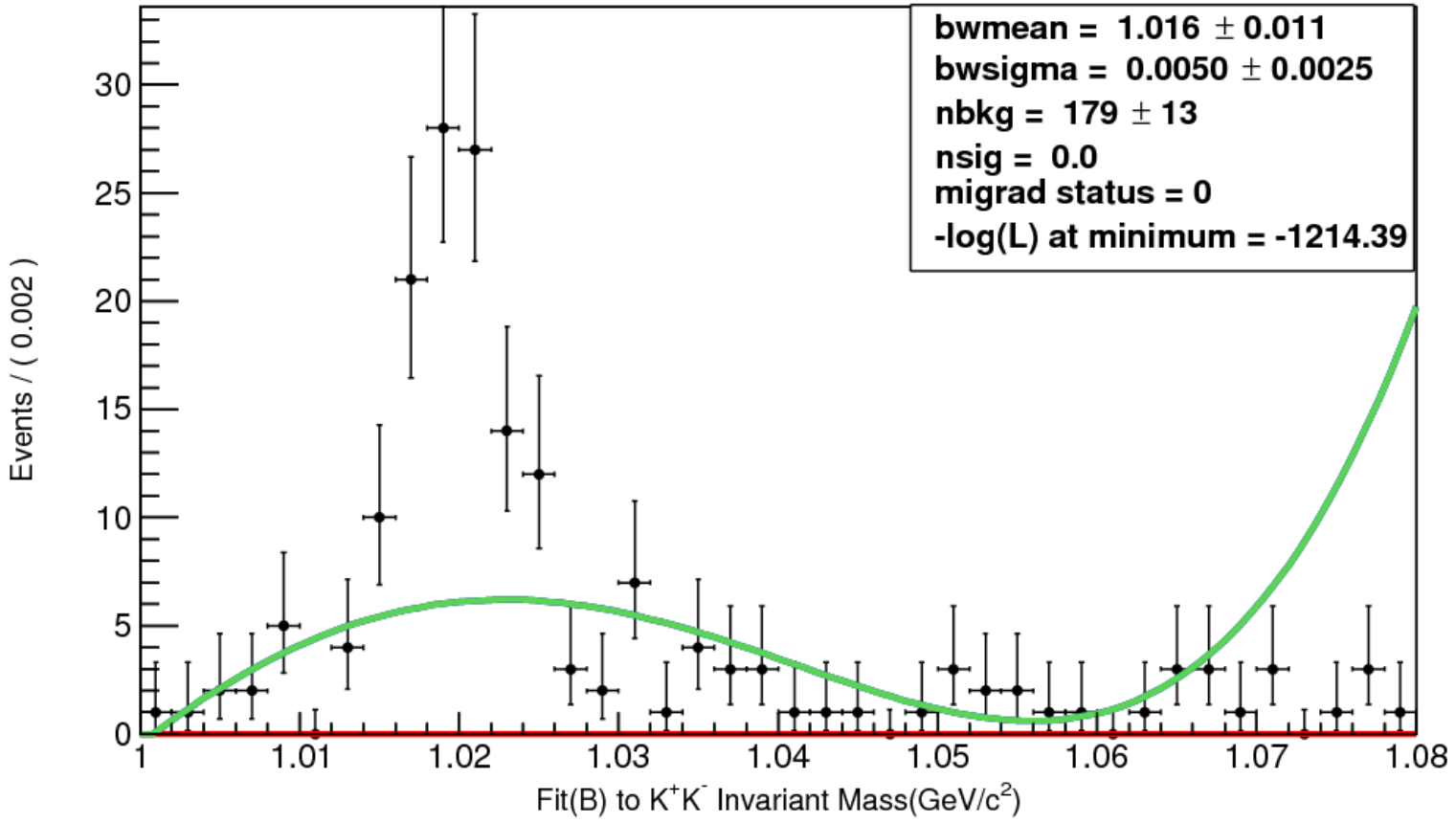

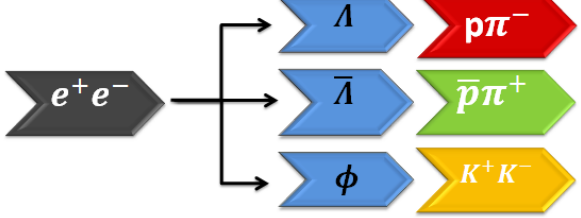

K^+K^- Invariant mass distribution of data after 4C kinematic fit under

$|M_{p\pi^-} - M_{\Lambda}| < 0.0137$, $|M_{\bar{p}\pi^+} - M_{\bar{\Lambda}}| < 0.0144$, $\chi^2_{4c} < 80$,
$|M_{p\pi^-K^-} - M_{\Omega}| > 0.0207$, $|M_{\bar{p}\pi^+K^+} - M_{\bar{\Omega}}| > 0.0207$ and
$|M_{p\bar{p}\pi^-\pi^+} - M_{J/\psi}| > 0.00796$ cuts

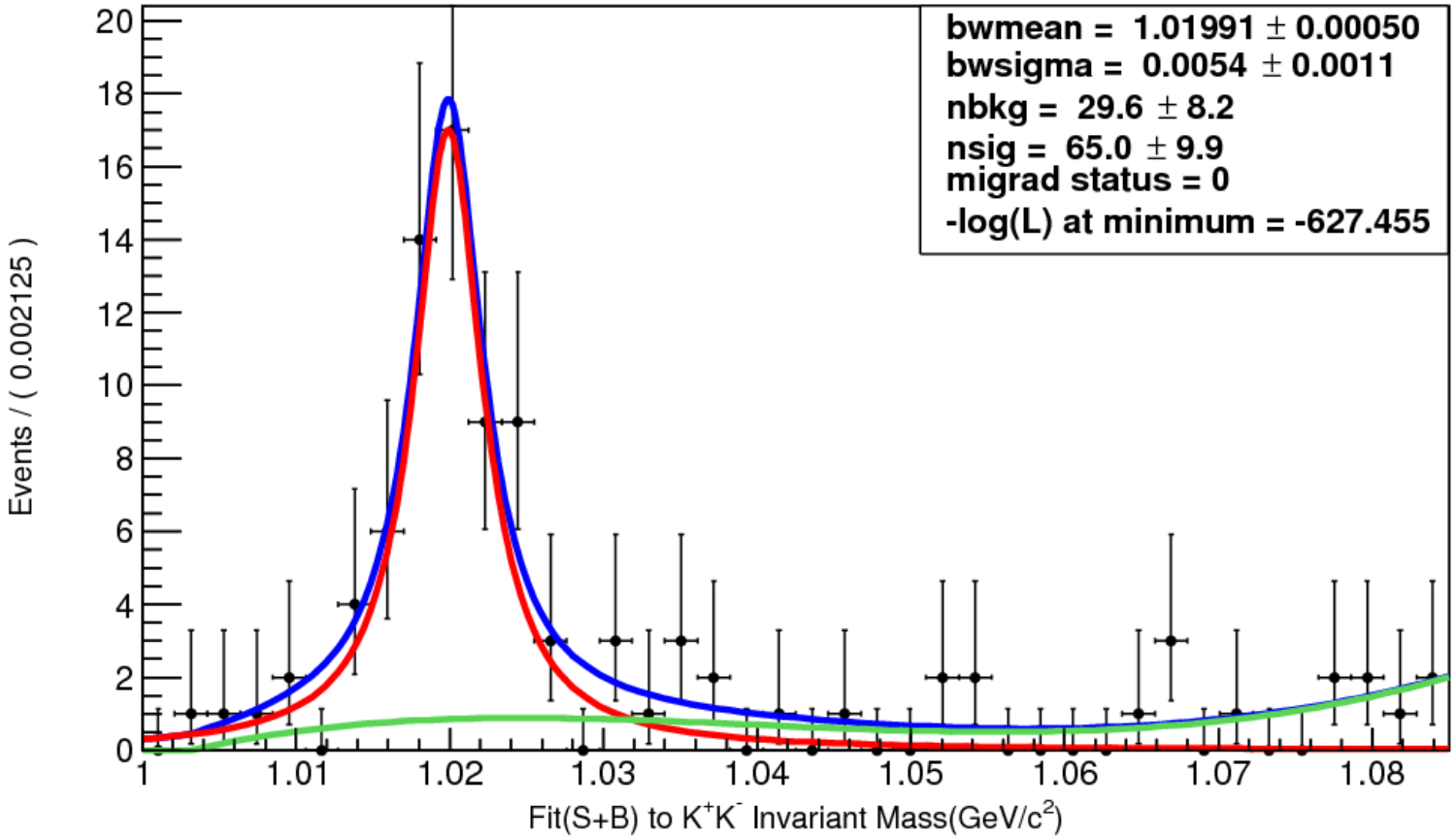

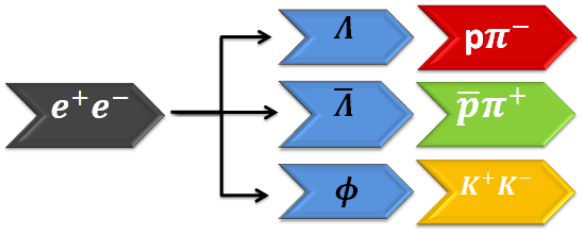

K^+K^- Invariant mass distribution of data after 4C kinematic fit under

$|M_{p\pi^-} - M_{\Lambda}| < 0.0137$, $|M_{\bar{p}\pi^+} - M_{\bar{\Lambda}}| < 0.0144$, $\chi^2_{4c} < 80$, $|M_{p\pi^-K^-} - M_{\Omega}| > 0.0207$, $|M_{\bar{p}\pi^+K^+} - M_{\bar{\Omega}}| > 0.0207$ and $|M_{p\bar{p}\pi^-\pi^+} - M_{J/\psi}| > 0.00796$ cuts

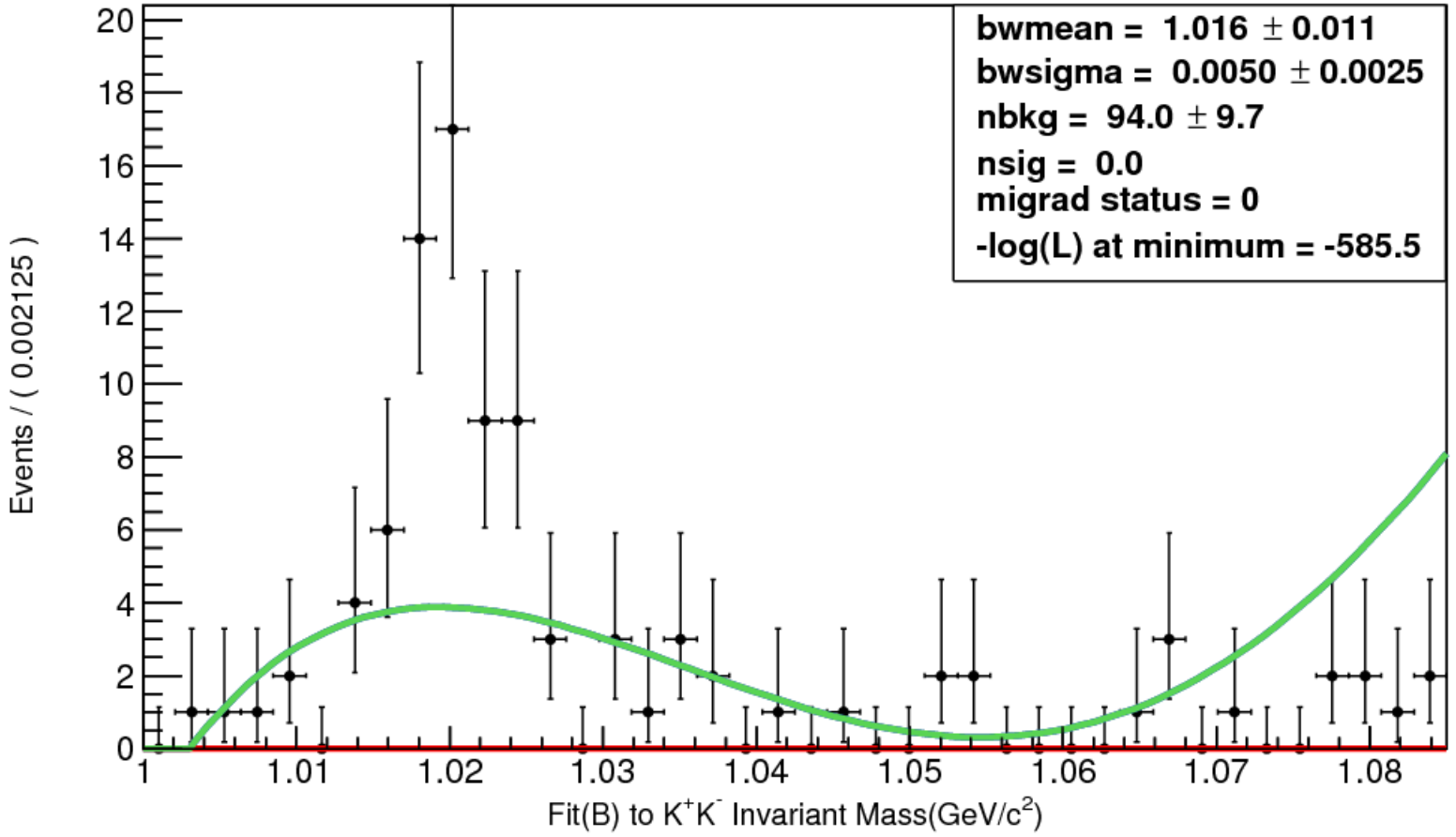

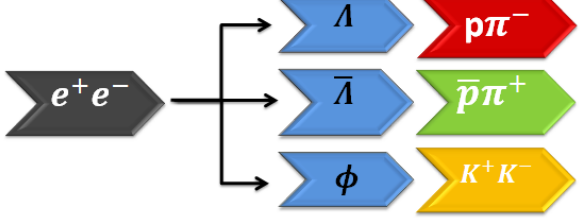

K^+K^- Invariant mass distribution of data after 1C kinematic fit under $|M_{p\pi^-} - M_{\Lambda}| < 0.01796$, $|M_{\bar{p}\pi^+} - M_{\bar{\Lambda}}| < 0.01972$, $\chi^2_{1c} < 80$, $|M_{p\pi^-K^-} - M_{\Omega}| > 0.025$, $|M_{\bar{p}\pi^+K^+} - M_{\bar{\Omega}}| > 0.025$ and $|M_{p\bar{p}\pi^-\pi^+} - M_{J/\psi}| > 0.010$ cuts

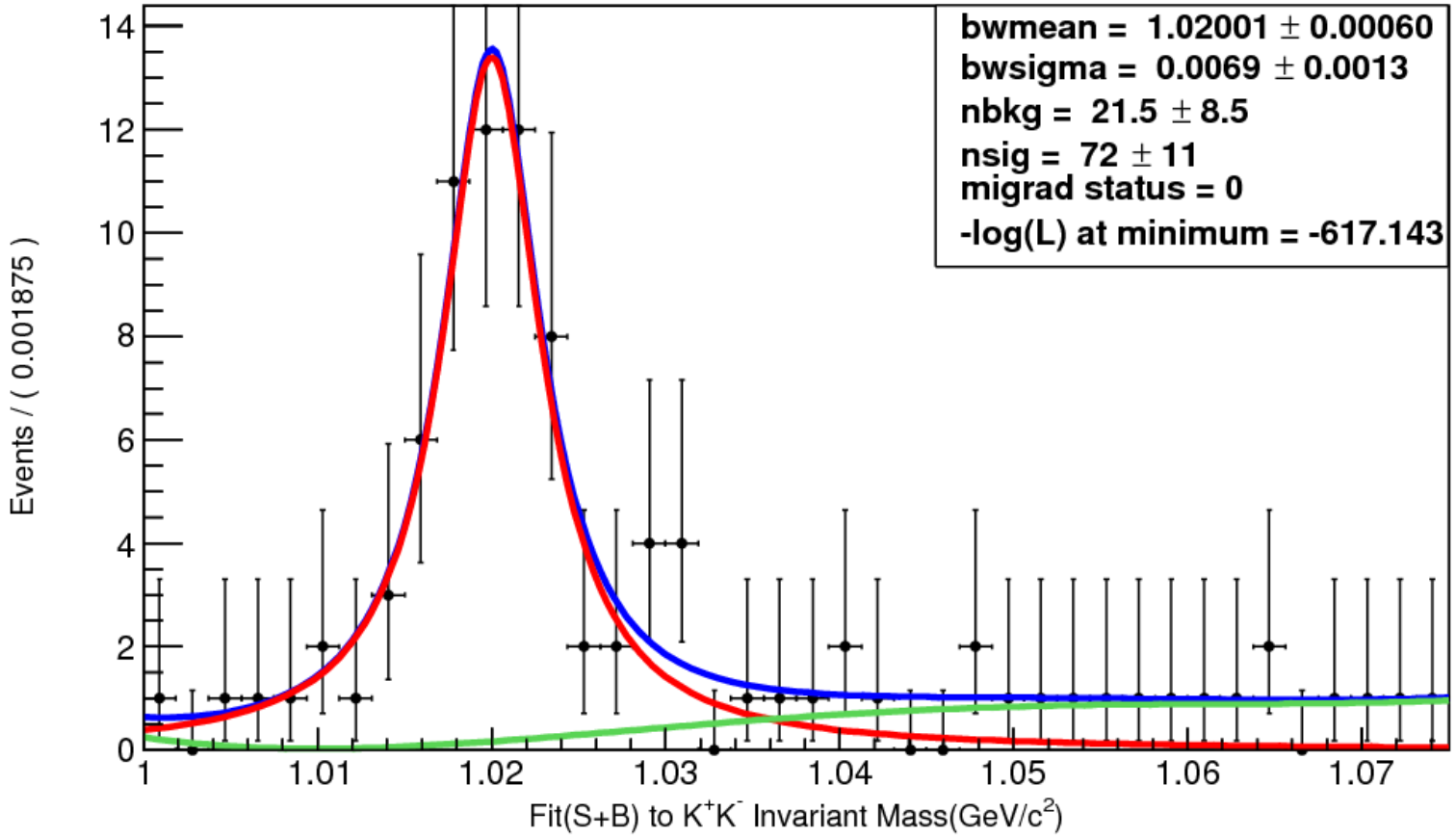

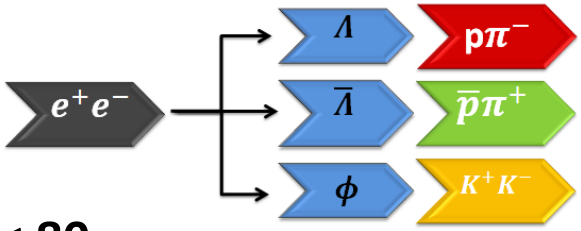

K^+K^- Invariant mass distribution of data after 1C kinematic fit under $|M_{p\pi^-} - M_{\Lambda}| < 0.01796$, $|M_{\bar{p}\pi^+} - M_{\bar{\Lambda}}| < 0.01972$, $\chi^2_{1c} < 80$, $|M_{p\pi^-K^-} - M_{\Omega}| > 0.025$, $|M_{\bar{p}\pi^+K^+} - M_{\bar{\Omega}}| > 0.025$ and $|M_{p\bar{p}\pi^-\pi^+} - M_{J/\psi}| > 0.010$ cuts

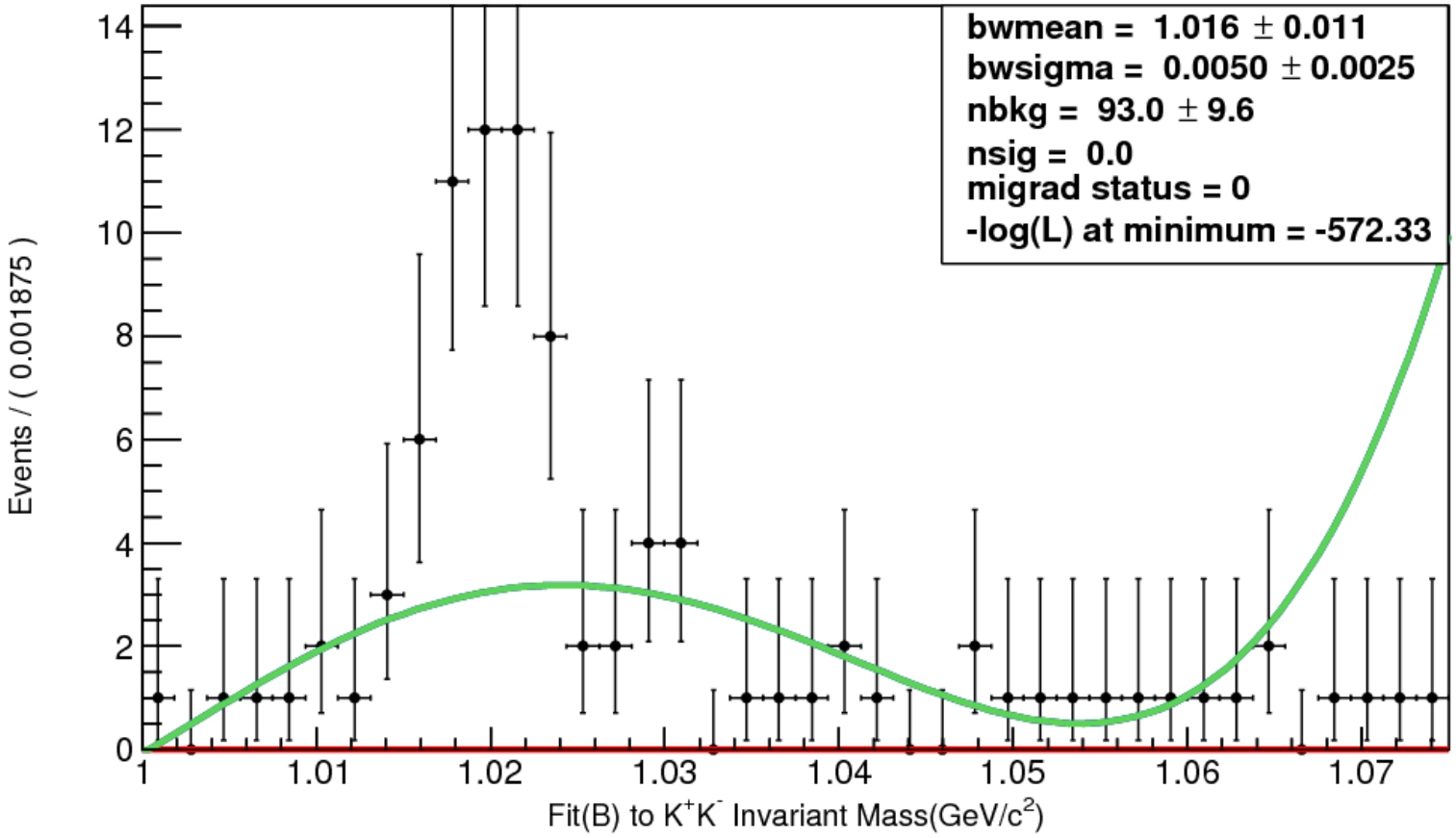

SCATTER PLOT after 4C and 1C kinematic fit

Scatter plot between $p\pi^-$ and K^+K^-

$|M_{\bar{p}\pi^+} - M_{\bar{\Lambda}}| < 0.01694$, $\chi^2_{4c\text{ and }1c} < 80$, $|M_{p\pi^-K^-} - M_{\Omega}| > 0.023$, $|M_{\bar{p}\pi^+K^+} - M_{\bar{\Omega}}| > 0.023$ and $|M_{p\bar{p}\pi^-\pi^+} - M_{J/\psi}| > 0.00889$ cuts

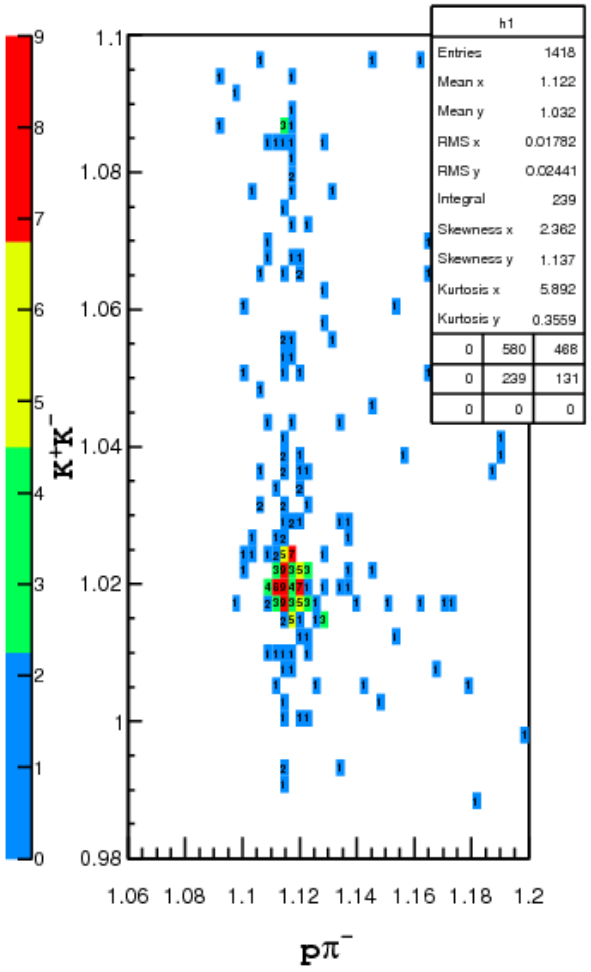

Scatter plot between $\bar{p}\pi^+$ and K^+K^-

$|M_{p\pi^-} - M_{\Lambda}| < 0.01566$, $\chi^2_{4c\text{ and }1c} < 80$, $|M_{p\pi^-K^-} - M_{\Omega}| > 0.023$, $|M_{\bar{p}\pi^+K^+} - M_{\bar{\Omega}}| > 0.023$ and $|M_{p\bar{p}\pi^-\pi^+} - M_{J/\psi}| > 0.00889$ cuts

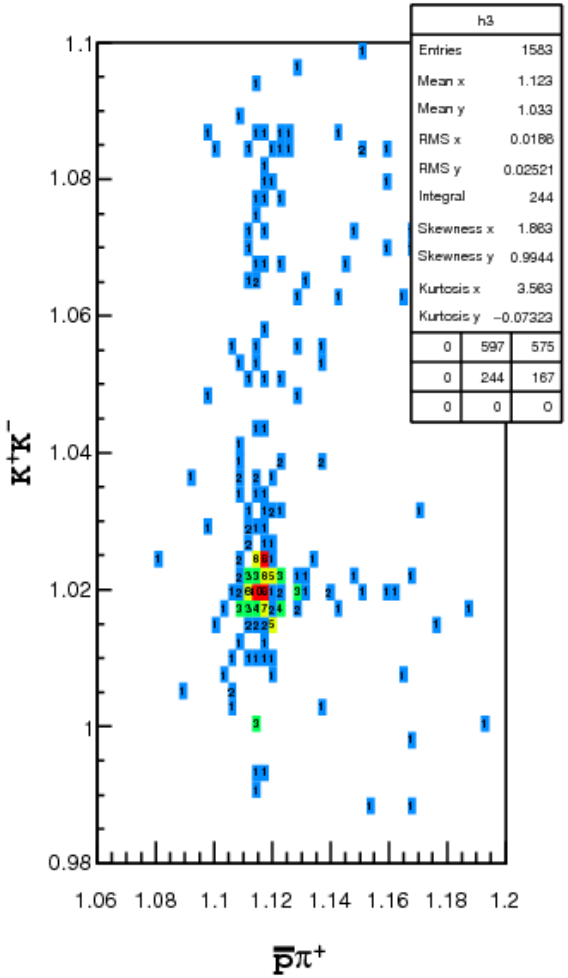

Scatter plot between $p\pi^-$ and $\bar{p}\pi^+$

$|M_{K^+K^-} - M_{\Phi}| < 0.011925$, $\chi^2_{4c\text{ and }1c} < 80$, $|M_{p\pi^-K^-} - M_{\Omega}| > 0.023$, $|M_{\bar{p}\pi^+K^+} - M_{\bar{\Omega}}| > 0.023$ and $|M_{p\bar{p}\pi^-\pi^+} - M_{J/\psi}| > 0.00889$ cuts

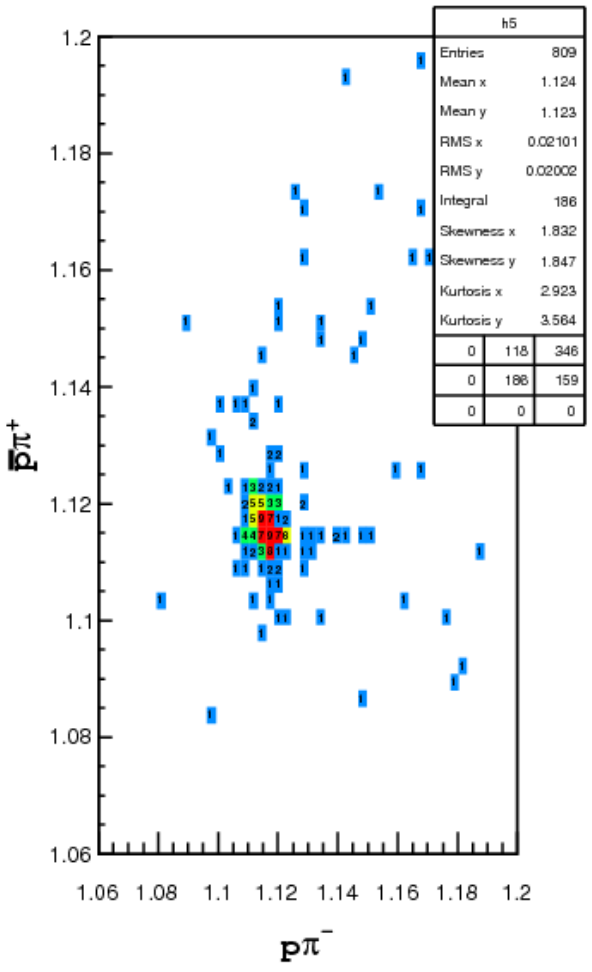

SCATTER PLOT after 4C kinematic fit

Scatter plot between $p\pi^-$ and K^+K^-

$|M_{\bar{p}\pi^+} - M_{\bar{\Lambda}}| < 0.0144$, $\chi^2_{4c} < 80$, $|M_{p\pi^-K^-} - M_{\Omega}| > 0.0207$, $|M_{\bar{p}\pi^+K^+} - M_{\bar{\Omega}}| > 0.0207$ and $|M_{p\bar{p}\pi^-\pi^+} - M_{J/\psi}| > 0.00796$ cuts

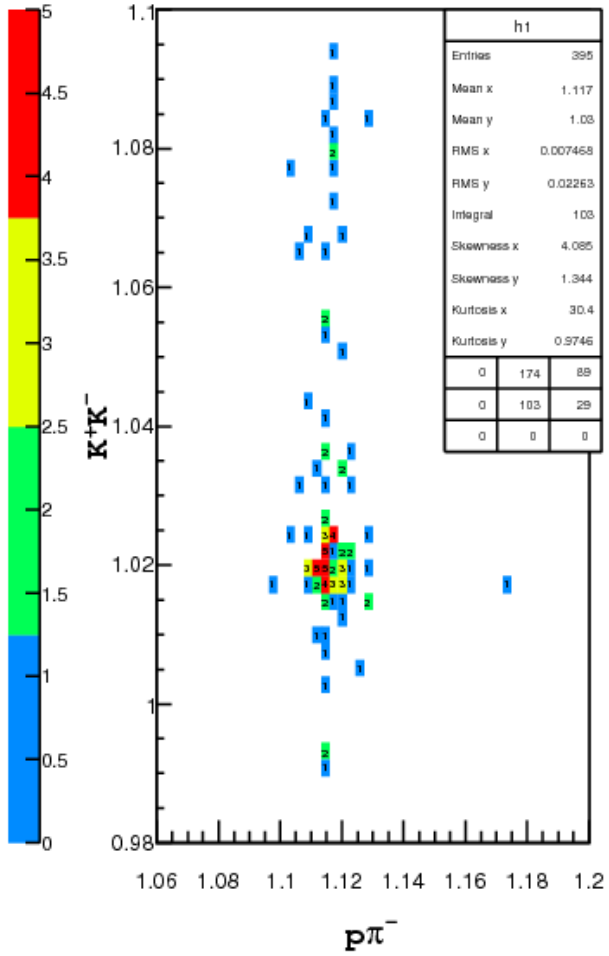

Scatter plot between $\bar{p}\pi^+$ and K^+K^-

$|M_{p\pi^-} - M_{\Lambda}| < 0.0137$, $\chi^2_{4c} < 80$, $|M_{p\pi^-K^-} - M_{\Omega}| > 0.0207$, $|M_{\bar{p}\pi^+K^+} - M_{\bar{\Omega}}| > 0.0207$ and $|M_{p\bar{p}\pi^-\pi^+} - M_{J/\psi}| > 0.00796$ cuts

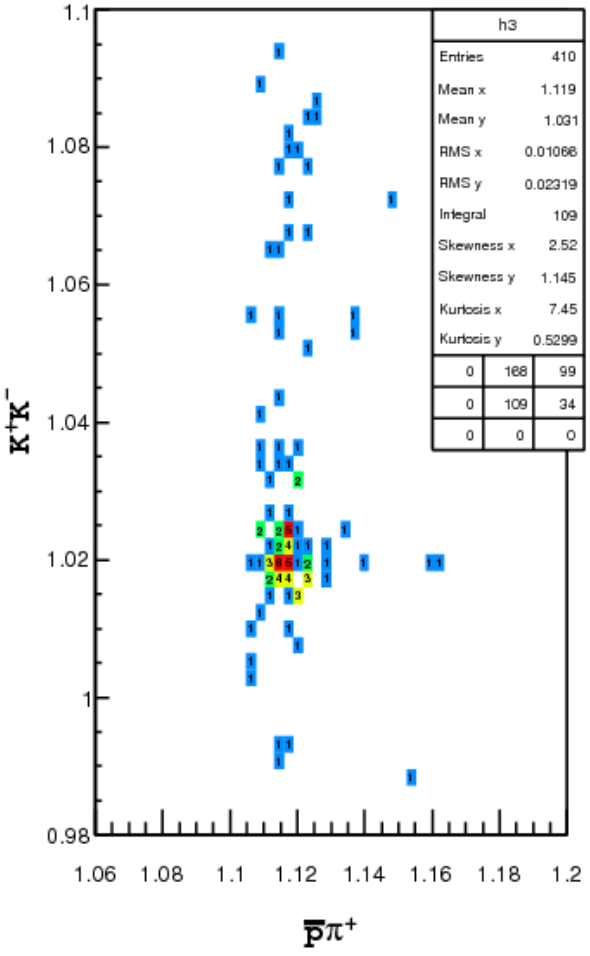

Scatter plot between $p\pi^-$ and $\bar{p}\pi^+$

$|M_{K^+K^-} - M_{\phi}| < 0.011187$, $\chi^2_{4c} < 80$, $|M_{p\pi^-K^-} - M_{\Omega}| > 0.0207$, $|M_{\bar{p}\pi^+K^+} - M_{\bar{\Omega}}| > 0.0207$ and $|M_{p\bar{p}\pi^-\pi^+} - M_{J/\psi}| > 0.00796$ cuts

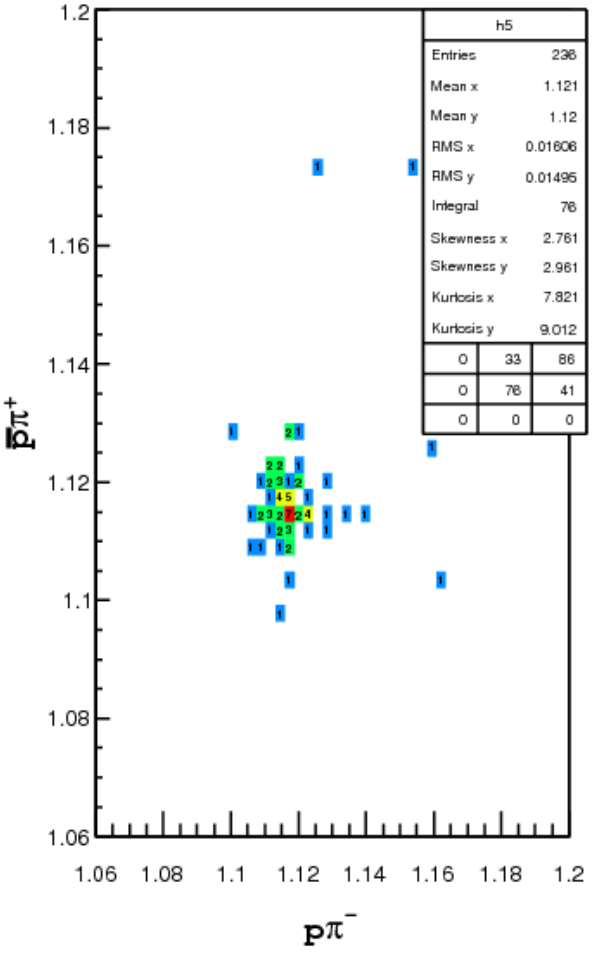

SCATTER PLOT after 1C kinematic fit

Scatter plot between $p\pi^-$ and K^+K^-

$|M_{\bar{p}\pi^+} - M_{\bar{\Lambda}}| < 0.01972$, $\chi^2_{1c} < 80$, $|M_{p\pi^-K^-} - M_{\Omega}| > 0.025$, $|M_{\bar{p}\pi^+K^+} - M_{\bar{\Omega}}| > 0.025$ and $|M_{p\bar{p}\pi^-\pi^+} - M_{J/\psi}| > 0.010$ cuts

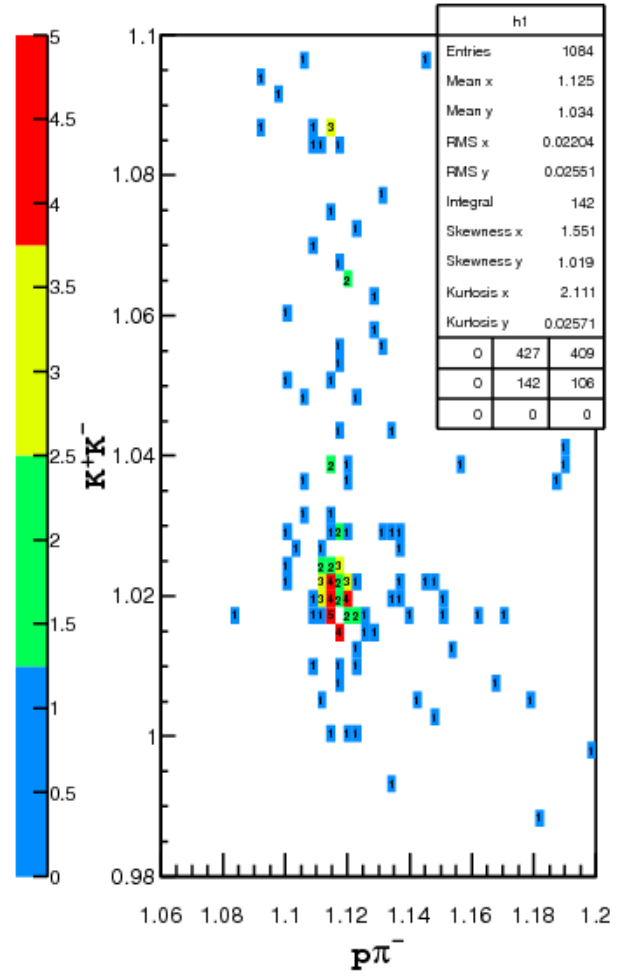

Scatter plot between $\bar{p}\pi^+$ and K^+K^-

$|M_{p\pi^-} - M_{\Lambda}| < 0.01796$, $\chi^2_{1c} < 80$, $|M_{p\pi^-K^-} - M_{\Omega}| > 0.025$, $|M_{\bar{p}\pi^+K^+} - M_{\bar{\Omega}}| > 0.025$ and $|M_{p\bar{p}\pi^-\pi^+} - M_{J/\psi}| > 0.010$ cuts

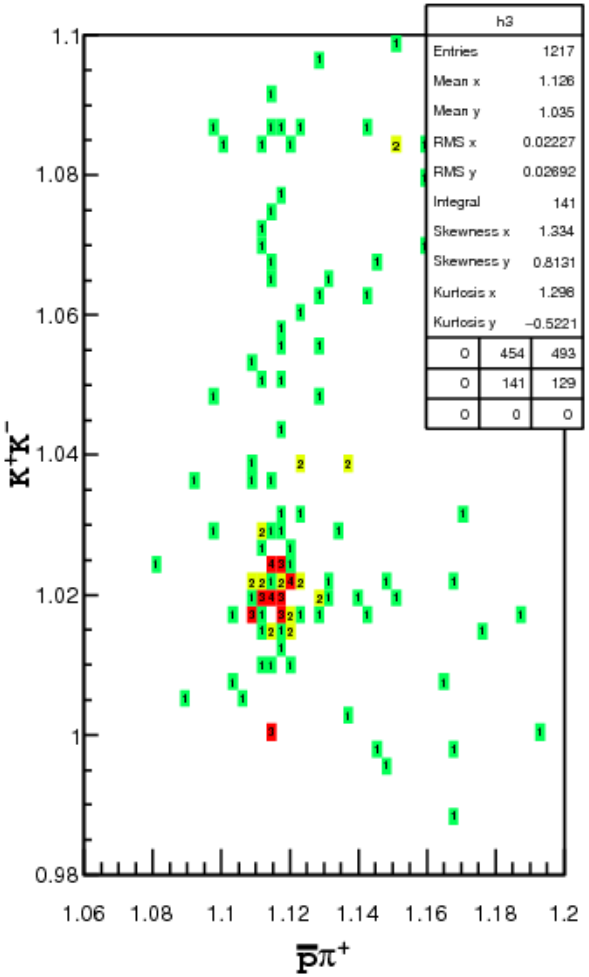

Scatter plot between $p\pi^-$ and $\bar{p}\pi^+$

$|M_{K^+K^-} - M_{\Phi}| < 0.012717$, $\chi^2_{1c} < 80$, $|M_{p\pi^-K^-} - M_{\Omega}| > 0.025$, $|M_{\bar{p}\pi^+K^+} - M_{\bar{\Omega}}| > 0.025$ and $|M_{p\bar{p}\pi^-\pi^+} - M_{J/\psi}| > 0.010$ cuts

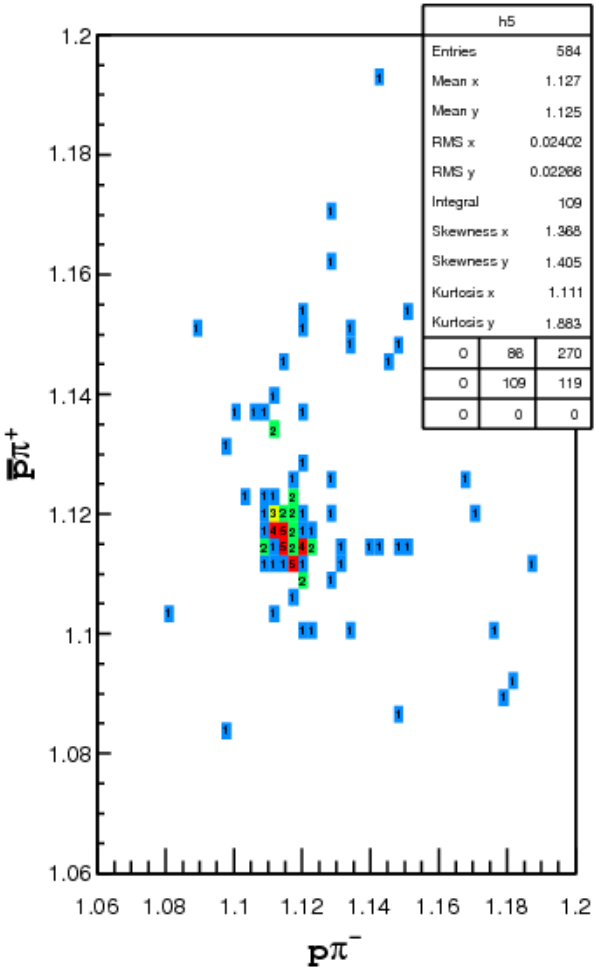

Background Analysis

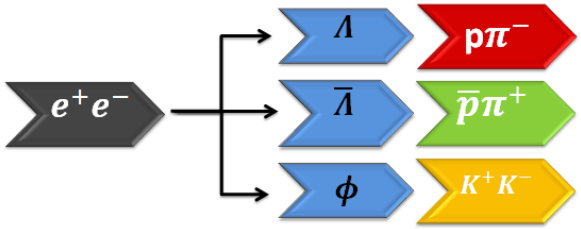

After making the final event selection of invariant mass distribution of K^+K^-, it is necessary to investigate the possible background events still affecting the signal region. For background analysis we have used 500 pb^{-1} inclusive MC data beside some exclusive MC sample generated using phase space generator. The possible background suggested by mclist is given in the table. From all the background decay channel given in table, exclusive cut of one prominent background decay channel has been applied in the final event selection.

Sr. No.	Decay Channels	$Events_{mclist}$
1	$Y(4260) \to J/\psi K^+K^-(J/\psi \to p\bar{p}\pi^+\pi^-)$	145
2	$Y(4260) \to J/\psi K^+K^-(J/\psi \to \Delta^{++}\bar{p}\pi^-)$	37
3	$Y(4260) \to J/\psi K^+K^-(J/\psi \to \Delta^{++}\Delta^{--})$	31
4	$Y(4260) \to J/\psi K^+K^-(J/\psi \to \Delta^{--}\pi^+p^+)$	31
5	$Y(4260) \to J/\psi K^+K^-(J/\psi \to \Lambda\bar{\Lambda})$	20
6	$Y(4260) \to J/\psi K^+K^-(J/\psi \to \Delta^0\bar{p}\pi^+)$	9
7	$Y(4260) \to J/\psi K^+K^-(J/\psi \to f_0' p\bar{p})$	9
8	$Y(4260) \to J/\psi K^+K^-(J/\psi \to \bar{\Delta}^0 p\pi^-)$	6
9	$Y(4260) \to J/\psi K^+K^-(J/\psi \to p\bar{p}\pi^+\pi^-\pi^0)$	4
10	$Y(4260) \to J/\psi K^+K^-(J/\psi \to \omega p\bar{p})$	4
11	$Y(4260) \to \omega\chi_{c0}(\omega \to \pi^+\pi^-, \chi_{c0} \to K^+K^-p\bar{p})$	3
12	$Y(4260) \to J/\psi K^+K^-(J/\psi \to \Delta^0\bar{\Delta}^0)$	2
13	$Y(4260) \to J/\psi\pi^+\pi^-(J\psi \to p\bar{p}f_0'')$	2
14	$Y(4260) \to \psi(2S)\pi^+\pi^-(\psi(2S) \to K^+K^-p\bar{p})$	2
15	$Y(4260) \to \omega\chi_{c0}(\omega \to \pi^+\pi^-\pi^0, \chi_{c0} \to K^+K^{*-}p\bar{p})$	2
16	$Y(4260) \to J/\psi K^+K^-(J/\psi \to \Lambda\bar{\Sigma})$	2
17	$Y(4260) \to J/\psi K^+K^-(J/\psi \to p\bar{p}\pi^+\pi^-\gamma_{FSR})$	2
18	$Y(4260) \to J/\psi K^+K^-(J/\psi \to \Sigma^{*+}\bar{\Sigma}^-)$	1
19	$Y(4260) \to J/\psi K^+K^-(J/\psi \to p\bar{p}\eta')$	1
20	$Y(4260) \to \psi(2S)\pi^+\pi^-(\psi(2S) \to p\bar{p}f_2)$	1
21	$Y(4260) \to J/\psi\pi^+\pi^-\gamma_{FSR}$	1
22	$Y(4260) \to J/\psi\pi^+\pi^-(J/\psi \to p\bar{p}K^+K^-)$	1
23	$Y(4260) \to J/\psi K^+K^-(J/\psi \to \gamma\Lambda\bar{\Lambda})$	1
24	$Y(4260) \to J/\psi\pi^+\pi^-(J/\psi \to \phi p\bar{p})$	1
25	$Y(4260) \to \pi^+\pi^-\pi^0\chi_{c2}$	1
26	$Y(4260) \to J/\psi K^+K^-(J/\psi \to p\bar{p}f_2)$	1
27	$Y(4260) \to J/\psi K^+K^-(J/\psi \to \Lambda\bar{\Lambda}\pi^0)$	1
28	$Y(4260) \to J/\psi K^+K^-(J/\psi \to p\bar{p}\rho^0)$	1
29	$Y(4260) \to J/\psi K^+K^-(J/\psi \to \Delta^{++}\Delta^{--}\pi^0)$	1
30	$Y(4260) \to \pi^+\pi^-\pi^0\chi_{c1}$	1

The possible background for $\Lambda\bar{\Lambda}\phi$

Detection Efficiency

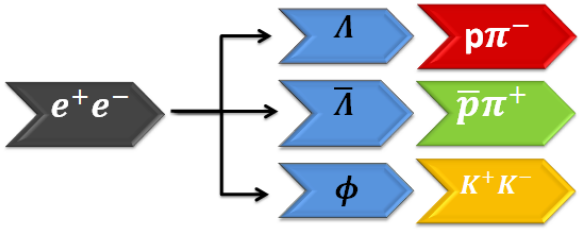

- In order to check the detection efficiency of a detector, a signal MC root file is generated using phase space (PHSP) generator.
- Detection efficiency = $\frac{N_{MC}(detected)}{N_{MC}(total)}$ x 100
- Where $N_{MC}(detected)$ and $N_{MC}(total)$ is the number of signal monte carlo events detected and total number of signal monte carlo events generated using phase space (PHSP) generator respectively.

Constraints	4C and 1C	4C	1C
Detected events (out of 900,000)	300200	142909	157291
Detection Efficiencey	33.35	15.87	17.47

Cross section Calculation of $e^+e^- \to \Lambda\bar{\Lambda}\phi$

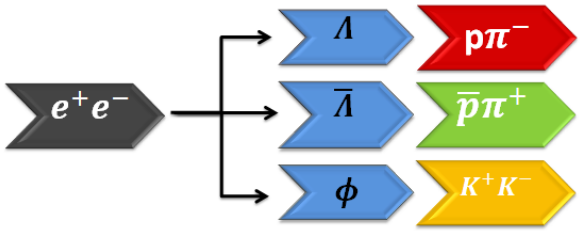

Using the following formula cross section is calculated for 4C and 1C , only 4C and only 1C:

$$\sigma\,(e^+e^- \to \Lambda\bar{\Lambda}\phi) = \frac{N_\phi^{obs}}{\mathcal{L}_{int} \times \mathcal{B}(\Lambda \to p\pi^-) \times \mathcal{B}(\bar{\Lambda} \to \bar{p}\pi^+) \times \mathcal{B}(\phi \to K^+K^-) \times \epsilon}$$

Cross section values are given in the table:

Constraints	4C and 1C	4C	1C
Cross Section	475.44 fb	447.86 fb	450.66 fb

where N_ϕ^{obs} is the number of observed signal of ϕ, $\mathcal{L}_{int}$ shows the data of integrated luminosity, $\mathcal{B}(\Lambda \to p\pi^-)$ is the branching fraction of $\Lambda \to p\pi^-$, $\mathcal{B}(\bar{\Lambda} \to \bar{p}\pi^+)$ is the branching fraction of $\bar{\Lambda} \to \bar{p}\pi^+$, $\mathcal{B}(\phi \to K^+K^-)$ is the branching fraction of $\phi \to K^+K^-$ and ϵ is the value of detection efficiency of the detector. Values of branching fractions $\mathcal{B}(\Lambda \to p\pi^-)$, $\mathcal{B}(\bar{\Lambda} \to \bar{p}\pi^+)$ and $\mathcal{B}(\phi \to K^+K^-)$ are taken from particle data group (PDG) 2016.

Systematic Uncertainty Estimation

Sr. No.	Sources of uncertainty in $\sigma(e^+e^- \to \Lambda\bar{\Lambda}\phi)$	Systematic uncertainty (%)		
		4c and 1C	4C	1C
1	Luminosity	1.0	1.0	1.0
2	Statistical error	0.300	0.415	0.210
3	MC Model	2.8185	6.647	11.026
4	$\mathcal{B}(\Lambda \to p\pi^-)$	0.7825	0.7825	0.7825
5	$\mathcal{B}(\bar{\Lambda} \to \bar{p}\pi^+)$	0.7825	0.7825	0.7825
6	$\mathcal{B}(\phi \to K^+K^-)$	1.0225	1.0225	1.0225
7	PID	6	6	6
8	Track identification	12	12	12
	Total uncertainty	13.8312	15.087	17.4572

Statistical significance of ϕ signal

Using the formula $S = \sqrt{|2 ln L_{max}(S+B) - 2 ln L_{max}(B)|}$

Constraints	4C and 1C	4C	1C
Statisticlal Significance	10.075	6.477	6.694

Summary and Analysis Results

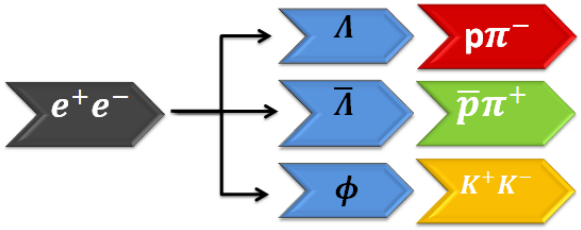

Analysis is performed using the data sets collected at center of mass energies $\sqrt{s}$ = 4190, 4200, 4210, 4220, 4237, 4246, 4260, 4270 and 4280 MeV with the BESIII detector and BEPCII collider. The decay channel $e^+e^- \to \Lambda\bar{\Lambda}\phi$ is studied for the very first time to measure the cross section. Real data of $4580.1\,pb^{-1}$ is used to check the number of events producing $\Lambda\bar{\Lambda}\phi$, for which we have used inclusive MC of $500\,pb^{-1}$ beside some exclusive MC sample generated using phase space generater to remove the background. Based on data of $4580.1\,pb^{-1}$, cross section of $e^+e^- \to \Lambda\bar{\Lambda}\phi$ is measured. For convenience analysis result is also given in table.

Center of mass energy $\sqrt{s}$ (GeV)	Reconstruction of $\Lambda\bar{\Lambda}\phi$	σ (fb) 4C and 1C	σ (fb) 4C	σ (fb) 1C
4.190, 4.200, 4.210, 4.220, 4.237, 4.246, 4.260, 4.270 and 4.280	$\Lambda \to p\pi^-$, $\bar{\Lambda} \to \bar{p}\pi^+$, $\phi \to K^+K^-$	475.44 $\pm 65.75(syst)$ $\pm 49.96(stat)$	447.86 $\pm 67.56(syst)$ $\pm 71.25(stat)$	450.66 $\pm 78.67(syst)$ $\pm 71.94(stat)$


Thankyou